Aus der Klinik mit Schwerpunkt Rheumatologie und Klinische Immunologie der
Medizinischen Fakultät Charité – Universitätsmedizin Berlin

DISSERTATION

Antagonizing Autocrine Interleukin-6 Receptor Signaling Inhibits Prostate Cancer Growth in Bone

zur Erlangung des akademischen Grades
Doctor medicinae (Dr. med.)

vorgelegt der Medizinischen Fakultät
Charité – Universitätsmedizin Berlin

von

Dennis Basel

aus Berlin

Datum der Promotion: 14.09.2018

meinen Eltern gewidmet

TABLE OF CONTENTS / INHALTSVERZEICHNIS

List of Figures / Abbildungsverzeichnis

Abbreviations / Abkürzungsverzeichnis

AP-1	activator protein-1
ATF4	activating transcription factor 4
Bcl-2	B-cell lymphoma 2
Bcl-xL	B-cell lymphoma-extra large
BMP-2	bone morphogenetic protein 2
BMPs	bone morphogenetic proteins
BSA	bovine serum albumin
CRPCa	castration-resistant prostate cancer
DKK-1	dickkopf-1
DNA	deoxyribonucleic acid
EDTA	ethylenediaminetetraacetic acid
EMT	epithelial-mesenchymal transition
FCS	fetal calf serum
FGF	fibroblast growth factor
FGF-23	fibroblast growth factor 23
FPP	farnesyl pyrophosphate
GH	growth hormone
GM-CSF	granulocyte macrophage colony stimulating factor
IGF-I	insulin-like growth factor I
IGF-II	insulin-like growth factor II
IL-1	interleukin-1
IL-11	interleukin-11
IL-17	interleukin-17
IL-6	interleukin-6
IL-8	interleukin-8
JAK	janus kinase
JNK	jun N-terminal kinase
LCS	lacunar-canalicular system
MAPK	mitogen activated protein kinase
Mcl-1	myeloid cell leukemia 1

M-CSF	macrophage colony stimulating factor
MITF	microphthalmia-associated transcription factor
MMP-9	matrix metalloproteinase 9
$NFAT_C1$	nuclear factor of activated T-cells, cytoplasmic 1
NFκB	nuclear factor kappa-light-chain-enhancer of activated B cells
NO	nitric oxide
OCF	osteoclastogenesis factor
OCIF	osteoclastogenesis inhibitory factor
OPG	osteoprotegerin
OPGL	osteoprotegerin ligand
OSX	osterix
P1NP	procollagen type I N-terminal propeptide
PBS	phosphate-buffered saline
PDGF	platelet-derived growth factor
PGE2	prostaglandin E2
PI3K	phosphatidylinositol 3-kinase
PKB	protein kinase B
PTH	parathyroid hormone
PTHR1	parathyroid hormone receptor type 1
PTHrP	parathyroid hormone-related protein
RANK	receptor activator of nuclear factor kappa B
RANKL	receptor activator of nuclear factor kappa B ligand
RNA	ribonucleic acid
RPMI	Roswell Park Memorial Institute medium
RT-PCR	reverse transcription polymerase chain reaction
RUNX2	runt-related transcription factor 2
S1P	sphingosine 1-phosphate
SOST	sclerostin
STAT	signal transducer and activator of transcription
TAMs	tumor-associated macrophages
TGF-β	transforming growth factor beta
TNF	tumor necrosis factor
TNF-α	tumor necrosis factor alpha

TRAcP	tartrate-resistant acid phosphatase
TRAcP 5b	tartrate-resistant acid phosphatase 5b
TRAF6	TNF receptor associated factor 6
TRANCE	TNF-related activation-induced cytokine
TUNEL	terminal deoxynucleotidyl transferase biotin-dUTP nick end labeling
VEGF	vascular endothelial growth factor
VEGF-A	vascular endothelial growth factor A
µCT	micro-computerized tomography

Abstract

Background:

In prostate cancer patients, high circulating levels of interleukin-6 (IL-6) correlate with disease progression and bone metastatic lesions. Studies have shown that IL-6 stimulates the “classical” vicious cycle of bone metastasis by inducing the expression of receptor activator of nuclear factor kappa B ligand (RANKL) on osteoblasts. As PC3 cells secrete large amounts of IL-6, we hypothesize that autocrine IL-6 signaling promotes tumor growth in bone by increasing the synthesis of receptor activator of nuclear factor kappa B (RANK) in cancer cells, sensitizing these cells for direct crosstalk with RANKL-bearing osteoblasts.

Materials and Methods:

The *in vitro* effects of human IL-6 on RANK and parathyroid hormone-related protein (PTHrP) mRNA expression in PC3 cells were assessed by using real-time quantitative reverse transcription PCR.

To determine *how* autocrine IL-6 signaling contributes to prostate cancer growth in bone, we inoculated human PC3 xenografts intra-tibially into nude mice and blocked autocrine IL-6 receptor signaling using tocilizumab and bone resorption using zoledronic acid for a period of 30 days. Tumors were analyzed by histomorphometry, immunohistochemistry for Ki-67 and RANK expression as well as by TUNEL staining. Osteolytic lesions were measured by X-ray images, the numbers of osteoclasts at the tumor-bone interface, serum RANKL and tartrate-resistant acid phosphatase 5b (TRAcP 5b) levels.

In a second experiment, we injected PC3 xenografts subcutaneously into nude mice and analyzed the tumors by calculating their volumes every 3 days, by immunohistochemical staining for RANK expression and by determining their mass following euthanasia of mice at day 58.

Results:

Treatment of PC3 cells with human IL-6 upregulated RANK and PTHrP mRNA expression *in vitro* and tocilizumab reduced this effect.

The intra-tibial xenograft murine model revealed that tocilizumab significantly inhibited PC3 tumor growth, associated with higher apoptosis and lower cell proliferation rates compared to untreated controls. Parameters of bone resorption were also significantly decreased in tocilizumab-treated mice, showing reduced osteolytic lesions in X-rays, osteoclast numbers at the tumor-bone interface, serum RANKL and TRAcP 5b levels.

In contrast, therapy with tocilizumab did not show any effects in the subcutaneous xenograft mouse model in terms of tumor volume, tumor mass and RANK receptor expression.

Conclusions:

In the current study, we demonstrate that PC3 tumor cells communicate directly with osteoblast lineage cells by signaling through feed forward loops involving IL-6, RANKL and RANK. This molecular triad promotes metastatic cancer growth in bone by (i) operating as an additional and amplifying element within the framework of the classical vicious cycle and by (ii) mediating cancer cell motility as well as directional migration towards a RANKL source.

Abstrakt

Hintergrund:

Erhöhte Werte von Interleukin-6 (IL-6) im Plasma korrelieren in Prostata-Krebspatienten mit Krankheitsprogression und dem Auftreten von Knochenmetastasen. Studien konnten zeigen, dass IL-6 die Bildung von 'receptor activator of nuclear factor kappa B ligand' (RANKL) auf Osteoblasten induziert und dadurch den „klassischen“ Teufelskreis der Knochenmetastasierung aktiviert. Da PC3-Tumorzellen große Mengen von diesem Zytokin sezernieren, stellen wir die Hypothese auf, dass autokrin wirksames IL-6 das Tumorwachstum im Knochen befördert, indem es die Synthese von 'receptor activator of nuclear factor kappa B' (RANK) in Krebszellen begünstigt und dadurch Tumorzellen für eine direkte Kommunikation mit RANKL exprimierenden Osteoblasten sensibilisiert.

Materialien und Methoden:

Die Wirkungen von IL-6 auf die RANK und 'parathyroid hormone-related protein' (PTHrP) mRNA Synthese von PC3-Zellen wurden mithilfe einer 'real-time quantitative reverse transcription PCR' ermittelt.

Um zu beurteilen wie autokrin wirksames IL-6 zum Tumorwachstum im Knochen beiträgt, injizierten wir PC3-Krebszellen in Tibiae von Nacktmäusen und hemmten für eine Dauer von 30 Tagen das autokrine IL-6-Signal per Tocilizumab sowie die Knochenresorption durch Zoledronsäure.

Die Neoplasien wurden mittels Histomorphometrie, immunohistochemischer Darstellung von Ki-67 und RANK sowie anhand des Ausmaßes der Apoptose mit TUNEL-Färbung analysiert. Osteolytische Läsionen wurden mittels Röntgenbilder, Plasmakonzentrationen von RANKL, 'tartrate-resistant acid phosphatase 5b' (TRAcP 5b) und der Anzahl von Osteoklasten an der Tumor-Knochen-Schnittstelle gemessen. Um die Rolle von IL-6 weiter zu definieren, injizierten wir PC3-Tumorzellen in einem zweiten Experiment subkutan in Nacktmäusen und berechneten die Volumina der daraus entstehenden Tumoren alle 3 Tage, stellten den Grad der Tumor-RANK-Synthese anhand von Immunohistochemie dar und analysierten die Tumormasse nach Versterben der Mäuse am 58. Tag.

Ergebnisse:

Humanes IL-6 bewirkte *in vitro* eine erhöhte RANK- und PTHrP-mRNA-Synthese, die Tocilizumab durch Blockierung der IL-6 Rezeptoren reduzierte.

In vivo verminderte Tocilizumab das Tumorwachstum im Knochen statistisch signifikant, das im Vergleich zur Placebogruppe mit einer erhöhten Apoptose- und einer erniedrigten Proliferationsrate assoziiert war. Tocilizumab behandelte Mäuse wiesen ebenfalls signifikant erniedrigte Knochenresorptionsparameter auf, was sich in kleineren osteolytischen Läsionen in Röntgenbildern, einer verminderten Anzahl von Osteoklasten an der Tumor-Knochen-Schnittstelle sowie in reduzierten Serumkonzentrationen von RANKL und TRAcP 5b widerspiegelte.

Im Gegensatz dazu zeigte die Therapie mit Tocilizumab keine Effekte im subkutanen Mausmodell bezüglich der Größe des Tumorvolumens, der Tumormasse sowie der RANK-Rezeptor-Synthese.

Schlussfolgerungen:

Die gegenwärtige Studie zeigt, dass PC3-Tumorzellen über positive Rückkopplungsmechanismen, bestehend aus den Zytokinen IL-6, RANKL und RANK, direkt mit Osteoblasten kommunizieren. Dieses Triumverat begünstigt metastatisches Tumorwachstum, indem es (i) als komplementäres und verstärkendes Element innerhalb des klassischen Teufelskreises agiert, und (ii) die Motilität sowie die direkte Migration von Krebszellen in Richtung eines RANKL-Gradienten vermittelt.

Chapter 1
Introduction

1.1 Bone Physiology

1.1.1 Bone Structure and Function

The skeleton of a human adult consists of 206 separate bones [1] and represents the passive part of the locomotor system. Bones can be classified as long, short, flat and irregular according to their shapes. Bone tissue consists of highly specialized bone cells and an extracellular matrix. The latter is a mélange of both organic and inorganic components: the organic constituent makes up 35 % of the extracellular matrix and is primarily represented by type 1 collagen fibrils (95 %) and proteoglycans (1 – 2 %) [2]. Inorganic minerals represent the remaining 65 % and are mainly stored as calcium hydroxyapatite crystals within the organic tissue [2]. Type I collagen mediates tensile strength, while the density of minerals confers compressive stability [3].
Macroscopically, there are two different architectural structures of bones: (i) cortical (compact) and (ii) trabecular (cancellous, spongy) bone [1].

(i) As a compact and dense tissue, cortical bone forms the solid outer layer of all bones. Compact bone is composed of overlapping parallel osteons, just as a wall is built with overlapping bricks [3]. Cortical bone accounts for about 80 % of bone mass and is particularly present in the shaft of long bones (e.g. tibia, femur) [1].

(ii) Cancellous bone forms a porous, spongy-like network of trabeculae which is mainly found in the epiphysis of long bones, vertebral bodies as well as flat bones [1]. The space between the tiny spicules of spongy bone is filled with red or yellow bone marrow where haematopoiesis takes place. The structure of the trabeculae is organized in such a manner that it corresponds to the maxima of compressive and tensile stress, a structural principle termed trajectory architecture [2].

Despite the macroscopic difference, mature compact and cancellous bones share a similar type of histological architecture which is characterized by the term lamellar bone [4]. Both bone types are built economically and their microstructures follow the principle of lightweight construction, providing maximal strength with minimal mass [2].

Bone tissue can be considered as a specialized connective tissue and as such, it primarily has mechanical functions. Cortical bone favors rigidity over flexibility permitting long bones to serve as levers for mechanical loading and bodily movements [3]. In contrast, cancellous bone favors flexibility over stiffness allowing vertebral bodies to absorb more energy and to function more like a spring than a lever [3]. Bone may also serve as a shield to protect internal organs such as the brain or the bone marrow. Since 99 % of the body's calcium is located in bone [1], osseous tissue can be viewed as a mineral storage that plays a central role in the regulation of the body's electrolyte homeostasis. Interestingly, it has recently been demonstrated that bone releases endocrine signals including fibroblast growth factor 23 (FGF-23) and undercarboxylated osteocalcin to communicate with internal organs such as the kidney, pancreas and the testes [5].

1.1.2 Bone Cells, Bone Modeling and Remodeling

1.1.2.1 Osteoblasts and Bone Formation

Osteoblasts are the bone-forming cells, residing on the inner and outer surfaces of bone. They derive from mesenchymal stem cells and their differentiation depends on multiple intracellular signaling cascades among which the Wnt signaling pathway has emerged as a determining driver. Wnt signaling is divided into two branches: the canonical (beta-catenin-dependent) and the non-canonical (beta-catenin-independent) pathway and both cascades have been implicated in the regulation of the osteoblast lineage [6]. In addition to Wnt signaling, other pathways such as Hedgehog, BMP and FGF signaling have been found to play a role in osteoblastogenesis [5]. Important transcription factors implicated in osteoblastic development include runt-related

transcription factor 2 (RUNX2) and osterix (OSX), while activating transcription factor 4 (ATF4) has been shown to regulate the production of osteoblastic proteins such as osteocalcin and receptor activator of nuclear factor kappa B ligand (RANKL) [5].

Osteoblast lineage cells are a group of cells that includes osteoblast precursors, matrix-producing osteoblasts, bone-lining cells and matrix-embedded osteocytes [7]. Active matrix-producing osteoblasts synthesize and secrete the organic component of the extracellular bone matrix called osteoid. They typically secrete large amounts of type 1 collagen as well as other proteins including alkaline phosphatase, osteocalcin [5], osteopontin, osteonectin and proteoglycans [8]. This non-mineralized matrix is then mineralized through the accumulation of calcium phosphate in the form of hydroxyapatite [5]. At the end of the bone forming phase, matrix-producing osteoblasts may “choose” one of three different fates: (i) become trapped within the bone matrix as osteocytes (ii) transform into inactive osteoblasts called bone-lining cells, or (iii) undergo apoptosis [9]. The mechanisms that govern these different destinies are not well understood. Besides their bone-forming task, osteoblasts fulfill a second important function in bone metabolism, that is, they control the differentiation and activity of bone-resorbing osteoclasts via the expression of cytokines that include macrophage colony stimulating factor (M-CSF), RANKL and osteoprotegerin (OPG), which will be further discussed in 1.1.2.3 and 1.1.3 below.

Regulation of osteoblastic lineage cells occurs locally and systemically. Stimulating local parameters include mechanical loading as well as factors such as Hedgehog (HH) proteins, Wnt family proteins, bone morphogenetic proteins (BMPs), fibroblast growth factors (FGFs) and transforming growth factor beta (TGF-beta) [5]. In contrast, local molecules that suppress osteoblast development include sclerostin (SOST) and dickkopf-1 (DKK1), both of which are inhibitors of the Wnt signaling pathway [6]. Systemic regulation takes place via the sympathetic nervous system as well as hormones such as leptin, (intermittent) parathyroid hormone (PTH) exposure, growth hormone (GH), insulin, insulin-like growth factor I (IGF-I) and sex hormones (testosterone and oestrogen) [5].

1.1.2.2 Osteocytes

As mentioned above, osteocytes are former osteoblasts that become trapped by unmineralized matrix (osteoid) during the process of bone formation. When mineralization occurs, osteocytes are encased in caves (lacunae) and remain in place for the rest of their lives [9]. Osteocytes represent the most abundant cell line within bone tissue, comprising more than 90 – 95 % of all bone cells in the adult skeleton [9, 10]. In comparison, osteoblasts compose less than 5 % and osteoclasts less than 1 % [10].

Osteocytes have long been considered as passive placeholders in bone, however, new evidence has established osteocytes as crucial sensors of mechanical loading in bone tissue [11, 12]. During osteocytogenesis, osteoblasts undergo a radical transformation in shape and function from a cuboidal to a neuron-like cell with long dendritic extensions surrounded by channels (canaliculi) [11]. This lacunar-canalicular system (LCS) forms a network that connects osteocytes with each other and with cells on the bone surface (osteoblasts and bone-lining cells), allowing them to communicate either directly through gap junctions or indirectly via paracrine signals [11]. Communication with bone surface cells is fundamental for osteocytes, because they can pass sensory inputs from within the bone to the bone surface, where bone formation and resorption originate [11]. Osteocytes detect mechanical loading through fluid flow shear stress within the LCS and convert this mechanical input into a chemical message that affects osteoblast and osteoclast activity [11, 12]. Osteocytes regulate osteoblast function by producing bone formation promoters (NO, IGF-I) as well as potent inhibitors (SOST, DKK-1), while osteoclast-mediated bone resorption is controlled via increased local production of RANKL and downregulation of OPG [11]. The fact that osteocytes are able to control the activity of osteoblasts and osteoclasts prompted different authors to conclude that osteocytes represent master orchestrators of the bone remodeling process [11, 13]. In addition, osteocytes function as endocrine cells by communicating with distant organs such as the kidney through the release of the hormone FGF-23 to regulate global serum phosphate concentration [5, 13].

Viability of osteocytes is promoted by mechanical loading, estrogens, bisphosphonates and calcitonin, while factors such as immobilization, glucocorticoids, TNF-alpha, IL-1 and withdrawal of estrogen foster osteocyte cell death [13].

1.1.2.3 Osteoclasts and Bone Resorption

Osteoclasts derive from circulating myeloid/monocyte progenitor cells and degrade mineralized bone tissue. Osteoclast precursors are drawn to bone surfaces by a variety of factors liberated at sites of bone resorption, where they fuse with each other to form giant and multinucleated bone-resorbing cells [14]. Osteoblast lineage cells express two factors that are essential and sufficient to promote osteoclast differentiation including M-CSF and RANKL [14, 15].

In order to degrade bone, osteoclasts attach to the bone matrix via foot-like structures called podosomes and then polarize, forming a sealed compartment between their ruffled plasma membrane and the bone surface [16]. This compartment is termed “Howship’s lacunae” and represents the bay where bone resorption takes place. To dissolve the mineral component of bone tissue, osteoclasts generate a low pH within the lacunae by transporting protons actively (V-H^+-ATPase) and Cl^- ions passively (chloride channel type 7) through their ruffled border to form HCl [16]. Osteoclasts then secrete a broad spectrum of lysosomal and non-lysosomal enzymes that degrade the organic phase of bone tissue, among which cathepsin K and tartrate-resistant acid phosphatase (TRAcP) are well-known [4, 16]. Since osteoclasts represent the principal bone degrading cells, they play a pivotal role in skeletal diseases associated with bone loss such as bone metastases and osteoporosis. Interestingly, recent studies have implicated osteoclasts in functions beyond bone catabolism by contributing to the regulation of bone formation, hematopoiesis, intraosseous angiogenesis as well as hormonal functions of osteocalcin [16].

Given the fact that osteoclasts degrade bone tissue 100 times faster than osteoblasts are able to restore resorbed lacunae during bone remodeling, osteoclasts need to be

tightly controlled [17]. Osteoclast differentiation and function is regulated by a variety of osteotropic molecules including hormones (PTH/PTHrP, glucocorticoids, calcitonin) as well as cytokines such as interleukin-6 (IL-6) and prostaglandin E2 (PGE2) which all impact the final effector molecules of the OPG/RANKL/RANK-axis [18].

1.1.2.4 Bone Modeling and Remodeling

Bone tissue adapts in response to mechanical and metabolic signals by two processes termed bone modeling (construction) and bone remodeling (reconstruction).
Bone modeling refers to a phenomenon that changes the size and shape of bone because bone formation and bone resorption take place at *different* sites [7]. Bone modeling increases bone mass not only during childhood but also during adulthood as a result of mechanical loading [1, 7]. At times of immobilization and unloading, bone mass decreases [1].
In contrast, bone remodeling describes a surface-based process in which bone resorption precedes new bone formation in the *same* location [7]. It involves osteoclasts that remove a certain amount of bone tissue, followed by the activity of osteoblasts that replace the lost bone. This process of constant bone turnover occurs throughout a person's life and renews about 5 – 10 % of the skeleton each year [19]. The bone remodeling cycle takes place asynchronously at multiple sites in the skeleton called basic multicellular unit (BMU) and can be divided into three different phases: (i) initiation, (ii) transition and (iii) termination [20].

(i) The initiation phase implies the recruitment of osteoclast progenitors, the differentiation, fusion as well as activation of osteoclasts and the onset of bone degradation. The depth of an osteoclastic resorption lacuna varies between 40 and 60 µm [21]. Signals that initiate a bone remodeling cycle include systemic hormones (PTH, 1,25-dihydroxyvitamin-D_3), local cytokines, low blood calcium, mechanical loading as well as microcracks. Osteoclast-mediated bone resorption lasts about 3 weeks in human adults and ceases with osteoclast apoptosis caused by high extracellular calcium levels.

(ii) The transition phase couples bone resorption to bone formation. Coupling represents the coordinated activity of osteoclasts and osteoblasts bone remodeling teams and is mediated by osteoclasts-derived coupling factors that act on osteoblast progenitors to stimulate bone formation. This osteoclast – osteoblast communication includes (1) direct cell-cell contact through the ephrinB2 ligand on osteoclasts and EphB4 receptor on osteoblast progenitors (2) the secretion of paracrine factors from osteoclasts including sphingosine 1-phosphate (S1P) and (3) the liberation of growth factors such as TGF-beta, BMPs and IGF-II from the bone matrix during bone resorption.

(iii) During the terminating phase of the bone remodeling process, osteoblasts refill the exact amount of bone tissue that has been removed by prior resorption [21]. This last sequence takes about 3 months and stops when osteoblastic activity is suppressed through the release of the osteocyte-derived factor sclerostin.

It is important to understand that bone remodeling needs to be tightly balanced in order to guarantee the integrity of the human skeleton. Unbalanced bone remodeling may facilitate the development of osteolytic bone diseases by means of two pathophysiological mechanisms. The first includes that osteoblasts are not able to completely refill the resorption lacunae, resulting in a net bone loss with each remodeling cycle [21]. The second mechanism implies uncoupling of the transition phase, leading to a remodeling cycle in which bone formation does not even initiate [22, 23].

It has long been thought that circulating hormones such as sex hormones, PTH, glucocorticoids and vitamin D3 function as regulators of bone remodeling, however, it has become clear in recent years that locally generated factors act as the key regulators [19]. These molecules are able to stimulate osteoclast differentiation via the upregulation of RANKL (IL-1, IL-6, TNF-alpha, IL-8, IL-11, IL-17, PGE2 and PTHrP) and downregulation of OPG (PTHrP, PGE2) [18, 24]. The fact that pro-inflammatory cytokines such as IL-6 favor bone resorption has led to the introduction of a new field in the research of bone biology termed osteoimmunology.

1.1.3 The RANKL/RANK/OPG-System – Regulation of Bone Resorption and Formation

The discovery of the RANKL/RANK/OPG-system in the late 1990s represented an immense advance in the understanding of bone biology. It is now clear that this axis functions as the key regulator of bone metabolism under physiological as well as pathological conditions.

RANKL (also known as TRANCE, OPGL or OCF) belongs to the TNF superfamily and is preferentially expressed by osteoblast progenitor cells [18], osteoblasts, osteocytes, bone marrow stromal cells and activated T-cells [25]. In bone, RANKL functions as the key mediator of osteoclastogenesis and thus bone resorption. The interaction of RANKL with its cognate receptor RANK, expressed on osteoclasts and their precursor cells enhances osteoclast formation, activation, adherence and survival [26]. Three isoforms of RANKL have been described. Two of them (RANKL1 and 2) correspond to transmembrane forms of RANKL, yet RANKL2 has a shorter intracellular domain [27]. RANKL3 represents a soluble molecule that arises either from alternative mRNA splicing or proteolytic cleavage of its membrane form and appears less efficient in mediating osteoclast differentiation [25, 27].

OPG (also known as osteoclastogenesis inhibitory factor, OCIF) was the first protein of the triad to be discovered and belongs to the TNF receptor superfamily. It is secreted by osteoblast lineage cells in response to bone anabolic agents such as 17β-estradiol, TGF-β as well as BMP-2 [27, 28] and has been shown to inhibit the generation and activity of bone-resorbing osteoclasts *in vitro* and *in vivo* by acting as a decoy receptor for RANKL [29]. It binds RANKL in a 1:1 ratio, preventing a possible RANKL-RANK interaction on osteoclast precursor cells [30]. Multiple studies have demonstrated that parental application of OPG results in osteopetrosis while a lack of this cytokine leads to osteoporosis [31]. OPG thus functions as a physiological negative regulator of bone resorption and can be interpreted as a bone protecting factor.

The third protagonist of the triad is RANK, the cognate receptor of RANKL, which was originally cloned from dendritic cells. As a TNF receptor superfamily member, RANK lacks intrinsic enzymatic kinase activity and must therefore recruit cytoplasmatic adaptor proteins to activate downstream signals [25]. Binding of RANKL to RANK stimulates multiple intracellular signaling pathways including the NFκB-, PI3K/Akt-, c-jun N-terminal kinase- (JNK), p38 MAPK- and ERK1/2-cascade [32]. The adaptor molecule TRAF6 plays a pivotal role in the activation of most of these pathways, resulting in the subsequent stimulation of crucial transcription factors including NFκB, AP1, $NFAT_C1$ and MITF that regulate osteoclast formation, activity and survival [32]. The transcription factor $NFAT_C1$, in particular, represents a master regulator of osteoclast differentiation and promotes the expression of osteoclast-specific genes including TRAP, calcitonin receptors and cathepsin K [33].

It is crucial to understand that the RANKL/RANK/OPG system functions as the final converting effector of most osteotropic molecules [34]. In general, osteoblasts receive input from a variety of factors such as hormones, growth factors, prostaglandins as well as cytokines and translate these signals to adjacent osteoclasts via the OPG/RANKL/RANK system [35]. OPG and RANKL are both produced by osteoblast lineage cells and have emerged as the two principal cytokines that regulate osteoclast differentiation and activation. In fact, the degree of local bone destruction in malignant and non-malignant bone pathologies depends on the balance of these two cytokines. Thus, the RANKL:OPG ratio correlates positively with bone degradation and negatively with bone formation, implying that an elevated ratio shifts the balance towards increased osteoclast-mediated bone resorption [31]. In patients with elevated bone erosion, such as bone metastases or postmenopausal osteoporosis, the RANKL:OPG ratio is significantly increased and reflects the severity of osteolytic activity [18, 26].

1.2 Cancer and Metastatic Cancer

1.2.1 Cancer

Cancer represents an acquired genetic disease of human body cells that evolves progressively during a multistep process. Gain of function mutations in proto-oncogenes and loss of function mutations in tumor suppressor genes result in aberrant activation of intracellular signaling pathways, allowing cancer cells to escape physiological control mechanisms. It has been postulated that a typical cancer cell demonstrates a dysregulation of nearly 13 intracellular signaling pathways [36].

Tumors are more than masses of proliferating cancer cells. They represent complex organs with recruited normal cells that support tumor growth by forming a “tumor microenvironment” [37]. Malignant cancer can be defined as a manifestation of eight essential alterations in cell physiology including the following hallmarks: tumors maintain proliferative signaling, show resistance to growth inhibitors, evade apoptosis, possess limitless replicative potential, sustain angiogenesis, activate tissue invasion as well as metastasis, reprogram energy metabolism and avoid immune destruction [37]. These acquired hallmark capabilities collectively allow cancer cells to survive, proliferate, and disseminate to distant organs.

1.2.2 Metastatic Cancer

Most primary cancers generate, sooner or later, pioneer cells that abandon their original environment and establish new colonies in distant organs [38]. Tumor spreading occurs through the bloodstream, the lymphatic vessels or both. Metastasis and tissue invasion are a fundamental trait of malignancy and are usually associated with poor prognosis, causing 90 % of human cancer deaths [38]. Certain primary tumors display a tropism to metastasize to specific organs. The distribution of metastases varies according to the origin and type of each cancer, yet, frequent sites among cancer cells include liver, adrenals, brain and bone. Advanced stages of prostate and breast cancer, for instance, show a marked preference for the skeleton [39-41].

1.3 Prostate Cancer and Its Metastasis

1.3.1 Prostate Cancer

Prostate cancer is the most frequently diagnosed malignant tumor in males in the Western world [42], affecting approximately 1 in 7 men at some point during their lifetime [43]. In the United States, prostate cancer is diagnosed on average every 3 minutes and death occurs from it every 15 minutes [44].

The growth and survival of prostate cancer cells depend on the presence of androgens and medical castration by androgen ablation therapy induces regression [45]. While the initial response rate is excellent, many tumors eventually evolve to castrate-resistant prostate cancer (CRPCa), which represents an incurable phenotype that progresses and metastasizes [45, 46]. Major epidemiological risk factors for the development of prostate cancer include a family history, advanced age and African American race [43].

1.3.2 Prostate Cancer Metastasis

Prostate cancer can metastasize to local lymph nodes or distant organs such as liver, lungs and brain, however, advanced prostate cancer has a remarkably high propensity to metastasize to bone [47]. In fact, 8 out of 10 patients who died because of prostate cancer showed skeletal metastases [47] which are usually located in the lumbar vertebral bodies, the pelvis and the rib cage [48]. The 5-year survival rate for localized prostate cancer is nearly 100 %, however, when prostate cancer has metastasized to distant organs, this rate drops to 28 % [43]. After diagnosis of bone metastasis, the median survival is approximately 2 – 4 years [48, 49]. In addition to bone metastatic tumor burden, age-related and cancer therapy-induced bone loss, caused by sex steroid deficiency, aggravate the skeletal health in these patients.

1.4 Pathophysiology of Bone Metastasis

1.4.1 Consequences of Bone Metastasis

Skeletal metastasis is a frequent and serious complication of malignant cancer. Once it has metastasized to bone, cancer disease is incurable. Thus, most cancer patients do not die due to the primary tumor but because cancer cells have spread to distant anatomic sites [39]. Bone metastasis affects over 400,000 patients in the United States each year [50] and remains a devastating diagnosis with a poor prognosis: While the median survival of bone metastatic breast and prostate cancer can be measured in years, the remaining life time of bone metastasis from advanced lung cancer is a matter of months [51]. Metastasis to bone causes significant morbidity as well as mortality and implies severe complications such as bone cancer pain, impaired mobility, pathological bone fractures, spinal cord or nerve root compression, hypercalcaemia of malignancy and bone marrow suppression with subsequent leukopenia, thrombopenia and anemia [39, 51, 52].

1.4.2 Classification of Bone Metastasis

Skeletal metastases have typically been classified by their radiographic appearance as either osteolytic or osteoblastic [52]. However, this classification only represents two ends of a continuum in which bone remodeling is strongly dysregulated. In reality, the great majority of bone metastases are heterogeneous and exhibit a mixture of both phenotypes with a predominance of an either osteolytic or osteoblastic response [39]. An explanation for the fact that both phenotypes appear within the same metastatic lesion provides the coupling process, stating that bone resorption follows bone formation and vice versa [53].

Predominantly lytic bone metastases are the most common phenotype and cause bone destruction because osteoclast-mediated bone resorption exceeds bone formation, resulting in a negative balance of bone turnover [54]. Osteolytic metastasis typically

occurs in melanoma [41], breast, lung, kidney as well as thyroid tumors [41, 52] and is recognized on radiographic imaging as a dark hole within the cortex [55]. Purely osteolytic lesions only develop in multiple myeloma patients and show no sign of bone-forming activity [56].

Conversely, predominantly osteoblastic lesions exhibit increased formation of new woven bone that overweighs bone resorption. Osteoblastic lesions arise in the majority of advanced prostate cancers and approximately 15 % of breast cancer patients [52] and appear radiographically as more dense, thus whiter, bone which is often described as osteosclerotic in appearance [55]. Although bone formation is elevated in this type of skeletal metastasis, the random and disorganized arrangement of collagen fibrils results in a weakened microarchitecture, so that pathological bone fractures easily occur.

Since most bone metastases display a stimulation of both bone formation and breakdown, it is not surprising that there is an augmentation of osteoclastic activity even in predominantly osteoblastic lesions. Histological examinations of osteoblastic metastases due to carcinoma of the prostate confirmed a general increase of bone catabolism in specimens [57, 58]. Moreover, high levels of urine and serum bone resorption markers were found regardless of the radiographic classification as predominantly osteolytic or osteoblastic, suggesting that osteoclast activity is markedly increased in all types of bone metastases [26]. The central role of bone-resorbing osteoclasts in all osseous lesions is the rationale for the use of anti-resorptive agents such as bisphosphonates or denosumab which currently represent the gold standard for the treatment of these patients.

1.4.3 The Vicious Cycle of Bone Metastasis

When tumor cells enter the bone microenvironment, they initiate a profound dysregulation of bone homeostasis known as “the vicious cycle” of bone metastasis. The vicious cycle offers a mechanistic explanation for the close relationship between bone breakdown and cancer expansion: The idea is that cancer cells interact with cells

of the bone microenvironment to establish a positive feedback loop that supports tumor growth and bone destruction, leading to skeletal morbidity [56]. From a simplistic view, this vicious cycle of bone metastasis is the result of a cooperation of at least three major protagonists including the following cells: first the metastasizing cancer cell, second, the bone residing osteoblast and/or stromal cell and third, the bone-resorbing osteoclast.

Once within bone, cancer cells produce osteolytic factors to indirectly enhance osteoclast formation. These tumor-derived molecules act on osteoblasts and/or stromal cells to induce RANKL expression and/or decrease OPG production. The net effect is a potent increase of the RANKL:OPG ratio that strongly favors osteoclast differentiation and activation. Subsequent bone resorption by osteoclasts releases stored growth factors as well as ionized calcium from the bone matrix which, in turn, stimulates tumor cell proliferation [56]. This reciprocal interaction of cancer cells and the bone microenvironment results in a vicious cycle that promotes both bone degradation and tumor burden (Fig. 1.1) [56].

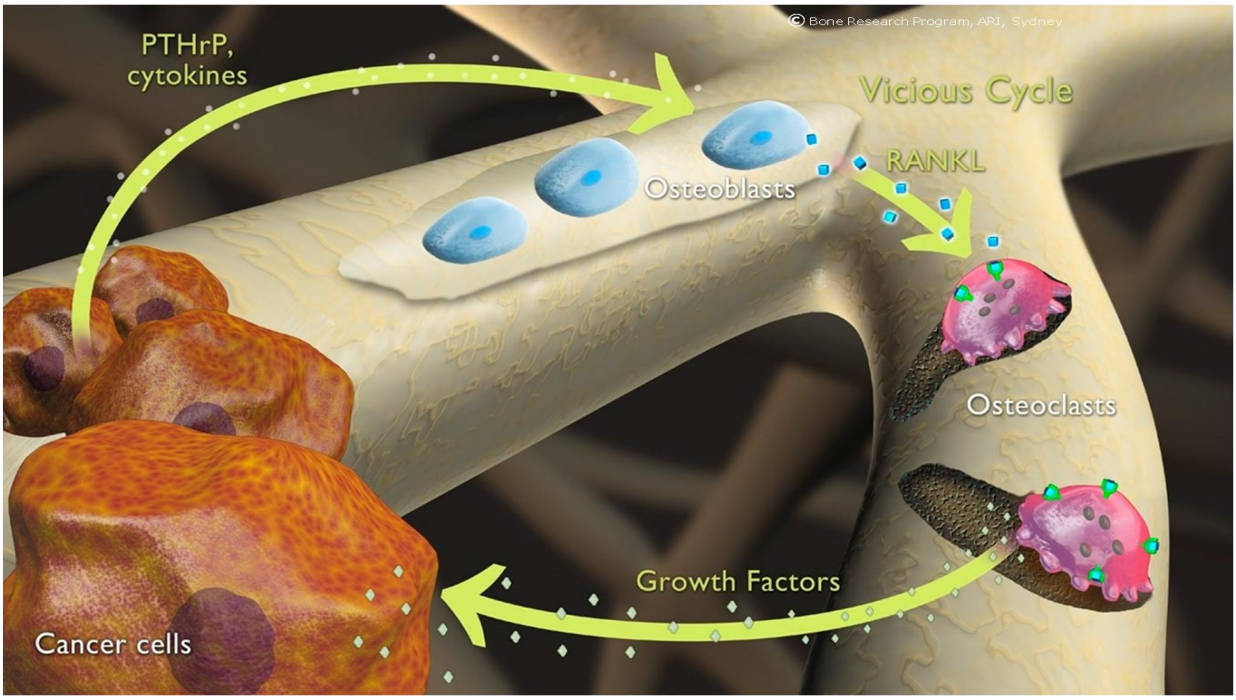

Fig. 1.1: The Vicious Cycle of Bone Metastasis.
Once within bone, metastatic cancer cells secrete osteoclast-activating factors such as parathyroid hormone-related protein (PTHrP) and cytokines which impact on the receptor activator of nuclear factor kappa B ligand (RANKL)/osteoprotegerin (OPG)

ratio, favoring RANKL synthesis while reducing the expression of OPG. Osteoblast-derived RANKL binds to receptor activator of nuclear factor kappa B (RANK) receptors on osteoclast precursor cells, stimulating osteoclastogenesis and thus osteoclast-mediated bone resorption, which in turn releases stored growth factors that fuel cancer growth in bone. Figure adapted from [59].

One of the most important factors to be secreted by cancer cells is PTHrP. This molecule is related to PTH, allowing it to bind and activate the same receptor (PTHR1) as its cousin [60]. In breast cancer bone metastasis, the prototype of osteolytic tumors, PTHrP functions as a primary stimulator of osteoclastogenesis through upregulation of RANKL and downregulation of OPG, leading to excessive osteolysis accompanied by hypercalcaemia of malignancy [18, 39, 61]. Other secreted factors by cancer cells have been shown to enhance osteoclast formation as well, including the following: IL-1, IL-6, IL-11 [39], TNF-alpha and PGE2 [61].

Bone tissue represents a storehouse of inactive growth factors which are released and activated during the process of bone degradation. Bone resorption releases molecules such as transforming growth factor beta (TGF-beta), insulin-like growth factors (IGFs), fibroblast growth factors (FGFs), platelet-derived growth factor (PDGF) and bone morphogenic proteins (BMPs) which can, in turn, promote the synthesis of PTHrP and proliferation of cancer cells [56]. These growth factors provide a fertile soil in which the tumor seed can easily expand. This “seed and soil” theory was first proposed by the English doctor Stephen Paget in 1889, hypothesizing that the “tumor seed” leaves the primary tumor location to grow within the “bone soil” [54]. This analogy of Paget can also be assigned to osteoblastic metastases, which share a similar pathophysiology with osteolytic lesions [52]. In osteoblastic lesions, cancer cells produce molecules that foster osteoblastic activity, which in turn produce unmineralized bone matrix, enriched with growth factors that drive tumor growth [52]. Important osteoblast-activating factors secreted by prostate cancer cells include endothelin-1 (ET1), PDGF and BMPs [62]. The secretion of new woven bone may help to confine cancer growth in bone, which explains why osteoblastic prostate cancer bone metastases grow more slowly as opposed to osteolytic lesions from other cancers [62]. Yet, as mentioned earlier, an increase in osteoclast activity and bone resorption also occurs in osteoblastic

metastases, justifying the use of bone resorption inhibitors such as bisphosphonates in this type of lesion.

1.5 Interleukin-6

1.5.1 Interleukin-6: Structure and Function

Interleukin-6 (IL-6) is a 184 amino acid-long protein [63] that belongs to the IL-6 family of cytokines. IL-6 represents a highly multifunctional molecule that has been implicated in the regulation of multiple biological systems such as acute phase reactions, immune regulation, hematopoiesis and many others [64]. Its dysregulation affects numerous diseases including many types of cancer, chronic inflammation, auto-immunity, osteoporosis and Alzheimer's disease [65]. As a member of the triumvirate of cytokines that drive the acute inflammatory reaction, IL-6 expression increases in response to a variety of pro-inflammatory factors including TNF-alpha, IL-1 (both complete the triad of cytokines), bacterial products, viral infections and necrotic cells [66]. Factors that repress IL-6 promoter activity involve steroidal hormones such as dihydrotestosterone (DHT), glucocorticoids and estradiol [67]. Many cell types are able to secrete IL-6, including B- and T-cells, monocytes, fibroblasts, endothelial cells as well as several tumor cells [64]. Note that human IL-6 binds to murine IL-6 receptors [67], whereas murine IL-6 does not activate human IL-6 receptors [68].

1.5.2 Interleukin-6 Receptor: Structure and Function

The IL-6 receptor belongs to the class 1 cytokine receptor family and consists of two different subunits: one that binds IL-6 with high affinity and one that initiates the intracellular signal [65]. The ligand-binding part of the IL-6 receptor exists in a soluble (sIL-6R) and membrane-bound (mIL-6R) form and associates directly with the cytokine [65]. This IL-6/IL-6R complex interacts with the membrane glycoprotein 130 (gp130) which functions as the crucial subunit for signal transduction by recruiting and activating

protein tyrosine kinases [65, 69]. All members of the IL-6 family of cytokines share the gp130 molecule as a signal transmitting component, which explains the functional redundancy of cytokines in this family [65].

The membrane-bound form of the IL-6R is only present on a limited amount of cells including osteoclasts [70], macrophages/monocytes, neutrophils, hepatocytes and some lymphocytes, while gp130 is synthesized by most if not all cells in the body [71]. Cells that do not express the IL-6R on their surface cannot respond to this cytokine, as gp130 alone is unable to bind to IL-6. However, circulating complexes of IL-6 and its naturally occurring soluble receptor (sIL-6R), which has been found in various body fluids such as urine and blood, can bind to gp130, conferring IL-6 responsiveness to cells that do not express the IL-6R on their membrane [63, 65]. The signaling process of the soluble IL-6R is termed trans-signaling and is thought to have agonistic biological activity, however, it has recently been reported that both signaling pathways might differ in that IL-6 trans-signaling is rather pro-inflammatory, while IL-6 classic signaling represents an anti-inflammatory/regenerative response [63]. Since most mIL-6R-expressing cells synthesize far more gp130 molecules than mIL-6R, they can respond to IL-6 in two ways, either via the IL-6/mIL-6R (IL-6 classic signaling) or through the IL-6/sIL-6R complex (IL-6 trans-signaling), whereas cells that simply produce gp130 can only be activated by the IL-6/sIL-6R complex [63]. IL-6 trans-signaling is blocked by the soluble glycoprotein 130 (sgp130) which functions as the naturally occurring antagonist of the IL-6/sIL-6R complex and the balance of the two soluble receptors (sIL-6R and sgp130) regulates IL-6 trans-signaling [72]. Interestingly, human osteoblasts have been shown to synthesize a non-functional form of the membrane-bound IL-6R, therefore IL-6 trans-signaling appears to be responsible for the effects of the cytokine on bone cells [72].

Binding of IL-6 to its receptors activates three distinct signaling pathways: the JAK/STAT-, the Ras/MAPK-, and the PI3K/PKB (Akt)-pathway, which account for its multifunctional effects in different cell lines [42, 73]. STAT3 represents the main transcription factor through which IL-6 signals, regulating genes that stimulate cell proliferation, block apoptosis and mediate angiogenesis [66]. As proof of principle, most effects of IL-6 can be abolished by disrupting the STAT3 pathway [66].

1.5.3 Interleukin-6 and Prostate Cancer Progression

More than 40 years ago, Charles Huggins showed that prostate cancer growth and survival initially depend on the presence of androgens [45]. Androgen blockage represents the mainstay of therapy, however, this medication fails to produce the desired effect in many men because prostate cancer eventually progresses to an androgen-independent and more aggressive phenotype [45]. The fact that androgen-independent prostate cancer cell lines secrete large amounts of IL-6 as opposed to androgen-dependent cells has led to a great effort in cancer research to determine whether this cytokine plays a fundamental or a bystander role.

Essential hints of an existing relationship between prostate cancer progression and IL-6 came from clinical studies which were mostly conducted in the late 1990s. In patients with neoplasia of the prostate, augmented circulating levels of IL-6 were associated with advanced stage [74-78], distant bone metastases [74, 75, 77], metastasis-related morbidity [69, 77] and unfavorable clinical outcome [69, 79]. In addition to these clinical trials, *in vitro* and *in vivo* research experiments demonstrated that IL-6-producing prostate cancer cell lines grow at a faster rate compared to their non-secreting counterparts, which leads to the conclusion that IL-6 acts as an autocrine growth factor [80-83]. Likewise, a consistent growth-stimulating effect of IL-6 has been reported in other malignancies such as renal cell carcinoma and multiple myeloma [81]. However, tumor growth not only depends on the rate of cell proliferation but also on the rate of cell death. IL-6 has been shown to protect cancer cells from undergoing programmed cell death by upregulating anti-apoptotic members of the Bcl-2 family such as Mcl-1 and Bcl-xL [84, 85]. Clinically important could be the finding that this cytokine confers resistance to cytotoxic agent-induced apoptosis in prostate cancer [85-88], breast cancer [89], multiple myeloma [90] and neuroblastoma cells [91].

As cancer cells progress through a multistep process to higher pathological grades of malignancy, they (often) develop a migratory and invasive phenotype. Several studies suggest that IL-6 promotes tissue invasion and migration of benign prostate epithelium, ovarian carcinoma [92] and human breast cancer cells [93, 94]. Interestingly, increased

motility and cell-cell separation in response to IL-6 have been postulated in ductal breast carcinoma cells as early as in the late 1980s [95, 96].

Activation of bone resorption and the consequent stimulation of the vicious cycle is a major strategy for cancer cells to survive and grow in bone metastatic lesions. A large body of evidence identifies IL-6 as a bone-resorbing cytokine and IL-6 appears to be involved in the promotion of bone breakdown in many pathological conditions including bone metastases [70], postmenopausal osteoporosis [97, 98], rheumatoid arthritis [99] and Paget's disease [100].
In patients with bone metastases, serum levels of IL-6 and sIL-6R are elevated and associated with poor clinical outcome [70]. In postmenopausal osteoporosis, the prototype of pathological bone loss, high IL-6 serum levels are strongly predictive for femoral bone breakdown and sIL-6R levels correlate negatively with bone mineral density of the lumbar spine [72]. Accordingly, IL-6 knock-out mice are protected from bone loss following estrogen deficiency caused by ovariectomy [98]. The mechanism involved is that IL-6 increases the pool of osteoclasts indirectly by stimulating RANKL production in osteoblasts and stromal cells [39]. As human osteoblasts express a non-functional form of the membrane-bound IL-6R, IL-6-induced osteoclastogenesis depends on trans-signaling mediated through the IL-6/sIL-6R complex [70, 72, 101, 102]. Other investigators have proposed that IL-6 stimulates osteoclast differentiation and thus bone resorption by elevating RANK expression on osteoclast precursors and decreasing basal OPG secretion from osteoblasts [35], however, conflicting results have been reported [101]. Interestingly, stimulation of bone resorption through RANKL-independent mechanisms via IL-6 has been postulated as well [103, 104].
In autoimmune arthritis, IL-6 together with TGF-beta has also been shown to support the development of naïve T-cells into osteoclastogenic Th17 cells which express RANKL on themselves and induce RANKL synthesis on osteoblasts/synovial fibroblasts via the secretion of IL-17 [33, 105].

Taken together, there is little doubt that IL-6 acts as an osteolytic factor but the question how IL-6 affects bone resorption remains to be completely elucidated. The majority of the current evidence suggests that IL-6 enhances bone breakdown by signaling through the OPG/RANKL/RANK system, in particular, by increasing RANKL expression in

osteoblasts. This cytokine can thus be considered as a molecule that potentially promotes tumor growth in bone by supporting the vicious cycle of bone metastasis.

1.6 Anti-Cancer Therapy

1.6.1 Zoledronic Acid

Zoledronic acid (ZA) is a third-generation bisphosphonate that has been approved for the treatment of diseases with high bone catabolism including bone metastases of malignancy, osteoporosis and Paget's disease [106]. Bisphosphonates represent analogs of pyrophosphate that accumulate in the mineralized bone matrix by binding with high affinity to hydroxyapatite crystals. They are released from bone surfaces at sites of active bone resorption and subsequently absorbed by osteoclasts [107]. Zoledronic acid represents a nitrogen-containing bisphosphonate that prevents prenylation of intracellular proteins by inhibiting a key enzyme in the mevalonate pathway called farnesyl pyrophosphate synthase (FPP synthase) [107]. Disruption of this enzyme has a profound effect on physiological cell metabolism, causing inhibition of osteoclast-mediated bone degradation [107, 108] as well as osteoclastic cell death [107].

Several animal studies of bone metastasis have shown significant efficacy of bisphosphonates including zoledronic acid in reducing the size of osteolytic lesions and osseous tumor burden [108-111]. Clinical trials have confirmed the bone protective effect of zoledronic acid by demonstrating a diminishment of skeletal-related events (SRE) in prostate and breast cancer patients with bone metastases [112, 113]. In bone lesions due to prostate cancer, zoledronic acid represents in fact the only bisphosphonate that has revealed statistically significant reductions in skeletal morbidity [49]. A possible explanation for these observations is the fact that zoledronic acid is a powerful inhibitor of bone breakdown and thus of the vicious cycle of bone metastasis, a mechanism which would reflect an indirect anti-tumor effect [49]. Alternatively, it has been suggested that zoledronic acid exerts direct anti-tumor actions *in vitro* and *in vivo*

by mechanisms similar to that observed in osteoclasts [109, 114]. However, an animal study conducted in our own laboratory indicates that nitrogen-containing bisphosphonates (exemplified by ibandronate) mediate their anti-tumor effects primarily indirectly through inhibition of bone resorption than direct cytotoxicity [108].

1.6.2 Tocilizumab

Tocilizumab is a humanized anti-human IL-6 receptor monoclonal antibody that prevents the binding of IL-6 to its receptors [115]. Tocilizumab binds selectively, competitively and with high affinity to the membrane-bound and soluble IL-6 receptor [115], thus inhibiting both IL-6 classic signaling and IL-6 trans-signaling [63].
So far, tocilizumab has been approved for the treatment of disorders such as moderate to severe rheumatoid arthritis, juvenile idiopathic arthritis and Castleman's disease [115]. Pilot studies have recently shown efficacy of the IL-6 receptor antagonist in autoimmune and inflammatory conditions, including Crohn's disease [116] and systemic lupus erythematosus [117]. Tocilizumab may also be of clinical benefit in neoplasias such as oral squamous cell carcinoma [118].

1.7 Hypothesis and Aims

Based upon the above discussion, the cytokine IL-6 promotes tumor growth in bone in an indirect manner, namely by stimulating the vicious cycle of bone metastasis. This model of the "classical" vicious cycle of bone metastasis has been very useful in elucidating the mechanisms that facilitate and maintain established cancer lesions in bone. However, owing to its monodirectionality and its dependence on three distinct cell types to become and remain activated (tumor cells -> osteoblasts -> osteoclasts), this model may be less suited to explaining cancer growth at early stages of the metastatic process, or when bone metastases expand rapidly as observed clinically during late stages of the disease. We thus believe that the growth kinetics of bone lesions include additional pathways within the classical vicious cycle that support and accelerate tumor growth and expansion in the bone environment.

In our studies, we utilized an osteolytic prostate cancer cell line, termed PC3, that secretes high quantities of IL-6 [80, 85] and expresses the membrane-bound (mIL-6R) as well as the soluble IL-6 receptor (sIL-6R) [80]. In bone, as mentioned above, it is well established that this cytokine activates RANKL synthesis in osteoblast lineage cells. As PC3 cells also express RANK [119], the cognate receptor for RANKL, it would be rational to assume, but it is unclear whether osteoblasts directly signal back to prostate cancer cells via RANKL-RANK interaction and if so, whether direct contact between these two cell lines contributes to tumor growth *in vivo*. Therefore, we hypothesize that autocrine IL-6 signaling in PC3 cells stimulates cancer growth in bone by enhancing tumor cell RANK expression, sensitizing tumor cells for direct communication between osteoblast lineage and cancer cells. As treatment of PC3 cells with RANKL enhances IL-6 production *in vitro* [119], direct RANKL-RANK communication could enforce IL-6 output levels by PC3 cells and activate the vicious cycle via establishing an additional pathway. We believe that this cytokine could play a central role in the initiation and progression of prostate cancer bone metastasis and may function as a therapeutic target in aggressive and/or androgen-independent prostate cancer.

The major **hypotheses** of this project are:

a) The bone microenvironment provides a fertile soil that is conducive to the growth of the prostate cancer cell line PC3.
b) Blocking autocrine IL-6 receptor signaling in the osteolytic prostate cancer cell line PC3 will reduce tumor growth in bone but not in the subcutis.

The **aim** of this study is to determine *how* tumor-derived IL-6 affects human prostate cancer growth in bone. This will be accomplished by:

a) Characterizing at the cellular level proliferation, apoptosis and gene expression in the bone metastatic prostate cancer cell line PC3 *in vitro* and *in vivo.*
b) Evaluating the comparative effects of tocilizumab and zoledronic acid on inhibition of tumor growth and bone resorption.
c) Evaluating the comparative effects of autocrine IL-6 receptor inhibition in an osseous and subcutaneous environment.

1.8 Rationale to Use Tocilizumab and/or Zoledronic Acid in an Animal Model of Bone Cancer Metastasis

In the present xenograft mouse model, the humanized anti-IL-6 receptor antibody tocilizumab (Tmab) and the bisphosphonate zoledronic acid (ZA), alone or in combination, were administered.

Zoledronic acid was chosen because it inhibits the vicious cycle of bone metastasis by suppressing osteoclast-mediated bone resorption, disrupting the supply of bone-derived growth factors to neoplastic cells (Fig. 1.2). By blocking cancer-induced osteolysis, zoledronic acid exerts indirect anti-tumor effects. The mode of action of tocilizumab is different. Tocilizumab inhibits autocrine IL-6 signaling in neoplastic cells by antagonizing the membrane-bound as well as the soluble IL-6 receptor. Note that tocilizumab specifically blocks the *human* IL-6 receptors and not the murine IL-6 receptors, which means that human neoplastic-derived IL-6 is able to bind to murine IL-6 receptors [67]. Since tocilizumab operates primarily on the tumor, the inhibition of the IL-6 signal cascade might lead to a potential direct anti-tumor effect (Fig. 1.2). This assumption is reasonable given the recent reports that IL-6 acts as an anti-apoptotic [84-86, 120] and pro-proliferative factor [80, 86, 121] *in vitro* on the osteolytic prostate cancer cell line PC3. If disruption of the autocrine IL-6 signal had direct anti-tumor effects independent of anti-resorptive action, then the combination of tocilizumab and zoledronic acid would reveal additive and/or synergistic effects.

However, as mentioned above, we hypothesize that antagonizing autocrine IL-6 receptor signaling in PC3 cells will desensitize cancer cells for beneficial RANKL-RANK communication with osteoblast lineage cells, resulting in less tumor-derived IL-6 production and therefore reduced activation of the vicious cycle. We thus believe that tocilizumab inhibits prostate cancer growth in bone *indirectly* and in a different manner than zoledronic acid.

As zoledronic acid and tocilizumab may inhibit tumor growth by different mechanisms, we sought to compare the effects of zoledronic acid and tocilizumab, alone or in combination, in mice bearing established prostate cancer bone metastasis to determine whether these treatments have comparable actions on neoplastic growth and to detect additive and/or synergistic effects. Both medications were administered at relatively high

doses to assure profound inhibition of osteoclastic bone resorption (zoledronic acid) as well as complete blockage of cancer IL-6 receptor signaling (tocilizumab), thus any differences would be due to other effects and not to varying effects of these drugs.

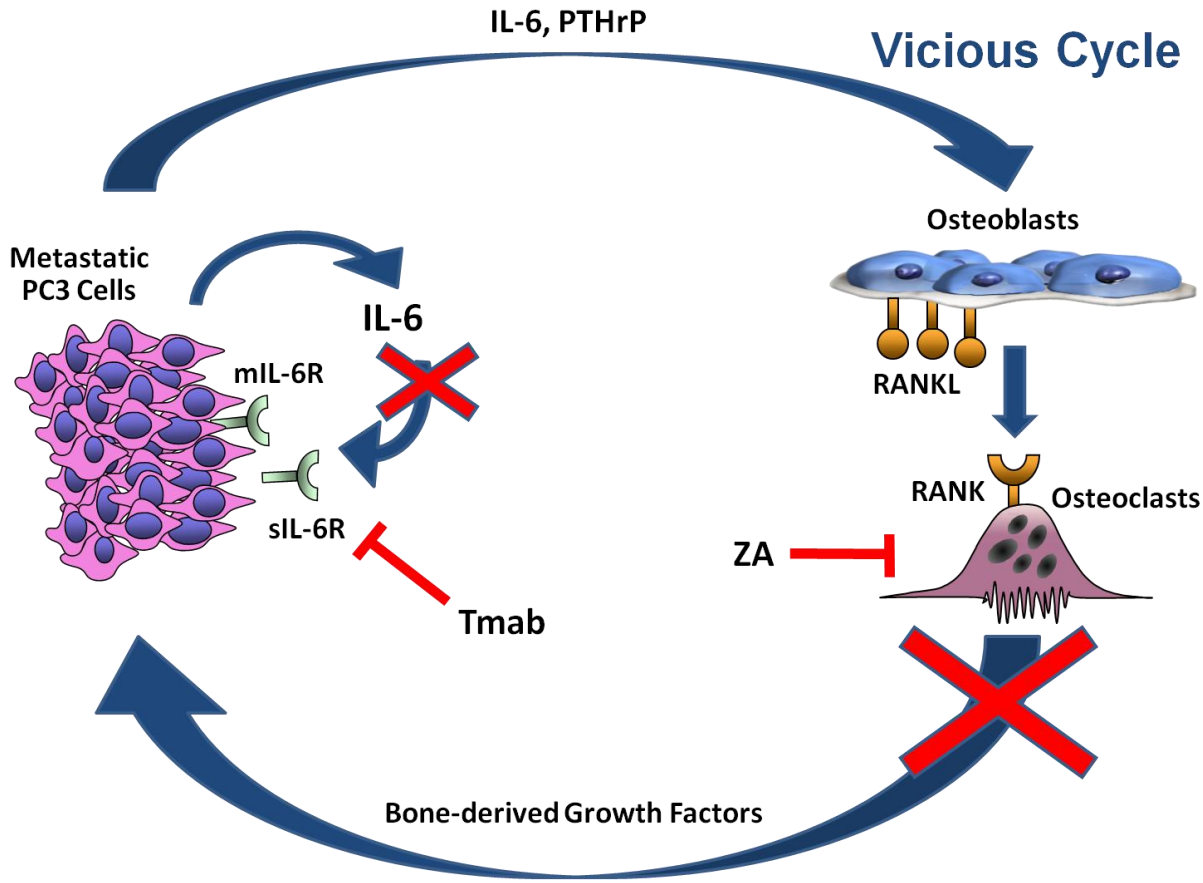

Fig. 1.2: Study Design.
PC3 cells secrete large amounts of interleukin-6 (IL-6) [80, 85] into their environment and they express the membrane-bound (mIL-6R) [80, 121] as well as the soluble IL-6 receptor (sIL-6R) [80]. *Paracrine* IL-6 signaling fuels metastatic tumor growth by stimulating the vicious cycle of bone metastasis because it induces receptor activator of nuclear factor kappa B ligand (RANKL) synthesis in osteoblasts. *Autocrine* IL-6 signaling either via the membrane-bound IL-6R (IL-6 classic signaling) or through the soluble IL-6R (IL-6 trans-signaling) in cancer cells might induce intracellular signal cascades that favor tumor expansion in bone. Tocilizumab (Tmab) specifically blocks

the *human* IL-6 receptors, antagonizing both IL-6 classic signaling and IL-6 trans-signaling, but tocilizumab does not block the murine IL-6 receptors. Zoledronic acid (ZA) inhibits osteoclast-mediated bone resorption, suppressing the activation of the “classical” vicious cycle. This figure emphasizes the possible different modes of action of the two medications.

Chapter 2
Materials and Methods

2.1 Prostate Cancer Cell Line

The androgen-independent bone metastatic prostate cancer cell line PC3 was obtained from the American Type Culture Collection (ATCC, Manassas, VA, USA).
The human prostate cancer cell line PC3 was established in 1979 and derives from lumbar bone metastasis of a 62-year-old Caucasian male [122].
All chemicals used in this study were purchased from Invitrogen (Carlsbad, CA, USA) unless stated otherwise.

2.2 Tissue Culture

2.2.1 Cancer Cell Line Propagation

PC3 cells were cultured in Roswell Park Memorial Institute medium (RPMI) supplemented with 10 % fetal calf serum (FCS, JRH Biosciences, KS) and 1 % penicillin/streptomycin solution. The cells were routinely subcultured when they reached approximately 80 % confluence.
Subculturing reagents including media, phosphate-buffered saline (PBS) and 0.05 % trypsin-EDTA were pre-warmed in a 37 °C water bath for about 10-15 minutes before use. The PC3 cell layer was viewed under an inverted microscope to determine confluence and contamination. The medium was removed aseptically with a Pasteur pipette attached to a vacuum pump aspirator. The cell layer was rinsed with PBS using a gently rocking motion before washing with 1 ml of 0.05 % trypsin-EDTA. This very trypsin was aspirated shortly after and 2 ml (75 cm^2 flask) or 4 ml (175 cm^2 flask) of trypsin-EDTA was added to the flask and then incubated at 37 °C for about 2 minutes. The detachment of cells from the bottom of the flask was observed through a microscope and the enzymatic reaction was neutralized by adding either 6 ml

(75 cm² flask) or 8 ml (175 cm² flask) fresh medium including 10 % FCS. The cell suspension was pipetted up and down and transmitted to a Falcon tube where the cells were carefully filtered with a syringe containing a 21-gauge needle to receive single cell suspension. An appropriate aliquot was chosen for cancer cell propagation in new flasks, attaining 80 % confluence in approximately 5 days. All new flasks were labelled and then incubated at 37 °C, 100 % humidity and 5 % CO_2.

2.2.2 *In Vitro* Incubation of PC3 Cells With Interleukin-6 and/or Tocilizumab

To investigate whether human interleukin-6 (IL-6) induces RANK and PTHrP mRNA expression in the prostate cancer cell line PC3, cells were seeded in a 6-well plate at a density of 1 x 10^5 cells per well (3,8 cm^2) in 2 ml supplemented RPMI (10 % fetal calf serum and 1 % penicillin/streptomycin) and allowed to adhere overnight. The next day, the wells were incubated for 4 hours with supplemented RPMI only (0.1 % BSA and 1 % penicillin/streptomycin) or supplemented RPMI, containing tocilizumab in a concentration of 200 µg/ml. Fetal calf serum was removed to avoid confounding effects due to growth factors present in the culture medium. After 4 hours of pretreatment, the medium was removed again and the wells were incubated with supplemented RPMI or supplemented RPMI, containing two different concentrations of human recombinant IL-6 (100 ng/ml and 200 ng/ml). The result is that one well represents the control group, two wells are treated with two different concentrations of human IL-6, two wells with IL-6 and tocilizumab and one well with tocilizumab only. After 24 hours, RNA was harvested and RANK or PTHrP synthesis levels were measured by real-time quantitative reverse transcription PCR. The experiments were independently repeated at least three times.

2.2.3 Cancer Cell Preparation For *In Vivo* Injection

The preparation of PC3 prostate cancer cells for inoculation into nude mice was performed as described in [123]. A modified technique was employed when necessary.

The osteolytic prostate cancer cell line PC3 was revived from frozen stocks and then passaged 1 – 2 times before preparing for implantation into mice. As trypsin contains proteases which may harm tumor cells by interfering with cell surface receptors, the non-enzymatic cell dissociation reagent Versene was chosen rather than trypsin to detach cells for *in vivo* injection.

Versene was warmed to room temperature, while media and PBS were pre-warmed as described above. The medium in the flask was aspirated and the cells were rinsed with PBS. Following a brief wash with Versene, 2 ml (75 cm^2 flask) or 4 ml (175 cm^2 flask) of Versene was transmitted again into the flask to cover the cell monolayer. The cell suspension was incubated at 37 °C for 30 minutes while monitoring cell separation and then passaged into a 50 ml Falcon tube. After washing the cells by two centrifugation steps at 250 g for 5 minutes in 10 ml PBS, an aliquot was extracted to determine cancer cell viability by trypan blue.

The trypan blue exclusion method is a routine tissue culture test to assess the amount of living cells present in a cell suspension. This method allows visual differentiation of viable and dead cells based on the fact that viable cells with intact cell membranes reject trypan blue, whereas dead cells with permeable membranes absorb it. Only suspensions with > 95 % of viable cells were selected for mouse inoculations in order to ensure maximum *in vivo* tumor growth. Following a last PBS washing and centrifugation step, PC3 cells were resuspended in 10 µl PBS at a concentration of 1 x 10^7 cells/ml for intra-tibial injection. For the subcutaneous mouse model, PC3 cells were suspended in a mixture of cold Matrigel and PBS (1:1) at a concentration of 2 x 10^7 cells/ml. Tumor cells were kept on ice until implantation.

2.3 Mouse Models of PC3 Cancer Growth

2.3.1 Mouse Maintenance

Male BALB/c nu/nu mice at five weeks of age (Animal Resources Centre, Canning Vale, WA, Australia) were selected for all animal experiments. Throughout this study, mice were accommodated under strict pathogen-free, temperature-, humidity- and noise-

controlled conditions at the animal facilities of the ANZAC Research Institute in accordance with Institutional Animal Welfare Guidelines and approved protocol 2009 – 012 by Sydney Local Health District Animal Welfare Committee, Sydney, Australia. All mouse procedures were conducted with reasonable care in a tissue culture hood under aseptic conditions while the application of freshly-made ketamine/xylazine (Sigma-Aldrich, St. Louis, MO, USA) (750 µl ketamine + 100 µl xylazine using sterile 0.9 % saline to dilute to 10 ml) via the intraperitoneal route maintained general anaesthesia. Food and water were always available, assuring a healthy nutritional state. Physical health of mice was closely monitored by inspecting daily for potential infection while body weight was checked twice a week. Mice were also observed for social stability as well as behavioral abnormalities. The animals were euthanized by anaesthetics and subsequent neck dislocation at the end-points of the experiments.

2.3.2 Intra-Tibial Tumor Cell Implantation

The intra-tibial xenograft murine model was chosen because this thesis aims to investigate the reciprocal interrelations between established neoplastic lesions and the bone microenvironment at a late stage of the bone metastatic process. The steps of tumor cell extravasation and growth of micrometastases are bypassed in this model as the cells are injected directly into the bone marrow cavity [124]. A disadvantage of this method includes the perforation of the bone cortex, causing an inflammatory reparative response that modifies the local bone microenvironment [124].
The injection of tumor cells into the tibiae of nude mice was performed as described in [123, 124]. A modified technique was employed when necessary.

To assure sterile working conditions, syringes (Hamilton Syringe Co., Reno, NV) were immersed in 100 % ethanol overnight and dried completely prior to use. Mice were anaesthetized via intraperitoneal (i.p.) injection of freshly made ketamine/xylazine. The analgesic carprofen (Rimadyl) (5 mg/kg) was administered subcutaneously so that mice do not suffer from any pain. The following technique was applied for the intra-tibial tumor cell inoculation: mice were placed in a supine position once they were narcotized

and the hind legs cleaned with 70 % ethanol. Shortly before injection, the concerned knee was gently flexed to access the proximal end of the tibia and the needle was then inserted into the tibial plateau, passing through the skin, the articular cartilage as well as the growth plate to reach the bone marrow cavity of the tibia. Once the needle was placed at this position, 1 x 10^5 PC3 cells suspended in 10 µl PBS (= 1 x 10^7 cells/ml) were injected into the right and left tibia, using a Hamilton glass syringe with 26 gauge needles. Inoculation speed was slow (20 – 30 seconds for 10 µl of suspension) in order to avoid leakage of cell suspension. All procedures were performed in a sterile biohazard hood and the needle was routinely changed between each injection. After tumor cell inoculation, mice were kept warm until they fully recuperated from anaesthesia.

2.3.3 Assessment of Intra-Tibial PC3 Tumor Growth

In the intra-tibial experiment, five-week-old male BALB/c nu/nu mice (n = 8) were randomly divided into four treatment groups: (1) control (PBS), (2) tocilizumab (50 mg/kg), (3) zoledronic acid (100 µg/kg) and (4) tocilizumab + zoledronic acid. Mice received treatments one day before tumor cell inoculation and then every 3 days. The dose of tocilizumab was selected based on prior intra-tibial mouse experiments conducted in our laboratory, while the dose of zoledronic acid was chosen based on a survey of the literature to assure profound suppression of bone breakdown despite the presence of osteolytic PC3 cells [125-127]. The development of osteolysis was verified by X-ray images 10 days after tumor cell implantation and the extent was then measured on day 17, 24 and 30. The experimental endpoint was reached on day 30 when mice were sacrificed for tissue harvest.

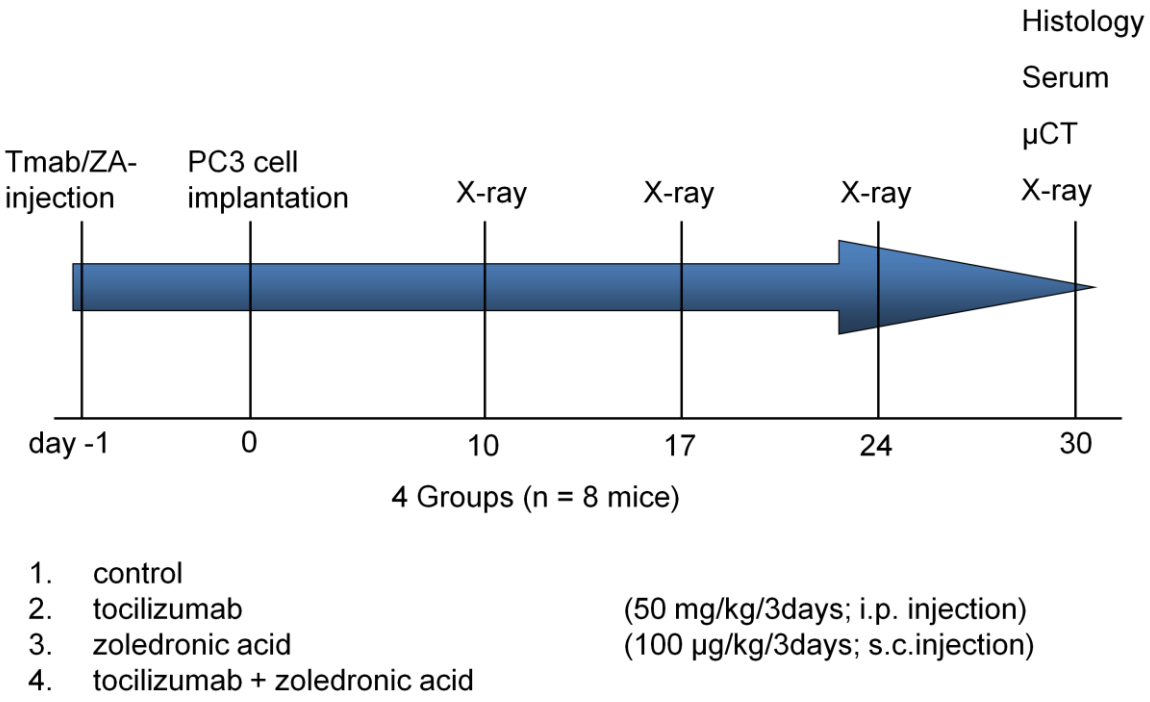

Fig. 2.1: Experimental Design of the PC3 Intra-Tibial Mouse Model.
The experimental design was implemented as described above. PC3 tumor cells were injected intra-tibially into five-week-old male BALB/c nu/nu mice. Treatments were given one day prior to tumor cell implantation and then every three days until endpoint. Tmab = tocilizumab; ZA = zoledronic acid; i.p. injection = intraperitoneal injection; s.c. injection = subcutaneous injection.

2.3.4 Subcutaneous Tumor Cell Implantation

The subcutaneous xenograft murine model was used to answer the question whether PC3 tumors respond to treatment without the presence of the bone microenvironment. Injection of cancer cells into the subcutis was performed according to [124].

In order to establish and enhance subcutaneous tumor growth, cancer cells need to be resuspended in Matrigel. Thus, PC3 neoplastic cells were prepared as mentioned above and suspended in a mixture of cold Matrigel and PBS (1:1) at a concentration of 2×10^7 cells/ml. Mice were anaesthetized and given analgesic as described above.

Once unconscious, the mice were placed in a lateral position and the area of interest was cleaned with 70 % ethanol. 100 µl of the tumor cell suspension and 100 µl of PBS for control purposes were then slowly injected within 30 seconds into the right and left flank of the hind legs, using a syringe equipped with a 25 gauge needle. To prevent leakage, slight pressure was applied to the skin lesion by using a band-aid. Mice rested in the same position until recovery and were monitored as described above.

2.3.5 Assessment of Subcutaneous PC3 Tumor Growth

In the subcutaneous murine model, five-week-old male BALB/c nu/nu mice (n = 10) were randomly divided into two treatment groups: (1) control (PBS) and (2) tocilizumab (50 mg/kg). Mice received treatments one day before tumor cell inoculation and then every 3 days until endpoint (day 58). To determine tumor progression, the length and width of the subcutaneous cancers were measured with a pair of callipers from day 7 onwards every 3 days. Tumor volumes were calculated with the help of the modified ellipsoidal formula [volume = (length x width^2)/2], in which the length was defined as the larger measurement [123]. Mice were euthanized by anaesthesia and neck dislocation when neoplasias reached 500 mm^3 in size (day 58). Following euthanasia, total tumor weight was determined.

2.4 Treatments

2.4.1 Zoledronic Acid

Zoledronic acid is a nitrogen-containing bisphosphonate that was purchased from Novartis (Novartis Pharmaceuticals Australia, North Ryde, NSW). In this thesis, zoledronic acid was administered subcutaneously at a dose of 100 µg/kg one day prior to tumor cell injection and then every 3 days until the experimental endpoint (30 days for the intra-tibial model). The dose was chosen based on a survey of the literature to assure profound suppression of bone breakdown despite the presence of osteolytic

PC3 cells [125-127]. Zoledronic acid was diluted (1:5) in PBS, stored in aliquots at -20 °C and thawed prior to use.

2.4.2 Tocilizumab

Tocilizumab is a humanized interleukin-6 receptor monoclonal antibody that was purchased by Roche Pharmaceutical Co., Ltd. In both *in vivo* experiments, tocilizumab was administered intraperitoneally at a dose of 50 mg/kg one day prior to tumor cell implantation and then every 3 days until the experimental endpoint (30 days for the intra-tibial model; 58 days for the subcutaneous model). Tocilizumab was also used for *in vitro* experiments at a dose of 200 µg/ml. The doses were selected based on prior *in vivo* and *in vitro* experiments conducted in our laboratory. Tocilizumab was diluted (1:4) in PBS, stored in aliquots at -20 °C and thawed prior to use.

2.4.3 Interleukin-6

Interleukin-6 (IL-6) is a pleiotropic cytokine that plays a major role in acute phase reactions, cancer progression and bone metabolism. Human recombinant IL-6 was purchased by R&D Systems (R&D Systems, Inc., Minneapolis, MN 55413, USA) and used for *in vitro* PC3 cell experiments at doses of 100 and 200 ng/ml. These doses were selected based on prior *in vitro* experiments with bone-seeking breast cancer cell lines in our laboratory.

2.5 Radiological Methods

2.5.1 Faxitron X-Rays

Faxitron X-ray was used to monitor the development of tumor-induced osteolytic lesions *in vivo*. At day 17, 24 and 30 post-inoculation, mice were anaesthetized as described

above and lytic lesions were made visible and assessed by digital radiography (MX-20 X-ray cabinet, Faxitron, Wheeling, IL, USA). Mice were exposed to X-ray doses of 26 kV for 10 seconds to examine the long bones (approximate 2 times magnification) [123].

2.5.2 Micro-Computerized Tomography

To attain a clearer understanding of the extent of bone lytic lesions, micro-computerized tomography (µCT) of the tibiae was performed by using a Skyscan 1172 scanner (SkyScan, Kontich, Belgium) after tissue harvest. This technique uses X-rays to create 3D images that visualize fine internal microstructures. Tibiae were scanned with 100 kV at 100 µA employing a 1 mm aluminium filter and a total of 1800 projections were collected at a resolution of 6.93 µm per pixel [123]. Reconstruction of sections was attained employing a modified Feldkamp cone-beam algorithm with beam hardening correction set to 50 % [123]. 3D images of tibiae were received by using VGStudio MAX 1.2 software (Volume Graphics GmbH, Heidelberg, Germany) [123].

2.6 Tissue Analysis

2.6.1 Radiological Measurement of Osteolytic Lesions

An interactive image analysis software (ImageJ, NIH, USA) was used to measure the area of osteolytic bone lesions on digitally recorded radiographs.
Dark sites on X-ray images corresponded to areas of PC3-induced osteolysis *in vivo*. The borders of these radiolucent zones within the tibiae were recognized and manually encircled. The area of lytic lesions was then calculated, presented as mm^2 at each time point and compared among experimental groups. Please consider that the 2-dimensional representation and calculation of osteolytic bone lesions in X-ray images may not illustrate the exact size of bone destruction *in vivo*.

2.6.2 Tissue Processing

For histological examination, tibiae of sacrificed mice were fixed for 36 hours in 4 % paraformaldehyde/0.1 M phosphate buffer (pH 7.4) and decalcified in 10 % EDTA at 4 °C for 2 weeks. Thereafter, the tibiae were embedded in paraffin. The paraffin blocks were put on ice for approximately 20 minutes before using the microtome (Leica Microsystems, Nussloch GmbH, 69226 Nussloch Germany; Model RM2125RT). Five-µm-thick sections were then cut from each specimen and stained with haematoxylin and eosin for histological analysis.

2.6.3 Histochemical Staining of Tartrate-Resistant Acid Phosphatase

Histochemical staining of tartrate-resistant acid phosphatase (TRAcP) as a biomarker for osteoclasts was conducted as described in [123].

In brief, mouse osteoclasts were stained for TRAcP by utilizing naphthol AS-MX phosphate (Sigma-Aldrich, Co., St. Louis, MO, USA) as a substrate and fast red violet Luria-Bertani salt (Sigma-Aldrich, Co., St. Louis, MO, USA) as a stain for the reaction product. Five-µm-thick sections were cut with the microtome, attached to coated slides and dried overnight. The slides were then put on a 60 °C hot plate for 10 minutes to remove the paraffin. After three rounds of 5 minute deparaffinization in xylene, the slides were rehydrated in a graded series of alcohols. The sections were briefly rinsed in distilled water and then incubated with 100 µl of TRAcP solution (50 mM tartrate, 0.01 % naphthol AS-MX phosphate, 0.06 % fast red violet Luria-Bertani salt in 0.1 M acetate buffer, pH 5.0) for 30 – 40 minutes at room temperature, while carefully observing for color appearance under a microscope. After washing the sections in distilled water, they were counterstained in Harris' hematoxylin for 30 seconds (Fronine, NSW, Australia, diluted 1 : 20 in distilled water), then washed in tap water and dried overnight. The next day, the sections were shortly immersed in xylene and finally fixed in a xylene-based mounting medium (Gurr, BDH, Poole, UK). Under the microscope, osteoclasts were recognized as big multinucleated purple colored cells, residing on the surfaces of cortical and trabecular bone.

2.6.4 TUNEL Staining

Apoptosis represents an orchestrated event in which cells are programmed to perish. Apoptosis can be initiated by two major pathways (extrinsic vs. intrinsic) which both converge to stimulate a series of proteases (caspases) that cleave key cellular proteins [128]. The effects of chemotherapeutics often depend on their ability to induce cancer cell death by apoptosis. TUNEL (terminal deoxynucleotidyl transferase d-UTP nick end labeling) assay is a commonly used method for detecting DNA fragmentation from cells that have undergone programmed cell death *in situ*. To quantify the amount of apoptotic cancer cells within the bone lesion, TUNEL staining was performed by using the ApopTag Peroxidase In Situ Apoptosis Detection Kit (Millipore Corporation, Billerica, MA 01821, USA) according to the manufacturer's protocol.

Five-µm-thick paraffin-embedded sections were deparaffinized, rehydrated and permeabilized using 1 µg/ml of proteinase K solution (Roche Diagnostics GmbH, 68298 Mannheim, Germany) in 10 mM Tris/HCl for 30 minutes at 37 °C in a humidified chamber. Following a brief wash, slides were incubated in 3 % peroxidase blocking solution for 10 minutes to inhibit endogenous peroxidase activity. After rinsing the sections, 30 µl equilibration buffer was added onto the sections and left for 10 minutes at room temperature. Excess liquid was tapped off and 25 µl TdT (terminal deoxynucleotidyl transferase) enzyme solution, consisting of 17.5 µl reaction buffer (70 %) and 7.5 µl TdT enzyme (30 %) was pipetted onto each section for labeling, then covered with parafilm and incubated at 37 °C in a closed humidified chamber for 60 minutes. For the negative control, the TdT enzyme was omitted from the mixture, so that only 25 µl reaction buffer was used. The parafilm was then carefully removed, the sections were rinsed in a working stop/wash buffer and after a brief wash in PBS, 25 µl anti-digoxigenin was applied to each section and incubated in a humidified chamber at room temperature for 30 minutes. Following a wash in PBS, 3,3-diaminobenzidine (DAB) was added onto the sections and incubated for 4 minutes while observing for color development. The reaction was stopped by tapping off DAB and dipping the slides into distilled water. The sections were washed and then counterstained in filtered Harris' hematoxylin (diluted 1 : 10 in distilled water) for 4 minutes. They were eventually dehydrated in a series of alcohols, cleared in fresh xylene and fixed in a xylene-based

mounting medium. TUNEL-positive prostate cancer cells were recognized as dark brown colored cells under the microscope.

To determine the ratio of TUNEL-positive cells, a representative section of each bone specimen was chosen and the positive as well as negative cells were counted in 3 random fields of non-necrotic areas of cancer (x 400 magnification).

2.6.5 Ki-67 Immunohistochemistry

Ki-67 represents a nuclear protein that is associated with cellular proliferation. As such, it is preferentially produced during the active phases of the cell cycle while cells in the G0 (quiescent) phase do not express this protein [123]. Immunohistochemical Ki-67 staining was performed to determine the proliferative fraction of cancer cells by using a primary polyclonal rabbit antibody to human Ki-67 (Thermo Fisher Scientific, Fremont, CA, USA) and a secondary goat anti-rabbit antibody (Vector Laboratories, Inc. Burlingame, CA, USA).

Five-µm-thick sections were deparaffinized, rehydrated and incubated for 10 minutes at room temperature in 3 % peroxidase blocking solution to cease the activity of endogenous peroxidase. The slides were then incubated for 30 minutes in 7 % goat serum made up of TBST buffer (200 mM Tris-HCl, 150 mM NaCl, 10 mM Tris-base, 0.5 % Tween) to block non-specific protein binding. The primary polyclonal rabbit antibody to human Ki-67 was pipetted onto the sections at a dilution of 1 : 750 and left overnight at 4 °C in a humidified chamber. Following a short wash on the next day, the sections were incubated with biotinylated goat anti-rabbit IgG by using a dilution of 1 : 150 in blocking serum for one hour at room temperature.
Vectastain Avidin-Biotin Complex (ABC) kit (Vector Laboratories, Inc. Burlingame, CA, USA) was pipetted onto the slides, left for 30 minutes and after adding 3,3'-diaminobenzidine (DAB; Vector Laboratories, Inc. Burlingame, CA, USA), the labelled antigens were visualized. The slides were rinsed in distilled water and counterstained in Harris' hematoxylin (diluted 1 : 10 in distilled water) for 4 minutes.

After a brief wash in tap water, the sections were dehydrated, cleared in xylene and fixed in a xylene-based mounting medium. Ki-67 positive tumor cells were detected as brown colored cells under the microscope.

To determine the ratio of Ki-67-positive cells, a representative section of each bone specimen was chosen and the positive as well as negative cells were counted in 3 random fields of non-necrotic areas of cancer (x 400 magnification).

2.6.6 RANK Immunohistochemistry

RANK is a type 1 transmembrane protein that functions as a cognate receptor for RANKL. To determine the expression of RANK on the surface of cancer cells, immunohistochemical RANK staining was performed by using a primary monoclonal mouse antibody to human RANK (R&D Systems, Inc., Minneapolis, MN 55413, USA) and a secondary horse anti-mouse antibody (Vector Laboratories, Inc. Burlingame, CA, USA) according to the manufacturer's protocol.

Five-µm-thick sections were deparaffinized, rehydrated through a series of alcohols and incubated in 3 % peroxidase blocking solution for 10 minutes to quench endogenous peroxidase activity. The slides were then left for 30 minutes in horse serum composed of PBS/BSA/Triton buffer (0.15 % BSA and 0.1 % Triton X100) to block non-specific protein binding. The primary antibody was added onto the sections at a dilution of 1 : 500 and incubated overnight at 4 °C in a humidified chamber. This was followed by the application of biotinylated horse anti-mouse IgG using a dilution of 1 : 150 in blocking serum for one hour at room temperature. Sections were then left for 30 minutes in Vectastain Avidin-Biotin Complex (ABC) kit and the labelled antigens were visualized following addition of 3,3'-diaminobenzidine (DAB) chromogen for 40 seconds. The slides were subsequently rinsed in distilled water and counterstained in Harris' hematoxylin (diluted 1 : 10 in distilled water) for 4 minutes. Following a brief wash in tap water, the sections were dehydrated, cleared in xylene and fixed in a

xylene-based mounting medium. RANK-positive tumor cells were identified as brown colored cells under the microscope.

2.6.7 Bone Histomorphometry

Bone histomorphometry represents a histological assessment of undecalcified bone. In this thesis, histomorphometric analysis was performed to quantify the following parameters: tumor area (mm^2), cortical bone area (mm^2) and static measures of bone resorption (number of TRAcP-positive cells/mm tumor-bone interface). Bone histomorphometry was performed as described in [123].

The OsteoMeasure system (Osteometrics, Atlanta, GA, USA) was used to analyze the 5-µm-thick sections stained with hematoxylin and eosin (x 12.5 magnification) and TRAcP (x 200 magnification). Longitudinal sections through the tibia with an approximate interval of 150 – 200 µm were cut, reflecting anterior, mid and posterior areas of the proximal tibia. To quantify the cancer area, a representative section with the largest tumor area in the proximal tibia was selected. Total tumor area was determined in each representative section and the mean was interpreted as an index of tumor load. All neoplastic areas were analyzed including the adjacent soft tissues where tumor cells broke through the cortical bone into its vicinity. Tumor area was not calculated when a neoplastic mass existed independently of a bone lesion because this situation was due to leakage during cancer inoculation (this situation was rare). The area of cortical bone tissue was quantified in the same sections.

In TRAcP stained sections, osteoclasts were recognized as purple multinucleated cells residing close to tumor-bone interfaces. The number of osteoclasts was counted in two random fields of each section and the ratio of osteoclast number per millimeter of tumor-bone interface was calculated.

2.7 Serum Biochemistry

Tartrate-resistant acid phosphatase 5b (TRAcP 5b) is an enzyme that is produced in high quantities by bone-resorbing osteoclasts. Despite its discovery in the early 1970s, the biological function of this enzyme is not known [129]. TRAcP 5b activity correlates strongly with bone resorption and may even reflect the degree of osteolytic tumor burden, however, recent studies suggest that secreted TRAcP 5b is rather associated with the number of osteoclasts than their activity [129, 130]. Levels of TRAcP 5b were analyzed by a solid phase immunofixed enzyme activity assay (Immunodiagnostic Systems Ltd., Boldon, UK) in mouse sera collected on day 30 of the intra-tibial PC3 tumor mouse model and performed according to the manufacturer's protocol.
Anti-mouse TRAcP antibody that uses TRAcP as antigen was added to the antibody coated microtiter wells. Following a washing step, controls and samples were pipetted into the wells and any mouse TRAcP present was bound by the antibody.
A chromogenic substrate solution was administered to all wells and then incubated for 2 hours to develop color. The addition of a stop solution terminated this reaction and the absorbance of the reaction mixture was measured by using a microtiter plate reader. The intensity of the color was directly proportional to the concentration of TRAcP 5b present in the sample.

Procollagen type I N-terminal propeptide (P1NP) is a marker of osteoblastic bone formation. Levels of mouse P1NP were measured using a specific enzyme immunoassay (Immunodiagnostic Systems Ltd., Boldon, UK) in mouse sera collected on day 30 of the intra-tibial PC3 tumor mouse model and performed according to the manufacturer's protocol.
The polyclonal antibody that utilizes mouse P1NP as antigen was coated onto the surfaces of the microtiter wells. After adding controls and samples to the wells, the plate was incubated with P1NP labelled with biotin for 1 hour. Following a brief wash, horseradish peroxidase labelled avidin was administered to the wells, binding selectively to complexed biotin. The addition of a chromogenic substrate resulted in color development. After pipetting stop solution into the wells, the optical density of each well was analysed by using a microtiter plate reader. The intensity of the color was inversely proportional to the amount of P1NP present in the sample.

RANKL levels were measured using a solid phase enzyme-linked immunosorbent assay (ELISA) (R&D Systems, Inc, Minneapolis, USA) in mouse sera collected on day 30 of the intra-tibial PC3 tumor mouse model and performed according to the manufacturer's instructions.

A polyclonal antibody specific for mouse RANKL was coated onto the microtiter wells. Controls and samples were added to the wells and mouse RANKL was bound by the coated antibody. Following a washing step, an enzyme-linked antibody that uses mouse RANKL as antigen was pipetted into the wells. Following a washing step, a chromogenic substrate solution was administered to all wells, leading to color development. After adding stop solution, the absorbance of each well was determined by using a microtiter plate reader. The intensity of the color was proportional to the quantity of mouse RANKL bound by the coated antibody.

2.8 Molecular Biology

2.8.1 RNA Extraction

Ribonucleic acid (RNA) isolation was conducted by using an extraction kit (innuPREP RNA Mini Kit; Analytik Jena AG, Jena, Germany) according to the manufacturer's protocol.

Lysis solution was added to the cell pellets and incubated for 5 minutes at room temperature. The genomic DNA was selectively bound and removed by centrifuging a spin filter for 2 minutes. A second centrifugation of a different spin filter caused selective binding of RNA onto the filter. After removing all contaminants by a washing step, pure RNA was eluted in RNase free water. The quality of the obtained RNA was verified by spectroscopy and on 1.2 % gel. RNA was stored at -80 °C to ensure its stability.

2.8.2 Reverse Transcription

Reverse transcription (RT) is a process in which an RNA-dependent DNA polymerase (reverse transcriptase) produces single-stranded complementary DNA (cDNA) from a messenger RNA template. Physiological cellular transcription involves the synthesis of mRNA from DNA, thus, reverse transcription represents the reverse of this process. Single-stranded cDNA was produced by using total cellular RNA together with a reverse transcriptase enzyme, a short primer complementary to the 3' end of the RNA, dNTPs and an RNase inhibitor. The resulting cDNA was then used for real-time quantitative reverse transcription PCR purposes.

A RT reaction (Superscript III Reverse Transcriptase kit, Invitrogen, Carlsbad, CA, USA) basically includes the following steps: template RNA, an oligo (dT) primer and a reaction mixture containing dNTPs were combined in a 0.5 ml tube and then incubated at 65 °C for 5 minutes. Following a quick chill on ice, a cocktail of other components including reverse transcriptase and RNase inhibitor was added into each tube and heated at 50 °C for 60 minutes. The enzyme-catalyzed reaction was inactivated by heating the mixture at 70 °C for 15 minutes.

2.8.3 Real-Time Quantitative Polymerase Chain Reaction

Real-time quantitative PCR is a method to multiply DNA or cDNA based on the principles of the standard PCR. It differs from the standard one in that it allows DNA concentrations to be determined in real time, i.e., after each cycle. PCR products can be quantified via a DNA-binding dye that fluoresces when it attaches to newly synthesized double-stranded DNA. As DNA templates augment during the PCR process, a detector measures the increase in fluorescence intensity. In this thesis, the DNA-binding dye SYBR Green (SYBR Green PCR Master Mix, Applied Biosystems, Foster City, CA) was used in combination with an iQ5 real-time PCR cycler (BioRad, Munich, Germany).

The standard PCR method relies on multiple thermal cycles which are, in turn, composed of three steps: The first step (denaturation) includes heating of the reaction to approximately 95 °C to separate the double-stranded DNA template.

The temperature is then reduced to permit annealing of the primer to the single-stranded DNA molecule, so that the polymerase can bind to the primer and begin DNA formation. In the last step (elongation), the Taq polymerase adds complementary dNTPs at the 3' end − at an optimum temperature of 72 °C − to synthesize a new DNA strand.

2.9 Statistical Analysis

All data were presented as mean ± SEM. Statistical analysis was performed using unpaired *t*-test (two groups) or one-way ANOVA (three or more groups). When multiple groups were compared by one-way ANOVA, the mean of the treatment groups was compared with the mean of the control group and a post hoc test using the Bonferroni method was employed to enable multiple comparisons. A p value < 0.05 was considered statistically significant. Statistical analysis was performed using GraphPad Prism 6 (GraphPad Software, Inc., La Jolla, CA, USA).

Chapter 3
Results

3.1 *In Vitro* Effects of Interleukin-6 and/or Tocilizumab on PTHrP Expression in PC3 Cells

The prostate cancer cell line PC3 was incubated *in vitro* with human recombinant interleukin-6 (IL-6) for 24 hours to test whether IL-6 increases the production of the osteolytic factor PTHrP. Measurements by real-time quantitative reverse transcription PCR revealed that application of 200 ng/ml of IL-6 improved PTHrP mRNA expression 2.3-fold in a highly significant manner; 100 ng/ml led to an almost 2-fold elevation of PTHrP synthesis (Fig. 3.1). Note that prior treatment of PC3 cells with the humanized IL-6 receptor antibody tocilizumab (200 µg/ml) totally blocked IL-6-induced changes and normalized tumor PTHrP output levels (Fig. 3.1).

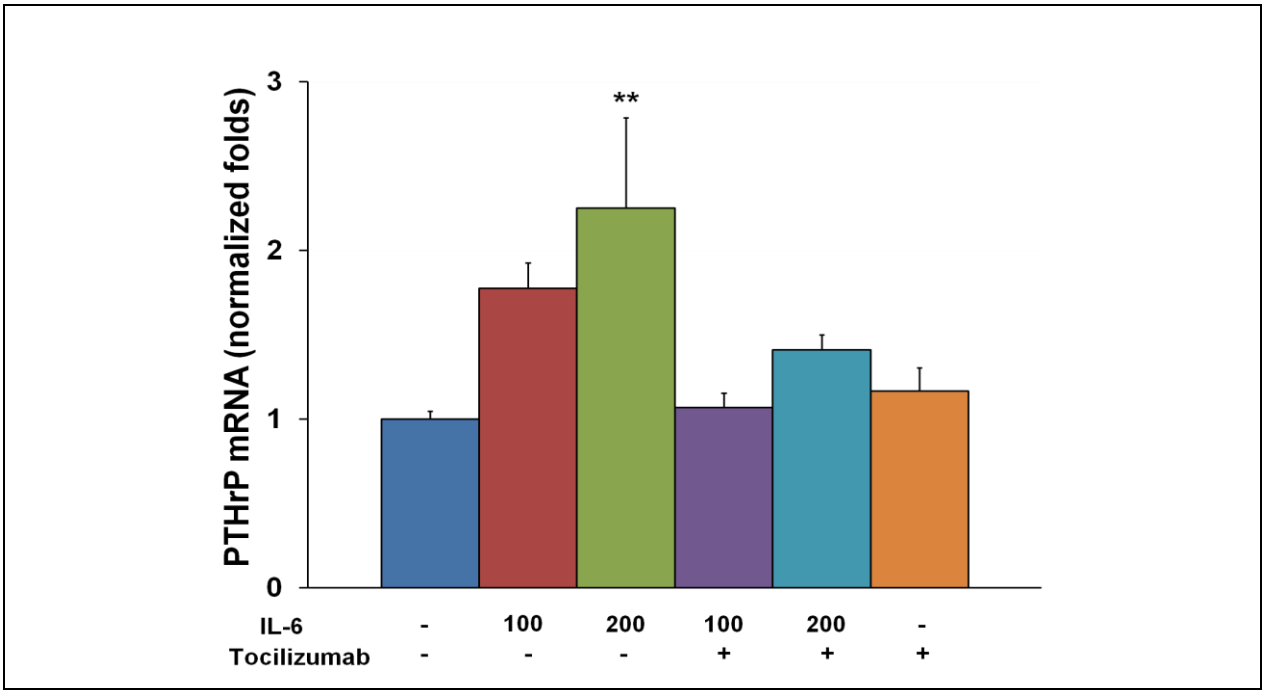

Fig. 3.1: *In Vitro* Effects of Interleukin-6 (IL-6) and/or Tocilizumab on Parathyroid Hormone-Related Protein (PTHrP) mRNA Expression.
Treatment of PC3 cells with human recombinant IL-6 for 24 hours at different concentrations enhanced tumor cell PTHrP production (IL-6 100 = 100 ng/ml;

IL-6 200 = 200 ng/ml; Tmab + = 200 µg/ml). In contrast, prior treatment of PC3 cells with tocilizumab completely prevented IL-6-induced changes on PTHrP mRNA synthesis. *Data are mean ± SEM (bars) and n = 5. ** denotes significantly different from controls (**, p < 0.01).*

3.2 *In Vitro* Effects of Interleukin-6 and/or Tocilizumab on RANK Expression in PC3 Cells

To determine whether IL-6 supports cancer cell adaptation in bone by increasing tumor RANK expression, PC3 cells were treated *in vitro* with human recombinant IL-6 for 24 hours. Administration of 100 ng/ml of IL-6 enhanced RANK mRNA formation 1.6-fold, while the concentration of 200 ng/ml of IL-6 resulted in a 2-fold rise of RANK mRNA production (p = 0.057) as measured by real-time quantitative reverse transcription PCR. Prior application of the IL-6 receptor antagonist tocilizumab reduced RANK mRNA synthesis by PC3 cells (Fig. 3.2).

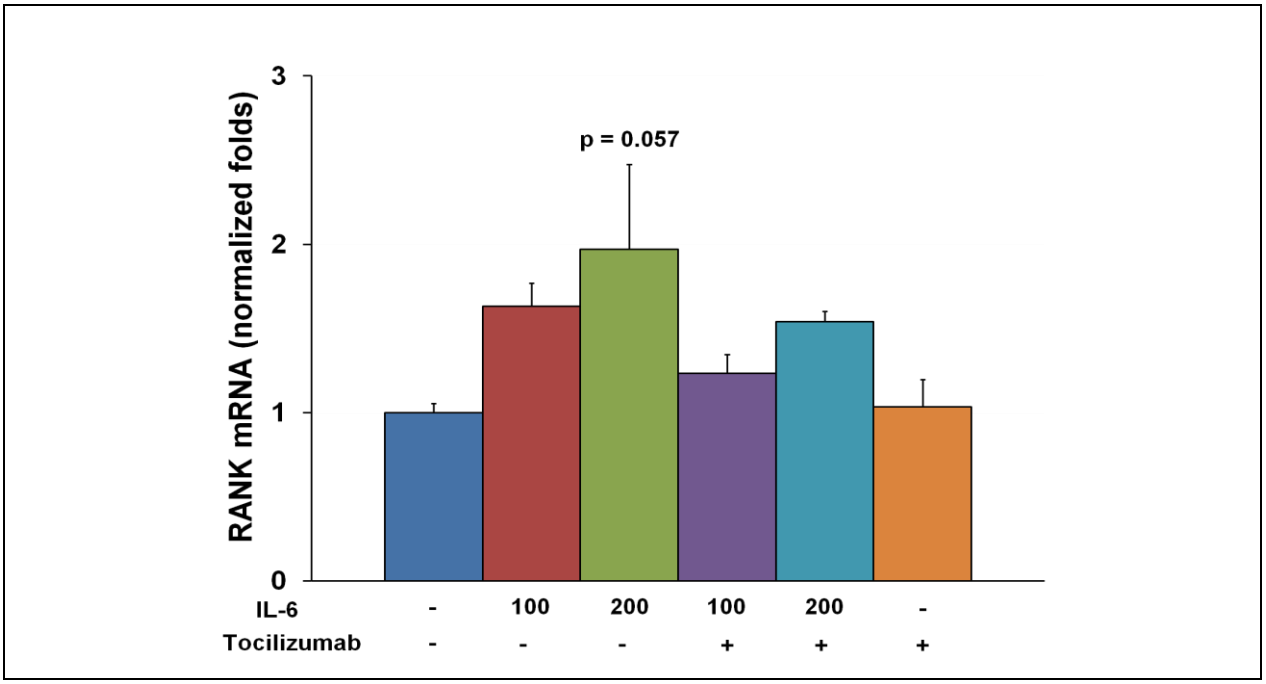

Fig. 3.2: *In Vitro* Effects of Interleukin-6 (IL-6) and/or Tocilizumab on Receptor Activator of Nuclear Factor Kappa B (RANK) mRNA Expression.
Incubation of PC3 cells with human recombinant IL-6 for 24 hours at different concentrations increased neoplastic RANK mRNA synthesis (IL-6 100 = 100 ng/ml;

IL-6 200 = 200 ng/ml; Tmab + = 200 µg/ml). Prior treatment of PC3 cells with tocilizumab diminished the impact of IL-6 on RANK production. *Data are mean ± SEM (bars) and n = 3.*

Zheng *et al.* have shown that *in vitro* co-cultures of RANKL-expressing osteoblasts and RANK-producing PC3 cells significantly enhance IL-6 output levels by cancer cells [131]. The above IL-6-RANK-related *in vitro* data now demonstrates that exogenously administered IL-6 is able to increase the expression of the cell surface receptor RANK in PC3 cancer cells. Since these cells secrete large quantities of IL-6 into their environment [80, 85], this cytokine could − in addition to its paracrine effect on RANKL synthesis in osteoblasts − upregulate RANK expression on cancer cells in an autocrine manner, sensitizing tumor cells to osteoblast-derived RANKL. This potential signaling pathway would involve IL-6, RANKL and RANK and might promote direct crosstalk between neoplastic and osteoblastic cells.

We examined whether these mechanisms are actually present *in vivo*. Specifically, we wondered whether antagonizing autocrine IL-6 receptor signaling in the osteolytic prostate cancer cell line PC3 affects tumor growth in bone and in soft tissues by the signaling pathways described above.

3.3 Effects of Tocilizumab on PC3-Induced Osteolytic Lesions

To determine whether blockage of autocrine IL-6 signaling via the human IL-6 receptor antibody tocilizumab (Tmab) inhibits PC3-induced bone destruction and neoplastic growth in bone, PC3 tumor cells were injected into the tibiae of five-week-old male nude mice. Osteolytic lesions were assessed by radiographic and micro-CT analysis. The development of bone erosions was verified by X-ray images 10 days after tumor cell implantation and then evaluated on day 17, 24 and 30. Osteolytic lesions within bone corresponded to darkened areas on X-rays and are indicated by thick black arrows as seen in Fig. 3.3A.

Over the course of 30 days, we found that tocilizumab, given at a dose of 50 mg/kg (body weight) one day prior to tumor cell inoculation and then every 3 days, significantly

reduced PC3-induced bone degradation at each time point of measurement (Fig. 3.3B). In detail, quantification of osteolysis at day 17 showed that blocking autocrine IL-6 signaling significantly diminished the osteolytic area by 69 % compared to controls (Fig. 3.3B; control: 0.333 mm^2, Tmab: 0.104 mm^2; $p < 0.05$ vs. control). Over the following days, osteolytic foci continued to expand in both experimental groups as determined by plain X-rays at day 24 and day 30, however, the tocilizumab-treated group maintained significantly decreased osteolytic levels at each moment, with a reduction of 51 % at day 24 (Fig. 3.3B; control: 0.900 mm^2, Tmab: 0.437 mm^2; $p < 0.05$ vs. control) and 48 % at day 30 compared to controls (Fig. 3.3B; control: 1.489 mm^2, Tmab: 0.778 mm^2; $p < 0.05$ vs. control). Representative micro-CT images from day 30 clearly emphasize the different degree of bone destruction within the two groups (Fig. 3.3A). Note that zoledronic acid treated mice did not present visible lytic bone lesions on X-rays at any moment, so that osteolysis could not be measured (images not shown).

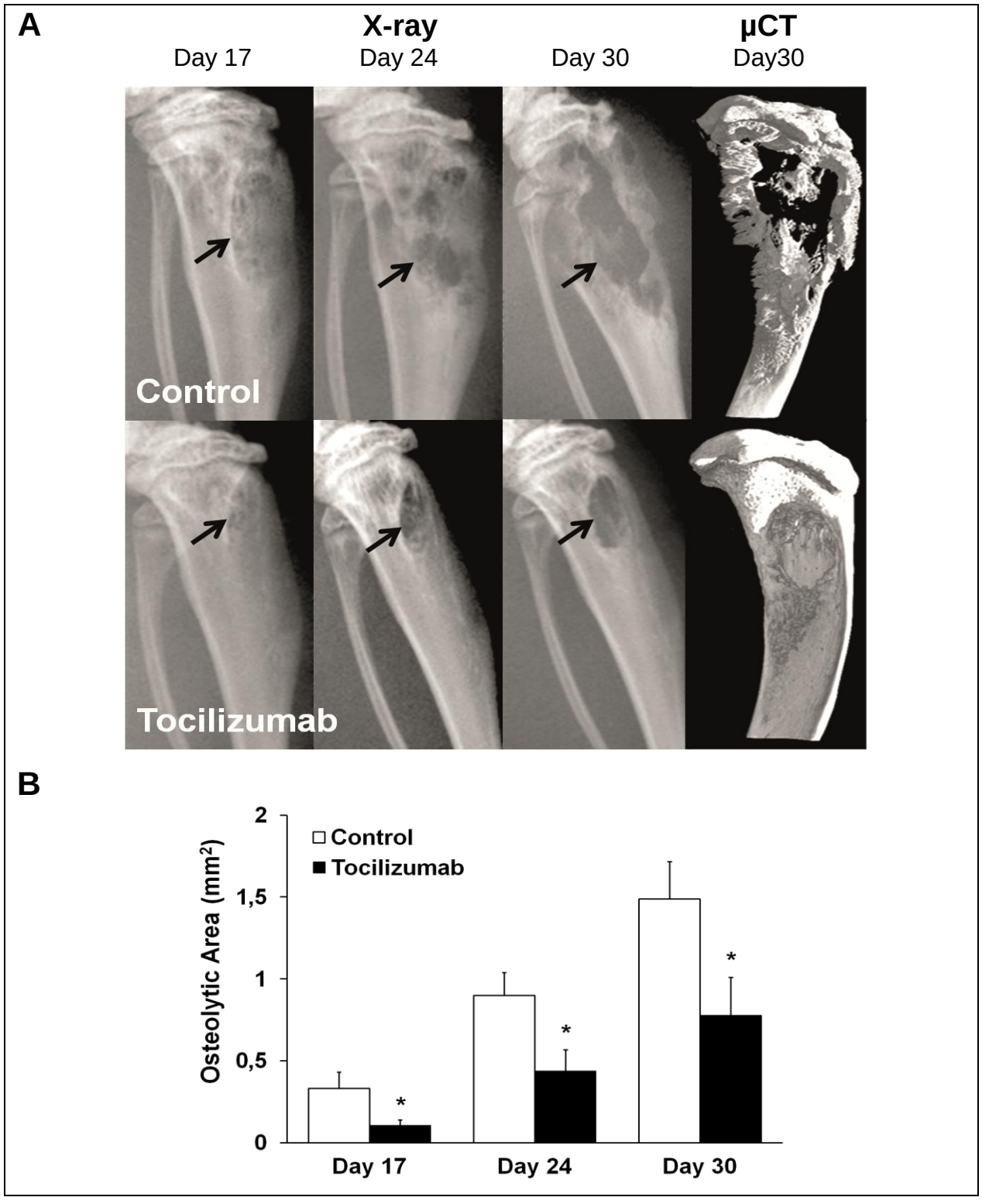

Fig. 3.3: Effects of Tocilizumab on Osteolysis in PC3 Cell Injected Tibiae of Nude Mice.

(A) Representative X-ray images and micro-computerized tomography (µCT) analysis of osteolytic areas in tibiae of nude mice treated with placebo (control) or tocilizumab from day 17, 24 and 30. Tocilizumab was administered at a dose of 50 mg/kg one day

prior to intra-tibial tumor cell injection and then every 3 days. Darkened areas within bone on X-rays represent osteolytic sites and are indicated by thick black arrows.
(B) Mean area of osteolytic lesions at day 17, 24 and 30 in tibiae of nude mice treated as mentioned above. Therapy with tocilizumab significantly decreased the enlargement of osteolytic spots at any time point of measurement compared to the control group. *Data are mean ± SEM (bars) and n = 8 in each group of animals except for control group (n = 7), in which one mouse died during the experiment. * denotes significantly different from controls (*, p < 0.05).*

3.4 Effects of Tocilizumab and/or Zoledronic Acid on Tumor Area and Cortical Bone Area

Representative hematoxylin and eosin-stained bone tissues illustrate the extent of tumor cell expansion in bone (Fig. 3.4A). Histomorphometric analysis revealed that treatment of nude mice with tocilizumab (Tmab) and/or zoledronic acid (ZA) significantly lowered tumor area while increasing cortical bone volume when compared to control animals (Fig. 3.4B and C).

Treatment of animals with tocilizumab reduced the intra-tibial PC3 tumor area by 54 % in contrast to controls (Fig. 3.4B; control: 4.521 mm^2, Tmab: 2.071 mm^2; $p < 0.05$ vs. control). Administration of zoledronic acid diminished neoplastic expansion to a greater extent, demonstrating a 67 % decrease in tumor area versus PBS-treated controls (Fig. 3.4B; control: 4.521 mm^2, ZA: 1.472 mm^2; $p < 0.01$ vs. control), however, statistical significance was not obtained compared to anti-IL-6 receptor therapy. Regarding cortical bone area analysis, therapy with tocilizumab showed a tendency to protect cortical bone from destruction by increasing its area up to 33 % versus untreated control mice ($p = 0.13$). Zoledronic acid treatment prevented the dissolving process of cortical bone more effectively, leading to a 57 % gain in cortical bone area compared to PBS-treated animals (Fig. 3.4C; $p < 0.01$ vs. control). Combined therapy with tocilizumab and zoledronic acid reduced the tumor burden and protected cortical bone from breakdown compared to controls, however, no additive effects were revealed (Fig. 3.4B and C).

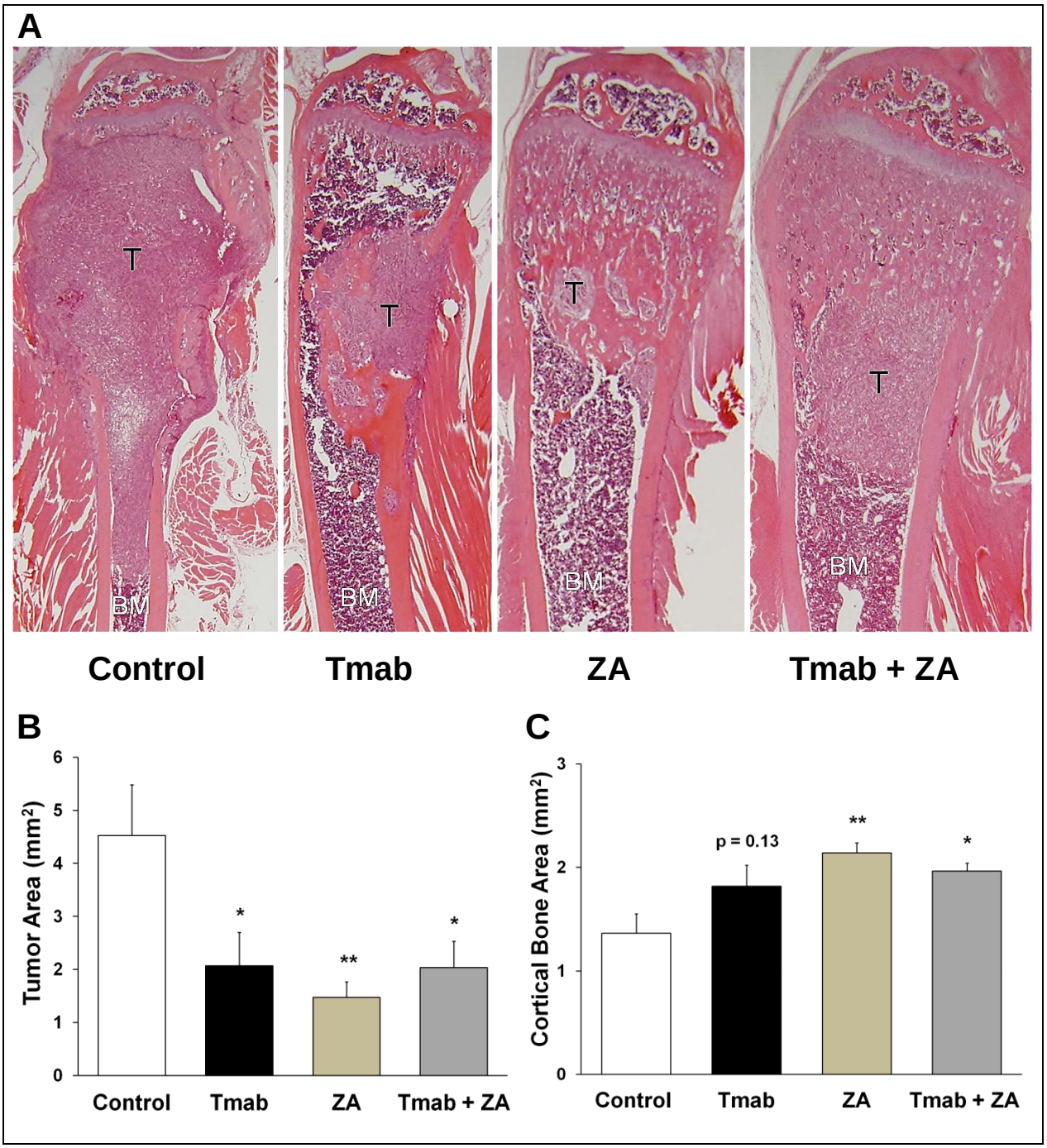

Fig. 3.4: Effects of Tocilizumab and/or Zoledronic Acid Treatment on Tumor Area and Cortical Bone Area.

(A) Representative hematoxylin and eosin-stained sections of PC3 cell injected tibiae from nude mice treated with placebo (control), tocilizumab (Tmab), zoledronic acid (ZA) or both tocilizumab and zoledronic acid (Tmab + ZA). Tocilizumab (50 mg/kg) and zoledronic acid (100 µg/kg) were administered one day prior to tumor cell implantation and then every 3 days. Tumor foci are marked as T, whereas the bone marrow cavity is symbolized by BM (x 12.5 magnification).

(B) Compared to controls, application of tocilizumab significantly reduced intra-tibial tumor spreading, however, mice treated with zoledronic acid exhibited a greater

reduction of tumor burden. Combined treatment with tocilizumab and zoledronic acid did not result in additive effects on tumor site reduction.
(C) Tocilizumab therapy tended to protect cortical bone from degradation compared to controls. Administration of zoledronic acid revealed a stronger trend on cortical bone preservation, though statistical significance was not reached when compared to anti-IL-6 receptor treatment. *Data are mean ± SEM (bars) and n = 8 in each group of animals except for control group (n = 7), in which one animal died during the experiment. * and ** denote significantly different from controls (*, p < 0.05; **, p < 0.01).*

3.5 Effects of Tocilizumab and/or Zoledronic Acid on PC3 Cell Apoptosis and Proliferation in Bone

Ki-67 and TUNEL staining were used to evaluate apoptotic and proliferative cancer cells. In sections, positive stained PC3 cells were identified as brown colored cells (Fig. 3.5A).

Histological quantification of TUNEL and Ki-67 stained cells showed higher apoptosis and lower proliferation rates in animals treated with tocilizumab and/or zoledronic acid (Fig. 3.5B and C). Anti-IL-6 receptor therapy with tocilizumab stimulated apoptosis in PC3 cells by 45 % ($p = 0.07$ vs. control; Fig. 3.5B) while zoledronic acid augmented the extent of TUNEL-positive tumor cells in a highly significant manner by 112 % ($p < 0.01$ vs. control; Fig. 3.5B) compared to untreated control mice. Both tocilizumab and zoledronic acid led to a similar decline concerning the assessment of Ki-67-positive mitotic cells: tocilizumab decreased the amount of proliferating cancer cells by 44 % ($p < 0.01$ vs. control; Fig. 3.5C), whereas zoledronic acid reduced the number of propagating tumor cells by 51 % ($p < 0.01$ vs. control; Fig. 3.5C). Concurrent application of tocilizumab and zoledronic acid increased apoptosis and decreased proliferation of cancer cells compared to controls but additive effects on tumor cell apoptosis and proliferation were not observed (Fig. 3.5B and C).

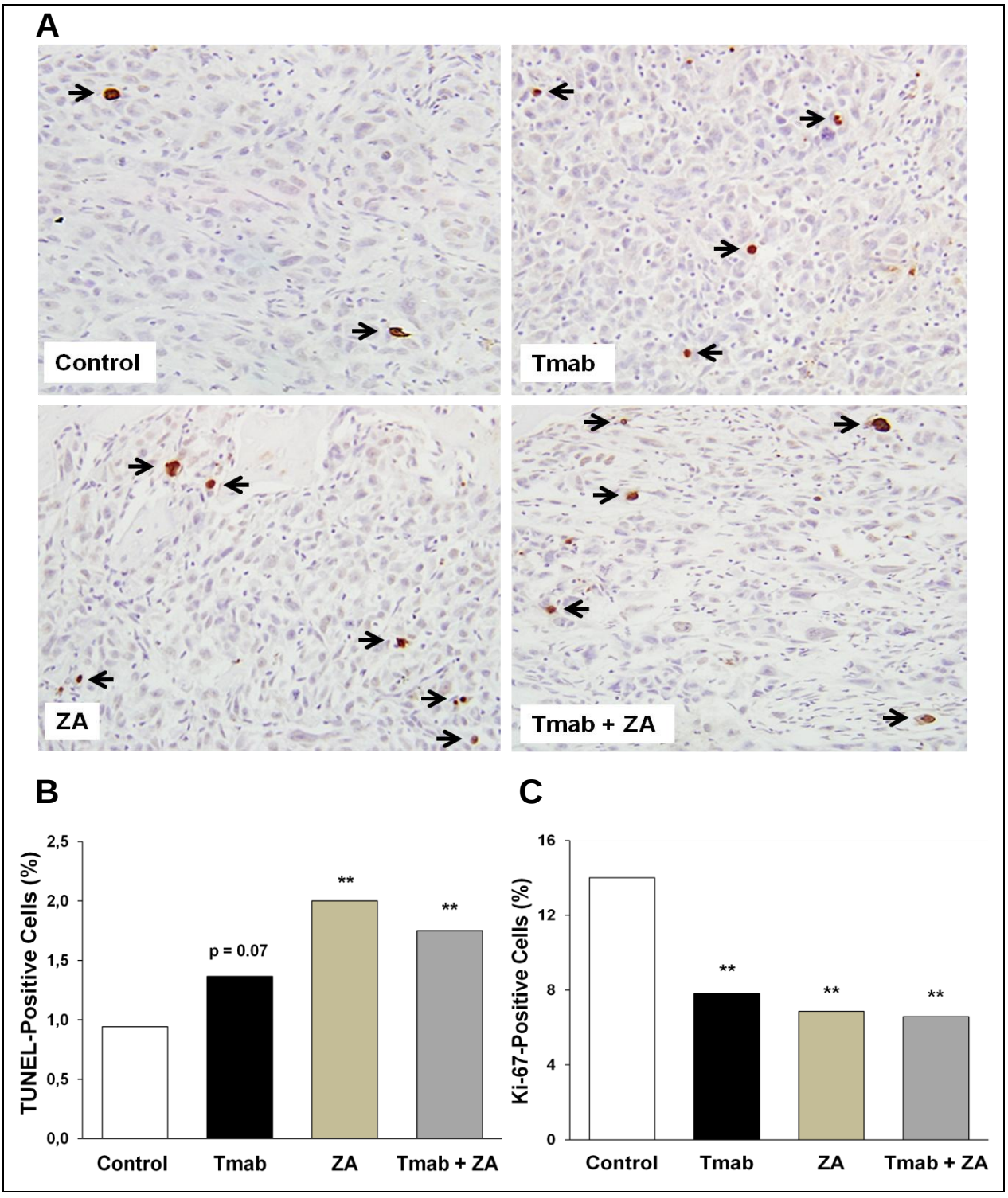

Fig. 3.5: Histological Assessment of Apoptosis (TUNEL Staining) and Proliferation (Ki-67 Immunostaining) of Tocilizumab and/or Zoledronic Acid Treated Mice.

(A) Representative TUNEL stained sections of PC3 prostate cancer cells in tibiae of nude mice treated with placebo (control), tocilizumab (Tmab), zoledronic acid (ZA) or tocilizumab and zoledronic acid (Tmab + ZA). TUNEL-positive apoptotic PC3 cells are identified as brown colored cells (x 400 magnification) as indicated by black arrows.

(B) The percentage of apoptotic cells was increased in all three treated groups compared to controls. Therapy with tocilizumab augmented the number of dying tumor cells, however, the degree of apoptotic cells was considerably more elevated in zoledronic acid treated mice. No additive effects were observed with combined treatments of tocilizumab and zoledronic acid.
(C) All three medication groups reduced the amount of propagating cancer cells in a significant and similar manner compared to control animals. *Data are mean ± SEM (bars) and n = 8 in each group of animals except for control group (n = 7), in which one animal died during the experiment. ** denotes significantly different from controls (**, p < 0.01).*

3.6 Effects of Tocilizumab and/or Zoledronic Acid on Osteoclast Numbers at the Tumor-Bone Interface

TRAcP staining was chosen in order to assess osteoclast differentiation and activity at the tumor-bone interface. TRAcP-positive osteoclasts were identified as purple colored cells, as indicated by black arrows in Fig. 3.6A.

Histological analysis revealed that tocilizumab and/or zoledronic acid treated animals displayed a significantly reduced number of TRAcP-positive osteoclasts compared to controls, indicating reduced osteolytic activity. Tocilizumab-treated animals showed 25 % less osteoclasts compared to control mice ($p < 0.01$ vs. control; Fig. 3.6B), in which tibiae exhibited a dense accumulation of bone-resorbing cells, lining the inner bone surfaces in the vicinity of the tumor (Fig. 3.6A). Sections obtained from mice treated with zoledronic acid showed a considerable smaller amount of TRAcP-positive osteoclasts at the conjunction, resulting in a 60 % decrease relative to controls ($p < 0.01$ vs. control; Fig. 3.6B). The combination of both medications tocilizumab and zoledronic acid produced results similar to those obtained with zoledronic acid treated animals (Fig. 3.6B).

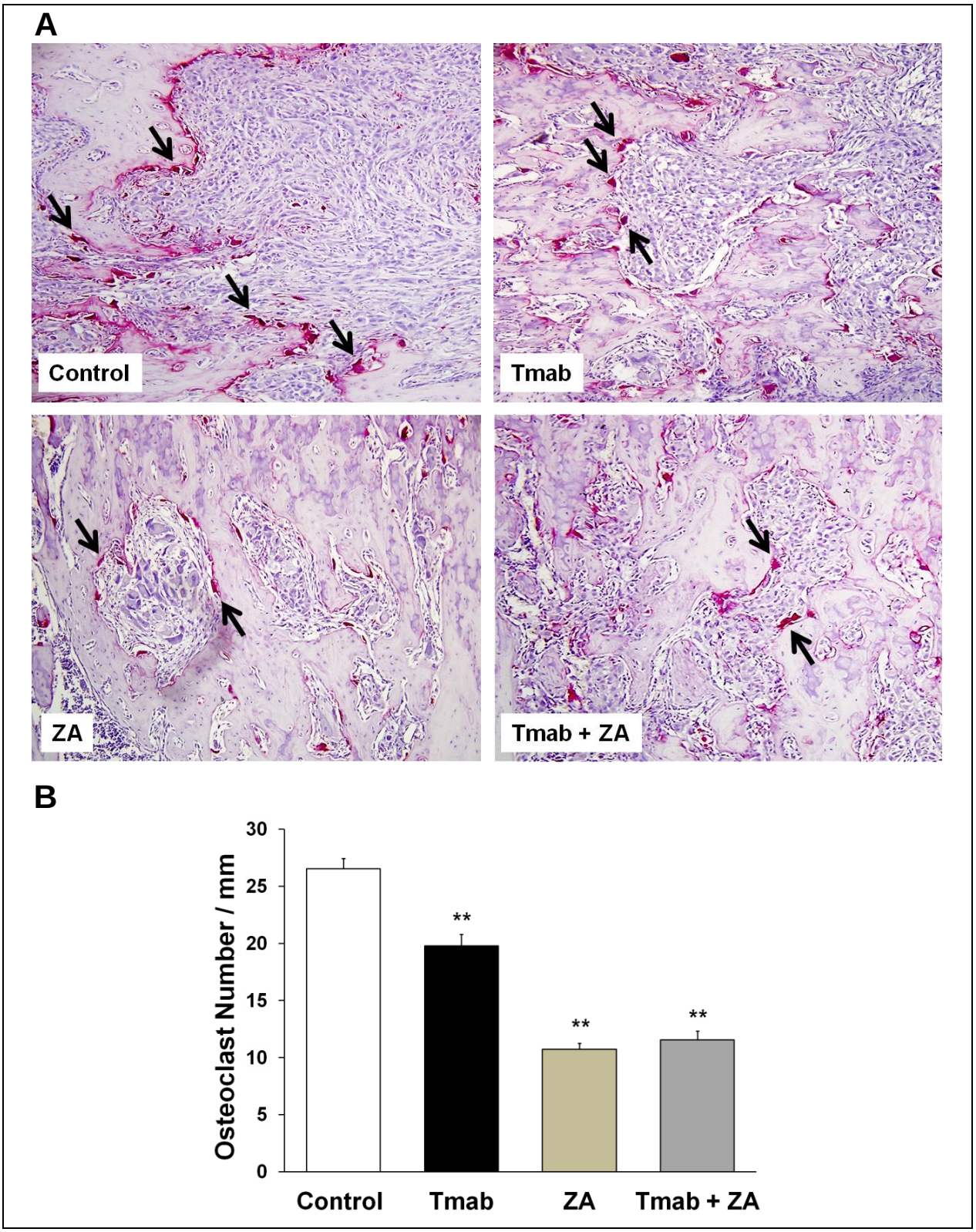

Fig. 3.6: Effects of Tocilizumab and/or Zoledronic Acid on Osteoclast Numbers at the Tumor-Bone Interface.

(A) Representative tartrate-resistant acid phosphatase (TRAcP) stained sections of osteoclasts in tibiae of nude mice treated with placebo (control), tocilizumab (Tmab),

zoledronic acid (ZA) or tocilizumab and zoledronic acid (Tmab + ZA). TRAcP-positive osteoclasts are identified as purple colored cells as indicated by black arrows (x 200 magnification).
(B) All three treatment groups demonstrated a significantly lower density of TRAcP-positive osteoclasts compared to controls, suggesting reduced bone destructive activity. Treatment with zoledronic acid or the combination of tocilizumab and zoledronic acid led to a greater decrease in osteoclast numbers than tocilizumab therapy alone. *Data are mean ± SEM (bars) and n = 8 in each group of animals except for control group (n = 7), in which one animal died during the experiment. ** denotes significantly different from controls (**, p < 0.01).*

3.7 Effects of Tocilizumab and/or Zoledronic Acid on Serum TRAcP 5b, Serum P1NP and Serum RANKL Levels

Circulating levels of tartrate-resistant acid phosphatase 5b (TRAcP 5b), procollagen type I N-terminal propeptide (P1NP) and receptor activator of NFκB ligand (RANKL) were measured to evaluate the degree of bone remodeling. These markers of bone turnover were determined in the sera of mice collected on day 30.

TRAcP 5b is an enzyme that is secreted by bone-resorbing osteoclasts and represents a marker of bone resorption and osteoclast number [129]. Consistent with the finding of diminished osteoclast numbers in TRAcP stained sections, reduced systemic TRAcP 5b levels are detected in the sera of mice in response to tocilizumab and/or zoledronic acid treatment compared to controls, suggesting reduced numbers of osteoclasts and their function. More specifically, tocilizumab reduced serum TRAcP 5b levels by 28 % ($p < 0.05$ vs. control), zoledronic acid by 32 % ($p < 0.01$ vs. control) and the combination of both by 38 % ($p < 0.01$ vs. control; Fig. 3.7A).

Another biomarker of bone metabolism reflects P1NP which is released by osteoblasts in the course of bone formation. The collected data demonstrated that the three treatment groups diminished the osteoblastic bone formation marker P1NP to a similar degree in contrast to controls. Due to the coupling process of bone resorption and bone formation, decreased osteoclastic activity results in diminished generation of osteoblasts and their bone-forming activity [19]. More accurately, tocilizumab diminished serum P1NP levels by 32 % ($p < 0.05$ vs. control), zoledronic acid by 36 %

(p < 0.05 vs. control), whereas the combination of tocilizumab and zoledronic acid led to a 29 % reduction relative to controls (p = 0.06 vs. control; Fig. 3.7B).

Serum RANKL levels were measured only in mice treated with tocilizumab. The IL-6 receptor antagonist significantly lowered circulating RANKL levels by 53 % compared to controls (p < 0.05 vs. control; Fig. 3.7C), which corresponds with the reduced amount of TRAcP-positive osteoclasts as well as the decreased levels of serum TRAcP 5b seen in tocilizumab-treated mice.

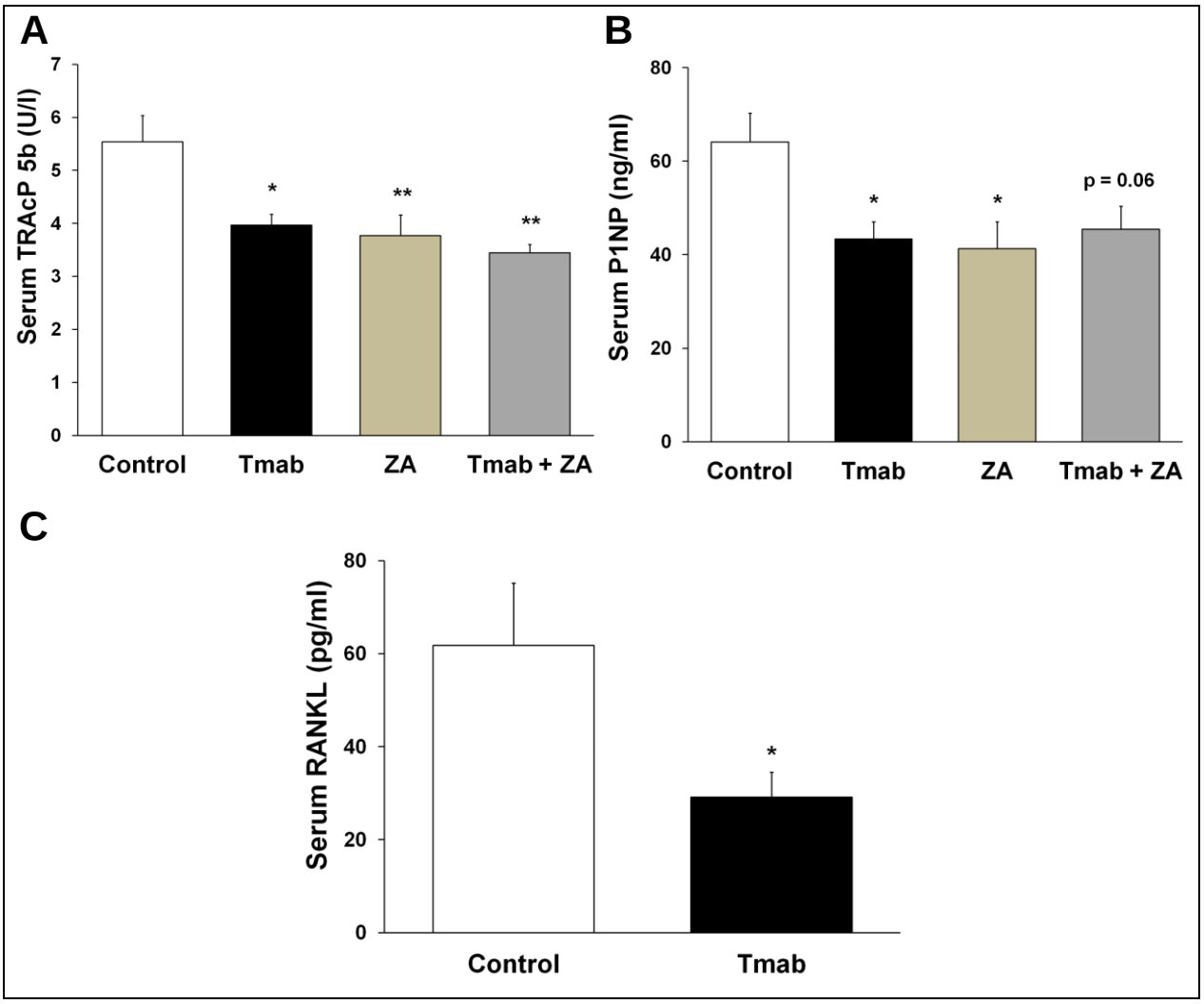

Fig. 3.7: Effects of Tocilizumab and/or Zoledronic Acid on Serum Tartrate-Resistant Acid Phosphatase 5b (TRAcP 5b), Procollagen Type I N-terminal Propeptide (P1NP) and Receptor Activator of Nuclear Factor Kappa B Ligand (RANKL) Levels.

(A) A solid phase immunofixed enzyme activity assay was used to measure serum TRAcP 5b levels in mice treated with placebo (control), tocilizumab (Tmab),

zoledronic acid (ZA) or tocilizumab and zoledronic acid (Tmab + ZA). The three treatment groups lowered systemic TRAcP 5b levels to a similar extent when compared to controls.
(B) A competitive enzyme immunoassay (EIA) was employed to quantify circulating P1NP levels in mice treated as mentioned above. All three medications led to a similar systemic decrease in the bone formation marker P1NP when compared to controls.
(C) A solid phase enzyme-linked immunosorbent assay (ELISA) was used to measure serum RANKL levels in mice treated with tocilizumab alone. Administration of tocilizumab significantly reduced systemic RANKL levels relative to controls, indicating decreased osteoclast numbers. *Data are mean ± SEM (bars) and n = 6 in each group of animals. * and ** denote significantly different from controls (*, $p < 0.05$; **, $p < 0.01$).*

3.8 Effects of Tocilizumab on Intra-Tibial PC3 Tumor RANK Expression

To further verify our *in vitro* data which showed that tocilizumab treatment reduced RANK mRNA synthesis in PC3 cells, immunohistochemical RANK staining of harvested bone tissues was performed (Fig. 3.8). The intensity of the brown dye correlates positively with tumor RANK production. As shown in the figure below, inhibition of autocrine IL-6 receptor signaling via tocilizumab largely reduced the strength of the brown stain compared to control mice, suggesting diminished RANK expression levels in intra-tibial PC3 tumors. Reduced *in vivo* RANK expression in response to tumor IL-6 receptor blockage is in line with our *in vitro* RANK data.

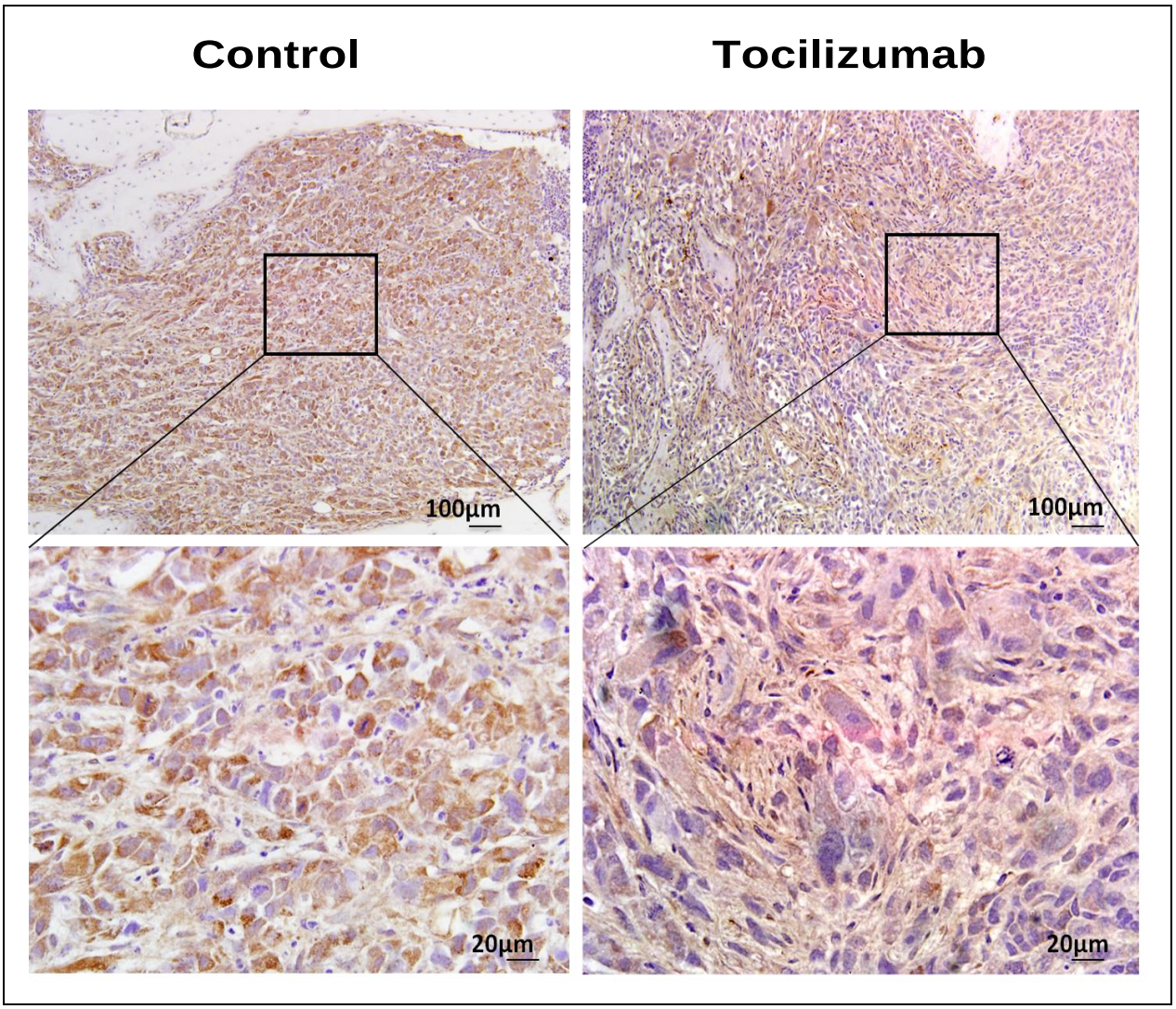

Fig. 3.8: Immunohistochemical Staining of Receptor Activator of Nuclear Factor Kappa B (RANK) in Bone Metastatic PC3 Tumors.
Representative RANK stained sections of PC3 tumors in tibiae of nude mice treated with placebo (control) or tocilizumab. The upper two images were magnified 100 times, the lower ones 400 times. The intensity of brown colored cells correlates positively with tumor RANK expression. The pictures illustrate that anti-IL-6 receptor therapy substantially decreased RANK production in PC3 cancer cells compared to untreated control mice.

3.9 Effects of Tocilizumab on Subcutaneous PC3 Tumor Growth

PC3 cells were inoculated subcutaneously at the flank of five-week-old male nude mice and treated for 58 days with tocilizumab (50 mg/kg/3days) to find out whether IL-6

receptor blockage has direct anti-tumor effects, i.e., tumor inhibitory actions that are not mediated by the tumor microenvironment. Seven days after subcutaneous tumor cell implantation, all animals developed palpable tumors. Neoplastic progression was measured every 3 days and cancer volumes were calculated by applying a formula described in materials and methods. Tumor mass (g) was determined following euthanasia of mice at day 58.

Compared to controls, therapy of mice with tocilizumab showed effects neither on tumor volume (Fig. 3.9A) nor on tumor mass (Fig. 3.9B), resulting in similar clinical tumor sizes. These outcomes indicate that blocking IL-6 receptor signaling in subcutaneous PC3 tumor lesions did not imply direct anti-tumor effects.

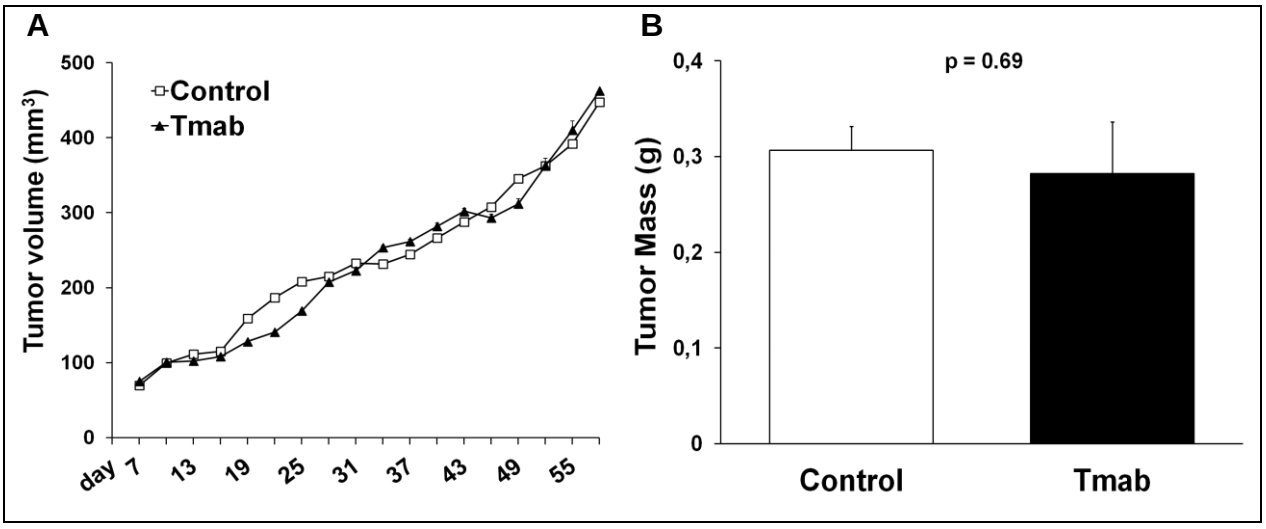

Fig. 3.9: Effects of Tocilizumab on Subcutaneous PC3 Tumor Growth.
(A) Analysis of subcutaneous tumor volume of nude mice treated with placebo (control) or tocilizumab (Tmab). Animals received tocilizumab (50 mg/kg) one day prior to tumor cell implantation and then every three days. Compared to controls, 58 days of anti-IL-6 receptor therapy had no effect on tumor volume (mm^3).
(B) Assessment of subcutaneous tumor mass of nude mice after 58 days of placebo or tocilizumab treatment. There is no difference in tumor mass (g) between the two groups after mice being sacrificed (p = 0.69). *Data are mean ± SEM (bars) and n = 10 mice in each group.*

3.10 Effects of Tocilizumab on Subcutaneous PC3 Tumor RANK Expression

Immunohistochemical RANK staining in subcutaneous PC3 tumors was conducted in order to compare RANK expression levels with those of PC3 bone metastasis. IL-6 receptor blockage appeared to have no effect on RANK synthesis in the subcutaneous mouse model, which contrasts with tocilizumab-induced inhibition of tumor RANK production in bone, indicating that the availability of bone cells is required to suppress RANK expression (Fig. 3.10).

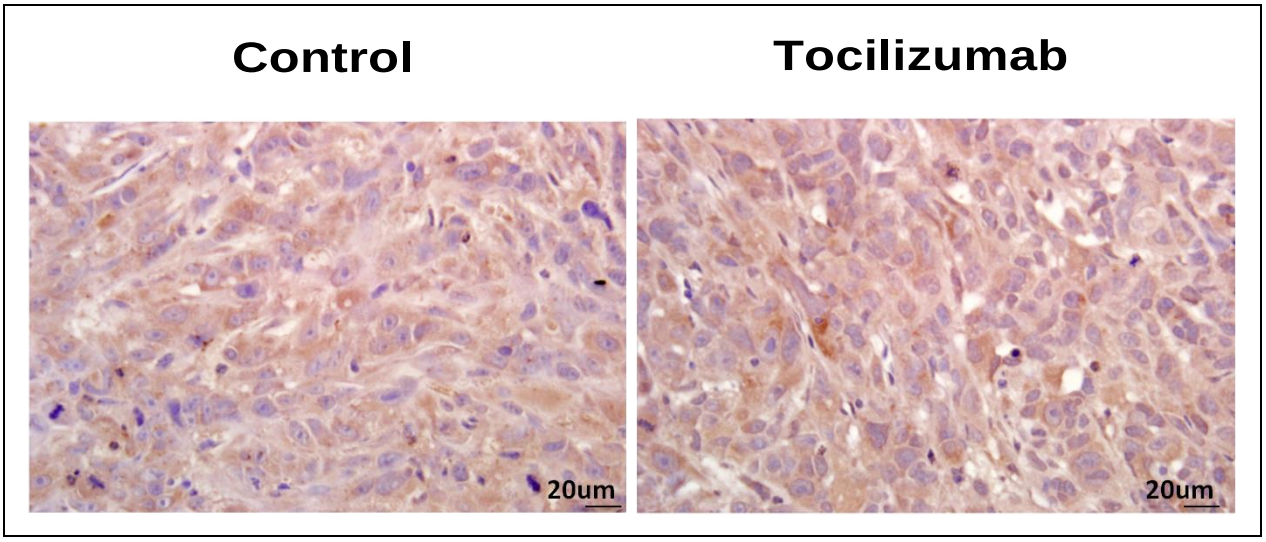

Fig. 3.10: Immunohistochemical Staining of Receptor Activator of Nuclear Factor Kappa B (RANK) in Subcutaneous PC3 Metastasis.
Representative RANK stained sections of subcutaneously inoculated PC3 tumors in nude mice after 58 days of treatment with placebo (control) or tocilizumab. The two images are magnified 400 times. The strength of brown colored cells correlates with tumor RANK expression. No difference in intensity of the brown color was observed when comparing the two pictures, suggesting that tocilizumab had no effect on RANK synthesis in subcutaneous PC3 cancers.

Chapter 4
Discussion

In the present study, we provide experimental evidence that cells of the osteoblast lineage communicate directly with prostate cancer cells by signaling through feed-forward loops that enhance tumor growth in bone. These signaling pathways mediate a complementary growth-stimulating function within the classical vicious cycle of bone metastasis as well as cancer cell migration and include cytokines such as IL-6, RANKL and RANK.

It is well accepted that the cytokine IL-6 acts within the bone microenvironment as an osteolytic factor by stimulating RANKL synthesis in osteoblast lineage cells. In the current study, we now demonstrate that autocrine IL-6 signaling in PC3 cells promotes RANK expression on the surface of these cells, sensitizing cancer cells to osteoblast-derived RANKL. Subsequent direct crosstalk between RANK-bearing tumor cells and RANKL-expressing osteoblasts increases IL-6 output levels by PC3 cells. As IL-6 stimulates RANK expression on neoplastic cells through *autocrine* IL-6 signaling and RANKL synthesis on osteoblasts via *paracrine* mechanisms, cancer-derived IL-6 creates the conditions required for its own synthesis, closing a feed-forward loop involving IL-6, RANKL and RANK (Fig. 4.1). Disruption of these self-amplifying signaling pathways significantly diminishes metastatic prostate cancer growth in bone in a xenograft mouse model.

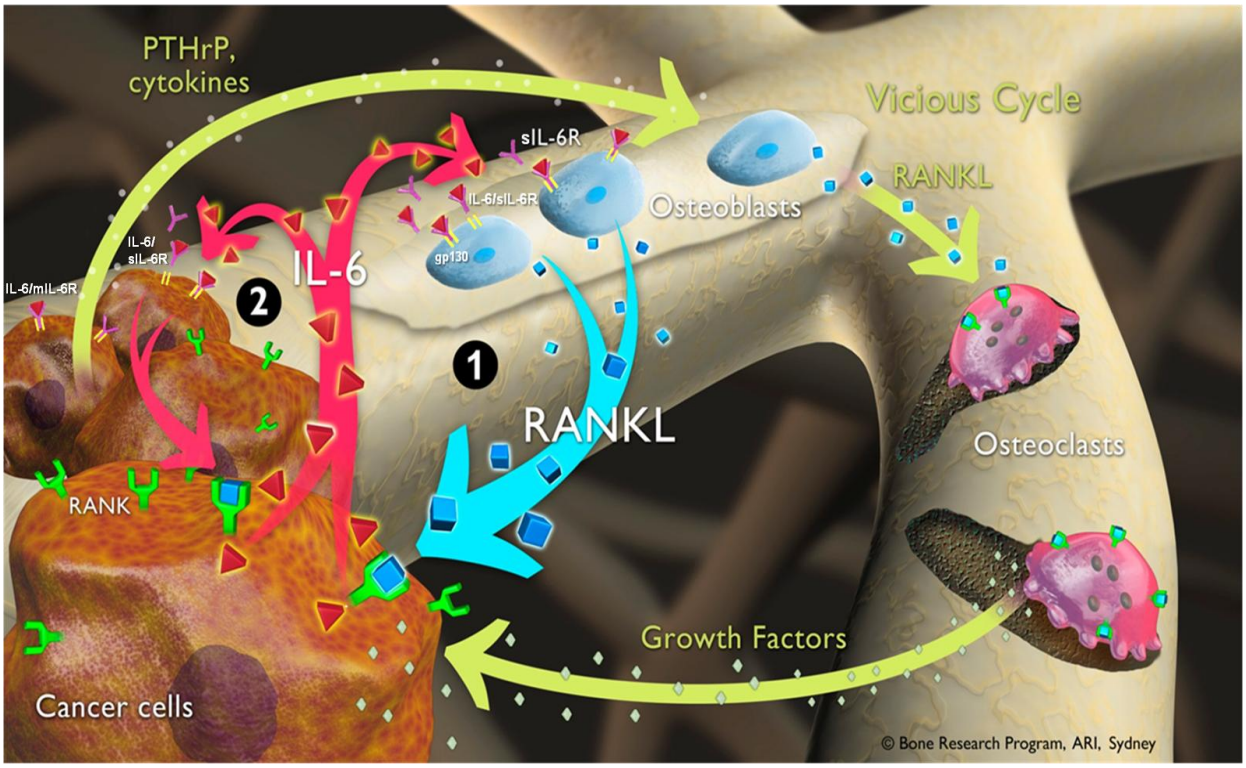

Fig. 4.1: IL-6/RANKL/RANK Autoamplification Loop Within the Classical Vicious Cycle of Bone Metastasis.

The proposed novel autocrine and paracrine signaling pathways are indicated by light red and blue arrows. The vicious cycle of bone metastatic growth is symbolized by yellow arrows. Osteolytic PC3 cells secrete large amounts of interleukin-6 (IL-6) into their environment, which then binds to IL-6 receptors, activating cancer cells and osteoblasts. Autocrine IL-6 signaling in neoplastic cells via the membrane-bound (mIL-6R) and/or soluble IL-6 receptor (sIL-6R) increases the expression of receptor activator of nuclear factor kappa B (RANK) [marked as number 2 in the figure], whereas the paracrine signal results in elevated synthesis of receptor activator of nuclear factor kappa B ligand (RANKL) in osteoblasts [marked as number 1 in the figure]. Augmented RANKL levels can either bind to RANK-bearing and thus sensitized tumor cells, conveying further amplification of the IL-6/RANKL/RANK feedforward loop as well as cancer cell migration or stimulate osteoclastogenesis and thus the release of tumor-promoting growth factors from the bone matrix. Autocrine IL-6 signaling in cancer cells also induces parathyroid hormone-related protein (PTHrP) production, enhancing cancer-induced bone breakdown. This illustration emphasizes the central role of the IL-6/RANKL/RANK triad within the framework of the “classical” vicious cycle of bone metastasis, stimulating bone erosion on the one hand, while mediating cancer cell migration on the other. Figure adapted from [59].

Multiple studies have shown that the cytokine IL-6 augments RANKL expression in osteoblast lineage cells [39, 101, 132], whereas *in vitro* treatment of PC3 cells with RANKL stimulates IL-6 synthesis [119, 131], closing a direct feed-forward loop between RANKL and IL-6. Since RANK is the only known activating receptor to RANKL, one can conclude that *in vitro* treatment of these cells with RANKL interacts with RANK, affecting in concert PC3 IL-6 output levels. In fact, Armstrong *et al.* demonstrate that *in vitro* activation of RANK by RANKL upregulates IL-6 protein levels 4-fold in PC3 cells [119]. Accordingly, Zheng *et al.* report that treatment of PC3 RANK-knockdown cells with RANKL strongly decreases IL-6 synthesis compared to RANK-expressing PC3 cells [131]. In addition to the effect of IL-6 on osteoblastic RANKL expression, we wondered whether PC3-derived IL-6 is also able to stimulate autocrine RANK production which would sensitize tumor cells to direct RANKL-RANK interaction with the host bone microenvironment. This setting would in fact represent an effective tool of adaptation for tumor cells within its new environment, a mechanism occasionally designated as osteomimicry.

To support our hypothesis, we show that IL-6 treatment induces RANK mRNA expression *in vitro* and that IL-6 receptor inhibition via tocilizumab reduces this effect. To examine the expression of RANK *in vivo*, immunohistochemistry from PC3-derived bone tumors was performed. There, we see a net decrease of tumor RANK production in tocilizumab-treated mice compared to controls, revealing that inhibition of autocrine IL-6 receptor signaling clearly affects tumor RANK synthesis *in vivo.* Moreover, we demonstrate that tocilizumab reduces circulating RANKL levels and osteoclast numbers in bone, which led us to formulate a refined model of the vicious cycle of bone metastasis: since autocrine IL-6 receptor inhibition in PC3 cells via tocilizumab results in reduced *in vitro* and *in vivo* tumor RANK expression levels, diminishing in concert with reduced serum RANKL levels the probability of a RANKL-RANK interaction between tumor and bone cells and therefore tumor-induced IL-6 production, it thus appears that the triad of IL-6/RANKL/RANK gives rise to a bone-specific feed-forward loop that results in a strong upregulation of all three parameters. In other words, autocrine IL-6 signaling in PC3 cells increases tumor RANK expression and serves as a sensitizer for direct RANKL-RANK crosstalk with osteoblasts, leading to elevated tumor IL-6 output levels. As IL-6 also induces RANKL synthesis on osteoblasts via paracrine signaling, tumor-derived IL-6 creates the conditions required for its own synthesis, closing an

IL-6/RANKL/RANK-loop. This cytokine can thus be considered as a molecule that mediates direct communication between invading cancer and resident osteoblastic/stromal cells. According to this notion, antagonizing autocrine IL-6 receptor signaling in PC3 cells via tocilizumab disrupts this autoamplification loop by downregulating all three parameters.

The growth-promoting effect of this molecular triad appears to be dependent on the presence of the bone microenvironment, since tocilizumab did not alter tumor growth in subcutaneous PC3 metastases. In line with our data, Zaki and coworkers found no difference in tumor volume and tumor weight compared to controls when they treated subcutaneous PC3 tumors in nude mice with the chimeric antibody siltuximab (CNTO 328), a potent inhibitor of human IL-6 [133]. The cause for the apparent tissue-dependent effect of IL-6 receptor inhibition could be attributed to the availability of RANKL. RANKL is present at high levels within the bone environment and is mostly derived from cells of the osteoblast lineage and activated T-cells [131]. Since athymic nude mice lack T-cells and since the cancer cells used in our studies do not synthesize RANKL [119], we conclude that RANKL is mainly expressed by osteoblasts in the setting of our studies.

The significantly reduced availability of RANKL within the subcutaneous environment appears to be the key reason why tocilizumab failed to inhibit subcutaneous PC3 tumor growth: less RANKL results in less RANKL-RANK interaction and therefore in less tumor-derived IL-6 secretion which, in turn, leads to reduced *autocrine* RANK and *paracrine* RANKL production. The finding that tocilizumab had no effect on RANK expression in subcutaneous PC3 tumors indicates that the amplifying effect of this molecular triad does not operate in soft tissue metastases. The existence of RANKL within the surrounding tumor environment determines whether or not this autoamplification loop is brought into action. In short: If RANKL is absent, this triad cannot be activated.

Supporting data comes from Morrissey and colleagues who demonstrated in a murine model by immunohistochemical staining that IL-6 expression was far more pronounced in intra-tibial PC3 tumors compared to subcutaneous PC3 metastases. They also performed immunohistochemistry on samples of patients with bone and soft tissue metastases due to prostate cancer to analyze the production of IL-6. There, they

estimated the intensity of IL-6 staining in RANKL-rich bone lesions to be 51 times stronger than that of RANKL-poor soft tissue metastases [134]. These findings are consistent with previously published results reporting that the concentration of IL-6 is significantly elevated in patients with osseous metastasis compared to ones with soft tissue or without bone metastases [74, 135]. However, it is unclear whether tumor growth in soft tissues may be suppressed by tocilizumab in immune competent mice, in which activated T-cells may synthesize RANKL to enable the interaction between RANKL-RANK and IL-6 from implanted tumors [131].

The boost of tumor-derived IL-6 expression within bone via the proposed IL-6/RANKL/RANK autoamplification loop has two major pathophysiological consequences: First, it mediates further bone destruction and secondly, the axis conveys migration of tumor cells and therefore metastatic cell behavior.

1) The quintessence of the vicious cycle of bone metastasis is the assumption that tumor expansion in bone mainly depends on its ability to induce osteolysis. With the successful creation of this cycle, metastatic cancer cells ensure their own nutritive supply, enabling proliferation and cell survival. Increased bone catabolism represents the linchpin of neoplastic growth and therefore the major strategy of cancer cells to prosper in bone. Studies have shown that IL-6 fosters bone destruction via effects on the OPG/RANKL/RANK-system, in particular, by increasing RANKL expression on osteoblastic and stromal cells [35, 39, 101, 132]. It is worth mentioning that IL-6 also promotes the production of other osteolytic factors such as PTHrP [70, 136], IL-1 [102, 136] and COX2/PGE2 [70, 136, 137]. As a matter of fact, we demonstrate in this thesis that treatment of PC3 cells with human IL-6 upregulates PTHrP expression *in vitro.* PTHrP is a well-known osteolytic factor and plays a significant role in the process of bone cancer lesions. In breast cancer bone metastases, the prototype of osteolytic tumors, PTHrP appears to function as the main mediator of osteoclast activation and bone degradation through upregulation of RANKL and downregulation of OPG by osteoblasts [39, 138]. Likewise, IL-6 also enhances PGE2 expression and vice versa and PGE2 has been shown to amplify osteoclast formation by signaling through the RANKL/RANK/OPG pathway as well [137]. Studies suggest that IL-6 functions as the mediator of PGE2-

induced suppression of OPG production by osteoblasts [72, 137]. Interestingly, RANKL-independent stimulation of bone resorption by IL-6 has also been postulated [103, 104]. The bottom line is that any of these IL-6-related mechanisms promotes tumor growth in bone by enhancing the vicious cycle of bone metastasis.

2) Previous data have demonstrated that RANKL-RANK signaling activates a number of crucial transcription factors that control the formation of epithelial-to-mesenchymal transition (EMT), osteomimicry as well as stem cell properties [139]. EMT is a physiological cellular program, normally involved in steps of embryogenesis and wound healing that tumor cells acquire to develop a migratory and invasive phenotype [37, 140]. Armstrong *et al.* have shown that RANK activation in PC3 cells via RANKL results in an upregulation of a cocktail of key genes involved in migration, chemotaxis and invasion, including IL-6, MMP-9, IL-1, TNF-alpha, GM-CSF, VEGF-A and members of the CXC chemokine family [119]. Similarly, RANKL-RANK signaling in a lymph node metastatic prostate cancer cell line (LNCaP) is capable of inducing a more aggressive cell behavior, resulting in increased cell motility, migration and invasion [139]. Moreover, the rich source of RANKL within bone may act as a “soil” factor to RANK-expressing tumor cells, facilitating the development of bone metastases [119, 141]. Accordingly, a high concordance of RANK-producing primary tumors and corresponding bone metastatic lesions has been reported [142]. In addition, blocking the RANKL-RANK signaling pathway *in vivo* via OPG significantly decreased osseous tumor burden in a melanoma model that does not trigger osteoclast activation [141]. This setting is interesting because it allowed Jones and coworkers to differentiate between *direct* effects of RANKL on tumor cells and *indirect* effects on osteoclasts. Since RANKL is not consumed for osteoclastogenesis in this setting, the results suggest that bone-derived RANKL acts *directly* on RANK-expressing melanoma cells through activation of cell motility [119, 141]. As neoplastic cells apply physiological mechanisms, it is not surprising to find RANKL-induced cell migration in normal, non-transformed cells as well. As such, RANKL causes mature osteoclasts to migrate towards a RANKL source [141]. In this context, direct crosstalk between cancer cells and osteoblast lineage cells through RANKL-RANK interaction may mediate cytoskeletal changes, triggering directional motility of cancer cells.

From these thoughts, we can recognize that autocrine/paracrine IL-6 receptor signaling kills two birds with one stone, meaning that activation of these signals promotes bone resorption on the one hand, while conveying cancer cell invasion on the other. By upregulating RANKL on osteoblasts either by paracrine IL-6 signaling or through the release of PTHrP, neoplastic cells initiate and maintain bone destruction, assuring their nutritive supply and space for migrating cancer cells. As autocrine IL-6 signaling induces RANK, cancer cells are sensitized for RANKL-RANK-regulated cell migration, filling in the spaces bone-resorbing osteoclasts created. These effects go hand in hand and are complementary.

As downstream signaling pathways of RANK are frequently involved in cell proliferation, one could assume that direct crosstalk increases cancer cell proliferation in bone, rendering tumor cells (more) independent from growth factors released during bone resorption. However, this mechanism does not seem to be operational since the combination with tocilizumab and zoledronic acid did not result in additive and/or synergistic effects in the course of our studies. In line with our interpretation, other research teams have reported that RANKL had no effect on proliferation or death on RANK-positive tumor cells [143]. It is thus important to understand that the proposed IL-6/RANKL/RANK axis forms a *complementary* and *amplifying* element for growth stimulation within the framework of the “classical” vicious cycle with bone resorption being the critical mediator influencing tumor growth. Direct crosstalk between tumor cells and osteoblasts might be of particular relevance during *early* stages of metastasis when local cell populations and cytokine concentrations are still low [59]. It may function as a mechanism to accumulate local IL-6 that initiates bone resorption to feed the incoming tumor “seed”. As this feedforward loop also mediates cancer cell migration, which accelerates tumor expansion in bone, direct crosstalk may represent a rationale for the observed increased growth kinetics of bone metastases at *late* stages of the disease. As the present study reveals that blocking RANKL-RANK interaction may offer a new therapeutic approach, it is of particular interest to notice that denosumab, a human monoclonal antibody to RANKL, represented a more effective therapy in a phase 3 study for the prevention of skeletal-related events in bone metastatic prostate cancer patients than zoledronic acid [144]. Our proposed mechanism of direct crosstalk between tumor cells and osteoblasts might be one factor amongst others why

denosumab is of greater clinical benefit as opposed to the current standard of care zoledronic acid.

It should be mentioned, however, that the bisphosphonate zoledronic acid, compared to tocilizumab, represents a slightly more effective medication in reducing tumor burden and preserving bone structure. Comparing both drugs, two major differences are found: first, zoledronic acid is almost twice as potent in limiting osteoclast numbers at the tumor-bone interface, secondly, the bisphosphonate is about 1.5 times more effective in inducing cancer cell apoptosis. The first finding is not surprising. Zoledronic acid is a potent nitrogen-containing bisphosphonate and represents the standard therapy for patients with pathological bone loss, leading to a strong inhibition of bone resorption through induction of apoptosis in osteoclasts. The second result underlines the pivotal role of the growth factors released by bone resorption even in cancer survival and inhibition of apoptosis, yet, direct anti-tumor actions by zoledronic acid cannot be excluded. In fact, it has recently been suggested that zoledronic acid exerts direct anti-tumor effects, however, an animal study of bone metastatic breast cancer cells conducted in our own laboratory indicated that nitrogen-containing bisphosphonates (exemplified by ibandronate) mediate their tumor inhibitory effects primarily through inhibition of bone resorption rather than direct cytotoxicity [108].

Combined treatment with tocilizumab and zoledronic acid did not result in additive and/or synergistic effects. The effects on tumor growth were associated with increased tumor cell apoptosis and decreased cell proliferation but no evident additive effects on tumor growth, apoptosis or proliferation rate were detected. The lack of additive effects with combination treatments indicates that both agents block PC3 cell tumor growth in bone by a common mechanism, and this occurs *indirectly*, predominantly through the inhibition of bone resorption. The indirect anti-tumor effects of tocilizumab can be explained with the disruption of our proposed bone-specific IL-6/RANKL/RANK loop, resulting in less osteoclast-mediated bone degradation and cancer cell migration. Moreover, tocilizumab failed to reduce tumor growth rates in subcutaneous PC3 metastases, which leads to the conclusion that the antibody lacks direct anti-tumor effects in our study.

However, as these direct tumor inhibitory actions by tocilizumab cannot be ruled out completely, growth-stimulatory effects, such as improved proliferation and evasion of apoptosis in response to autocrine IL-6 signaling have to be taken into consideration. It has been shown that many cancer cells generate their own growth signals, decreasing their dependence on stimulation from the surrounding environment. Different groups have recently postulated that endogenously produced IL-6 by prostate cancer cells results in the acquisition of a growth advantage compared to non-IL-6 secreting parental cells [80-82]. Clinically, elevated and autocrine synthesis of IL-6 correlates with progression and metastasis of prostate cancer [145]. Since PC3 cells secrete large amounts of IL-6 and express the corresponding membrane-bound as well as soluble IL-6 receptor, it is generally assumed that this cytokine acts as an autocrine growth factor on these cells [81, 86].

As tumor growth not only depends on the rate of cell proliferation but also on the rate of cell death, acquiring resistance to apoptosis is fundamental to cancer progression and a hallmark of probably all types of neoplasias [38]. Experiments show that IL-6 is capable of upregulating anti-apoptotic members of the Bcl-2 family, such as Mcl-1 [84] and Bcl-xL [85] in IL-6 secreting prostate cancer cell lines. In addition, IL-6 confers resistance to cytotoxic agent-induced apoptosis in PC3 cells [85, 86]. In the same way, IL-6 is a well-known inducer of paclitaxel resistance in breast cancer [89].

According to this logic, simultaneous administration of tocilizumab and zoledronic acid should have acted synergistically because both drugs would block tumor growth by different mechanisms: zoledronic acid would inhibit tumor growth indirectly by suppressing osteoclast-mediated bone breakdown, while tocilizumab would inhibit cancer expansion directly by stimulating PC3 cell apoptosis and blocking cell proliferation. However, as IL-6 receptor inhibition showed neither additive effects in the combination with zoledronic acid in bone metastatic lesions nor did the medication alone reduce cancer spread in subcutaneous PC3 metastases, it remains very unlikely that tocilizumab mediates direct anti-tumor effects in our experiments.

Over the past decade, neoplastic lesions have increasingly been considered as complex organs, which are composed of a heterogeneous amount of cancer cells and a stroma that includes immune cells, fibroblasts and endothelial cells, representing the “other half” of the tumor [37]. The role of the immune system in cancer progression

appears to be a double-edged sword, conveying anti-tumor effects on the one hand, while supporting its progression on the other. The multifunctional cytokine IL-6 has been shown to fulfill immune evasive functions by favoring the accumulation of regulatory T-cells (Tregs) [146], while constructing, in concert with other cytokines, a tumor-stimulating TH17 immune response [147]. Since athymic nude mice exhibit a deficiency in T-cells, the effects mentioned above appear negligible in our study. However, it should be considered that although some components of the immune system are missing, B-cells, dendritic cells and granulocytes are all relatively intact, and that there is a compensatory increase in both natural killer cells (NK cells) and macrophages in nude mice [148]. The transcription factor STAT3 has been shown to function as a point of convergence for various oncogenic signaling pathways that is constitutively activated both in tumor and immune cells in the tumor environment [146]. As a STAT3 activator, IL-6 could function as immunological brakes in macrophages, NK cells and neutrophils by reducing their cytotoxic anti-tumor immune responses [146]. Increased STAT3 activity also promotes the generation of immature dendritic cells in the tumor microenvironment [146]. Moreover, the recruitment of tumor-associated macrophages (TAMs) by IL-6 could propagate the development of a tumor-friendly environment: these cells mediate immunosuppressive functions [149] as well as trophic activities [149, 150] on cancer cells.

NFκB represents another important transcription factor, which has been shown to be crucial for the initiation and progression of tumor-promoting inflammation [146]. This transcription factor can be activated by more than 150 stimuli and the pro-inflammatory cytokine IL-6 is one of them [151]. Studies have demonstrated that constitutively active NFκB within the inflammatory environment is linked to the upregulation of anti-apoptotic, pro-proliferative and angiogenic factors [146]. In addition, inflammatory mediators downregulate DNA repair pathways and cell cycle checkpoints, elevating the mutation rate within inflamed tissues 4-fold compared to normal milieus, hence contributing to the accumulation of random genetic alterations [152].

The suppression of these immune-mediated tumor-stimulating effects through downregulation of tumor-derived IL-6 via tocilizumab might have contributed to decrease PC3 cancer growth in bone, however, it is unlikely that they played a major role due to T-cell deficiency. It is difficult to estimate the full extent of the function of IL-6

on tumor-promoting inflammation and immunoevasion because these issues remain mostly unresolved.

We can recognize that the multifunctional cytokine IL-6 supports bone cancer metastasis in multiple ways and might thus represent an interesting target for drug therapy. To date, there exists no official data for the efficacy of tocilizumab in restraining the progression of prostate cancer bone metastasis. Our animal study represents to our knowledge the first evidence that this antibody retards the growth of osteolytic prostate cancer lesions. Since tocilizumab could inhibit autocrine *and* paracrine IL-6 receptor signaling in *human* bone metastatic disease, this antibody might in fact constitute a potential therapeutic agent.

Even though bone metastases in prostate cancer display a predominantly osteoblastic appearance, osteolytic changes usually precede bone formation, and elevated bone breakdown remains a dominant feature of metastatic prostate cancer [56]. Inhibition of bone degradation with anti-resorptive medications has been shown to significantly delay skeletal-related events in patients with advanced prostate cancer, emphasizing the fundamental role of bone resorption in the growth even of osteoblastic metastases [131]. Therefore, findings from a predominantly osteolytic cancer cell line such as PC3 are of clinical relevance for the treatment of osteoblastic tumors [131]. According to the literature, it is important to get at least a 50 % inhibition in tumor growth in mouse models in order to predict clinical responses in patients [148]. The presented thesis fulfills this demand, yet, the neutralizing antibody did not stop the osteolytic process. This is not unexpected. Other factors in addition to IL-6 are also involved in bone resorption and in fact, IL-6 maintains many reciprocal interrelations with other pro-resorptive cytokines, forming a whole network in which they often act in synergism [153].

As animal trials have limitations, any study in immunodeficient mice must consider several points when one attempts to extrapolate findings to other xenograft mouse models or even humans [154]. First, as we only used one osteotropic prostate cancer cell line in our studies, the results obtained cannot automatically be generalized for other osteolytic cancers and require further research to be confirmed. Secondly, it is

now well established that tumor cell lines can bear little resemblance to primary cancers [154], an important argument why many mouse xenotransplantation models are rarely predictive of a clinical response in patients. Thirdly, the mouse xenograft model may mimic certain steps of bone cancer metastasis but it does not represent the exact conditions in humans owing to species difference, course of progression and lack of immune responses.

In summary, we have identified a self-amplifying signaling triad, involving IL-6, RANKL and RANK that drives prostate cancer growth in bone. Our results bring new insight into the pathogenic mechanisms of IL-6 in osteolytic prostate cancer bone metastasis, albeit further research needs to be done in order to elucidate and define the complex role of this cytokine. Future studies should aim to confirm a causal relationship between autocrine IL-6 receptor inhibition and reduced activation of the IL-6/RANKL/RANK triad and to further define the effects of IL-6 on the tumor microenvironment. In this context, it might be interesting to see whether specific blockage of IL-6 trans-signaling may differ from global inhibition of IL-6 activity. Overall, our findings demonstrate the importance of autocrine/paracrine IL-6 signaling in supporting prostate cancer growth in bone and provide a rationale for the concept that abrogation of this signal may represent a beneficial strategy for the treatment of patients with prostate cancer bone metastasis.

Chapter 5
Conclusions and Future Directions

The present study demonstrates that PC3 prostate cancer cells communicate directly with osteoblasts through a molecular triad that consists of IL-6, RANKL and RANK. This axis functions as a complementary autoamplification loop within the “classical” vicious cycle of bone metastasis driving prostate cancer cell growth in bone. The major aim of this study was to investigate **how** the cytokine IL-6 affects bone metastatic prostate cancer growth. To address this question, *in vitro* experiments and a rodent model of malignant bone as well as subcutaneous disease were employed.

The goal was to investigate whether the tumor-promoting effects of IL-6 are due to direct actions on the tumor or to indirect effects mediated by the bone microenvironment. By comparing the anti-tumor effects of tocilizumab with zoledronic acid, either dosed alone or in combination, this thesis evaluates how inhibition of autocrine IL-6 receptor signaling impacts prostate cancer cell growth in bone. The subcutaneous xenograft murine model was used to answer the question whether tocilizumab shows direct anti-tumor effects, that is, if PC3 tumors respond to treatment without the presence of the bone microenvironment.

The selected doses of tocilizumab were efficacious in significantly decreasing cancer expansion and bone breakdown in metastatic PC3 lesions compared to controls. The effects on tumor growth were associated with diminished cancer cell proliferation and increased tumor cell apoptosis. Regarding the effect on bone homeostasis, therapy with tocilizumab was associated with reduced parameters of bone resorption. The nitrogen-containing bisphosphonate zoledronic acid also represents an effective medication plan to diminish neoplastic burden and to preserve bone structure and architecture. Zoledronic acid treated mice exhibited a similar decrease in overall tumor area and osteolysis. Higher doses of zoledronic acid were administered in order to assure profound inhibition of cancer-induced bone erosion and to distinguish between direct and indirect effects of IL-6 on tumor growth. Simultaneous application of tocilizumab and zoledronic acid did not result in additive and/or synergistic effects.

Decreased PC3 tumor growth in bone in response to tocilizumab treatment may have several causes:

1) Inhibition of the vicious cycle of bone metastasis is very likely to be the main mechanism for the anti-tumor effects of tocilizumab. In this thesis, I present the following evidence to support this notion.

   First, the triad of L-6, RANKL and RANK forms a self-amplifying signaling pathway within the bone microenvironment by which prostate cancer cells communicate directly with osteoblasts. *Paracrine* IL-6 signaling promotes RANKL expression on osteoblasts while the *autocrine* signal stimulates RANK synthesis on PC3 cancer cells, sensitizing neoplastic cells to direct RANKL-RANK interaction which, in turn, enhances tumor IL-6 output levels. Direct crosstalk between RANK-expressing cancer cells and RANKL-producing osteoblasts promotes PC3 cancer growth in bone by supporting tumor-induced bone resorption and cancer cell migration. Treatment with tocilizumab interrupts this autoamplification loop by downregulating tumor RANK expression. Less RANK results in less RANKL-RANK interaction between osteoblasts and tumor cells and therefore in less tumor-derived IL-6 secretion. The IL-6/RANKL/RANK axis can thus be interpreted as an additional signaling pathway within the “classical” vicious cycle of bone metastasis.

   Secondly, autocrine IL-6 signaling increases PTHrP synthesis in PC3 cells *in vitro* and tocilizumab reverses this effect, offering an indirect mechanism by which IL-6 promotes osteoclastic bone destruction through the release of a well-known osteolytic factor.

2) Direct anti-tumor effects by tocilizumab may have participated to reduce tumor proliferation. However, since the combined treatment of tocilizumab and zoledronic acid did not result in additive and/or synergistic effects, direct cancer inhibitory actions by tocilizumab do not appear as a reasonable explanation. Moreover, tocilizumab therapy failed to decrease neoplastic growth rates in a subcutaneous xenograft mouse model, strongly suggesting that abrogation of autocrine IL-6 receptor signaling lacks direct anti-tumor effects at the doses tested. Apparently, tocilizumab requires the presence of the bone microenvironment to mediate its anti-tumor actions. This assumption leads to the conclusion that the tumor inhibitory

effects of tocilizumab are conveyed mainly indirectly, namely by the inhibition of communication between cancer and bone cells, nevertheless, direct anti-tumor effects cannot be ruled out completely.

3) The inhibition of immune-mediated tumor-promoting effects by IL-6 may have contributed to retarding tumor expansion in bone. The multifunctional cytokine IL-6 has been shown to support cancer-promoting inflammation [146, 147, 152] as well as evasion from anti-tumor immune responses [146]. As PC3 bone metastases were established in athymic nude mice that lack T-cell-mediated immune reactions, it is unlikely that these anti-tumor effects had a significant impact in this study, however, it is difficult to estimate the full extent of the effects of IL-6 on these issues because they remain to be investigated.

Further studies are required to define the complex role of IL-6 in the tumor microenvironment and to confirm a causal relationship between autocrine IL-6 receptor inhibition and reduced activation of the IL-6/RANKL/RANK triad. In this context, it might be interesting to see whether specific blockage of IL-6 trans-signaling may differ from global inhibition of IL-6 activity. Collectively, our results bring new insight into the pathogenic mechanisms of IL-6 in prostate cancer bone metastasis. In this thesis, I have shown the importance of *autocrine* and *paracrine* IL-6 signaling in supporting prostate cancer growth in bone and the findings provide a rationale for the concept that abrogation of this signal may represent a beneficial future strategy for the treatment of patients with prostate cancer bone metastasis. Taken together, this thesis represents a comprehensive investigation of the tumor-promoting role of IL-6 in the pathogenesis of osteolytic bone metastasis due to prostate cancer.

Chapter 6

References / Literaturverzeichnis

[1] Brandi ML. Microarchitecture, the key to bone quality. Rheumatology (Oxford). 2009;48 Suppl 4:iv3-8.

[2] Leonhardt H, Tillmann B, Töndury G, Zilles K, editors. Anatomie des Menschen Lehrbuch und Atlas. 3rd ed. Stuttgart: Georg Thieme; 2003. p. 46-81

[3] Seeman E, Delmas PD. Bone quality--the material and structural basis of bone strength and fragility. N Engl J Med. 2006;354(21):2250-61.

[4] Welsch U. Lehrbuch Histologie. 2nd ed. München: Elsevier Urban & Fischer; 2006.

[5] Long F. Building strong bones: molecular regulation of the osteoblast lineage. Nat Rev Mol Cell Biol. 2012;13(1):27-38.

[6] Wang Y, Li YP, Paulson C, Shao JZ, Zhang X, Wu M, et al. Wnt and the Wnt signaling pathway in bone development and disease. Front Biosci (Landmark Ed). 2014;19:379-407.

[7] Sims NA, Vrahnas C. Regulation of cortical and trabecular bone mass by communication between osteoblasts, osteocytes and osteoclasts. Arch Biochem Biophys. 2014;561:22-8.

[8] Del Fattore A, Teti A, Rucci N. Bone cells and the mechanisms of bone remodelling. Front Biosci (Elite Ed). 2012;4:2302-21.

[9] Franz-Odendaal TA, Hall BK, Witten PE. Buried alive: how osteoblasts become osteocytes. Dev Dyn. 2006;235(1):176-90.

[10] Bonewald LF. Osteocytes as dynamic multifunctional cells. Ann N Y Acad Sci. 2007;1116:281-90.

[11] Schaffler MB, Cheung WY, Majeska R, Kennedy O. Osteocytes: master orchestrators of bone. Calcif Tissue Int. 2014;94(1):5-24.

[12] Rochefort GY, Pallu S, Benhamou CL. Osteocyte: the unrecognized side of bone tissue. Osteoporos Int. 2010;21(9):1457-69.

[13] Bonewald LF. The amazing osteocyte. J Bone Miner Res. 2011;26(2):229-38.

[14] Boyce BF. Advances in the regulation of osteoclasts and osteoclast functions. J Dent Res. 2013;92(10):860-7.

[15] Teitelbaum SL. Bone resorption by osteoclasts. Science. 2000;289(5484):1504-8.

[16] Cappariello A, Maurizi A, Veeriah V, Teti A. The Great Beauty of the osteoclast. Arch Biochem Biophys. 2014;558:70-8.

[17] Deetjen P, Speckmann EJ, Hescheler J, editors. Physiologie. 4th ed. München: Elsevier Urban & Fischer; 2005. p. 194

[18] Dougall WC, Chaisson M. The RANK/RANKL/OPG triad in cancer-induced bone diseases. Cancer Metastasis Rev. 2006;25(4):541-9.

[19] Sims NA, Martin TJ. Coupling the activities of bone formation and resorption: a multitude of signals within the basic multicellular unit. Bonekey Rep. 2014;3:481.

[20] Matsuo K, Irie N. Osteoclast-osteoblast communication. Arch Biochem Biophys. 2008;473(2):201-9.

[21] Eriksen EF. Cellular mechanisms of bone remodeling. Rev Endocr Metab Disord. 2010;11(4):219-27.

[22] Andersen TL, Hauge EM, Rolighed L, Bollerslev J, Kjaersgaard-Andersen P, Delaisse JM. Correlation between absence of bone remodeling compartment canopies, reversal phase arrest, and deficient bone formation in post-menopausal osteoporosis. Am J Pathol. 2014;184(4):1142-51.

[23] Delaisse JM. The reversal phase of the bone-remodeling cycle: cellular prerequisites for coupling resorption and formation. Bonekey Rep. 2014;3:561.

[24] Zupan J, Jeras M, Marc J. Osteoimmunology and the influence of pro-inflammatory cytokines on osteoclasts. Biochem Med (Zagreb). 2013;23(1):43-63.

[25] Walsh MC, Choi Y. Biology of the RANKL-RANK-OPG System in Immunity, Bone, and Beyond. Front Immunol. 2014;5:511.

[26] Blair JM, Zhou H, Seibel MJ, Dunstan CR. Mechanisms of disease: roles of OPG, RANKL and RANK in the pathophysiology of skeletal metastasis. Nat Clin Pract Oncol. 2006;3(1):41-9.

[27] Theoleyre S, Wittrant Y, Tat SK, Fortun Y, Redini F, Heymann D. The molecular triad OPG/RANK/RANKL: involvement in the orchestration of pathophysiological bone remodeling. Cytokine Growth Factor Rev. 2004;15(6):457-75.

[28] Schoppet M, Preissner KT, Hofbauer LC. RANK ligand and osteoprotegerin: paracrine regulators of bone metabolism and vascular function. Arterioscler Thromb Vasc Biol. 2002;22(4):549-53.

[29] Udagawa N, Takahashi N, Yasuda H, Mizuno A, Itoh K, Ueno Y, et al. Osteoprotegerin produced by osteoblasts is an important regulator in osteoclast development and function. Endocrinology. 2000;141(9):3478-84.

[30] Baud'huin M, Duplomb L, Teletchea S, Lamoureux F, Ruiz-Velasco C, Maillasson M, et al. Osteoprotegerin: multiple partners for multiple functions. Cytokine Growth Factor Rev. 2013;24(5):401-9.

[31] Malliga DE, Wagner D, Fahrleitner-Pammer A. The role of osteoprotegerin (OPG) receptor activator for nuclear factor kappaB ligand (RANKL) in cardiovascular pathology - a review. Wien Med Wochenschr. 2011;161(23-24):565-70.

[32] Roodman GD, Windle JJ. Paget disease of bone. J Clin Invest. 2005;115(2):2008.

[33] Danks L, Takayanagi H. Immunology and bone. J Biochem. 2013;154(1):29-39.

[34] Baud'huin M, Lamoureux F, Duplomb L, Redini F, Heymann D. RANKL, RANK, osteoprotegerin: key partners of osteoimmunology and vascular diseases. Cell Mol Life Sci. 2007;64(18):2334-50.

[35] Liu XH, Kirschenbaum A, Yao S, Levine AC. The role of the interleukin-6/gp130 signaling pathway in bone metabolism. Vitam Horm. 2006;74:341-55.

[36] Mukherjee S. Der König aller Krankheiten: Krebs – eine Biographie. Köln: Dumont; 2012.

[37] Hanahan D, Weinberg RA. Hallmarks of cancer: the next generation. Cell. 2011;144(5):646-74.

[38] Hanahan D, Weinberg RA. The hallmarks of cancer. Cell. 2000;100(1):57-70.

[39] Mundy GR. Metastasis to bone: causes, consequences and therapeutic opportunities. Nat Rev Cancer. 2002;2(8):584-93.

[40] Weilbaecher KN, Guise TA, McCauley LK. Cancer to bone: a fatal attraction. Nat Rev Cancer. 2011;11(6):411-25.

[41] Coleman RE. Skeletal complications of malignancy. Cancer. 1997;80(8 Suppl):1588-94.

[42] Culig Z, Steiner H, Bartsch G, Hobisch A. Interleukin-6 regulation of prostate cancer cell growth. J Cell Biochem. 2005;95(3):497-505.

[43] seer.cancer.gov [Internet]. Bethesda: National Cancer Institute; [cited 2015 May 9]. http://seer.cancer.gov/statfacts/html/prost.html

[44] Walsh PC. Using prostate-specific antigen to diagnose prostate cancer: sailing in uncharted waters. Ann Intern Med. 1993;119(9):948-9.

[45] Feldman BJ, Feldman D. The development of androgen-independent prostate cancer. Nat Rev Cancer. 2001;1(1):34-45.

[46] Gartrell BA, Saad F. Managing bone metastases and reducing skeletal related events in prostate cancer. Nat Rev Clin Oncol. 2014;11(6):335-45.

[47] Jin JK, Dayyani F, Gallick GE. Steps in prostate cancer progression that lead to bone metastasis. Int J Cancer. 2011;128(11):2545-61.

[48] Eaton CL, Coleman RE. Pathophysiology of bone metastases from prostate cancer and the role of bisphosphonates in treatment. Cancer Treat Rev. 2003;29(3):189-98.

[49] Saad F, McKiernan J, Eastham J. Rationale for zoledronic acid therapy in men with hormone-sensitive prostate cancer with or without bone metastasis. Urol Oncol. 2006;24(1):4-12.

[50] Coleman RE, Guise TA, Lipton A, Roodman GD, Berenson JR, Body JJ, et al. Advancing treatment for metastatic bone cancer: consensus recommendations from the Second Cambridge Conference. Clin Cancer Res. 2008;14(20):6387-95.

[51] Coleman RE. Clinical features of metastatic bone disease and risk of skeletal morbidity. Clin Cancer Res. 2006;12(20 Pt 2):6243s-9s.

[52] Bronner F, Farach-Carson MC, Rubin J, editors. Bone resorption. 1st ed. London: Springer; 2005. p. 157-166.

[53] Guise TA, Mohammad KS, Clines G, Stebbins EG, Wong DH, Higgins LS, et al. Basic mechanisms responsible for osteolytic and osteoblastic bone metastases. Clin Cancer Res. 2006;12(20 Pt 2):6213s-6s.

[54] Gruber R. Reader's digest of the pathophysiology of bone metastases. Wien Med Wochenschr. 2012;162(17-18):370-3.

[55] Theriault RL, Theriault RL. Biology of bone metastases. Cancer Control. 2012;19(2):92-101.

[56] Roodman GD. Mechanisms of bone metastasis. N Engl J Med. 2004;350(16):1655-64.

[57] Coleman RE. Metastatic bone disease: clinical features, pathophysiology and treatment strategies. Cancer Treat Rev. 2001;27(3):165-76.

[58] Urwin GH, Percival RC, Harris S, Beneton MN, Williams JL, Kanis JA. Generalised increase in bone resorption in carcinoma of the prostate. Br J Urol. 1985;57(6):721-3.

[59] Zheng Y, Chow SO, Boernert K, Basel D, Mikuscheva A, Kim S, et al. Direct crosstalk between cancer and osteoblast lineage cells fuels metastatic growth in bone via auto-amplification of IL-6 and RANKL signaling pathways. J Bone Miner Res. 2014;29(9):1938-49.

[60] Wysolmerski JJ. Parathyroid hormone-related protein: an update. J Clin Endocrinol Metab. 2012;97(9):2947-56.

[61] Thomas RJ, Guise TA, Yin JJ, Elliott J, Horwood NJ, Martin TJ, et al. Breast cancer cells interact with osteoblasts to support osteoclast formation. Endocrinology. 1999;140(10):4451-8.

[62] Ibrahim T, Flamini E, Mercatali L, Sacanna E, Serra P, Amadori D. Pathogenesis of osteoblastic bone metastases from prostate cancer. Cancer. 2010;116(6):1406-18.

[63] Rose-John S. IL-6 trans-signaling via the soluble IL-6 receptor: importance for the pro-inflammatory activities of IL-6. Int J Biol Sci. 2012;8(9):1237-47.

[64] Naka T, Nishimoto N, Kishimoto T. The paradigm of IL-6: from basic science to medicine. Arthritis Res. 2002;4 Suppl 3:S233-42.

[65] Hong DS, Angelo LS, Kurzrock R. Interleukin-6 and its receptor in cancer: implications for translational therapeutics. Cancer. 2007;110(9):1911-28.

[66] Naugler WE, Karin M. The wolf in sheep's clothing: the role of interleukin-6 in immunity, inflammation and cancer. Trends Mol Med. 2008;14(3):109-19.

[67] Keller ET, Wanagat J, Ershler WB. Molecular and cellular biology of interleukin-6 and its receptor. Front Biosci. 1996;1:d340-57.

[68] Wallner L, Dai J, Escara-Wilke J, Zhang J, Yao Z, Lu Y, et al. Inhibition of interleukin-6 with CNTO328, an anti-interleukin-6 monoclonal antibody, inhibits conversion of androgen-dependent prostate cancer to an androgen-independent phenotype in orchiectomized mice. Cancer Res. 2006;66(6):3087-95.

[69] Corcoran NM, Costello AJ. Interleukin-6: minor player or starring role in the development of hormone-refractory prostate cancer? BJU Int. 2003;91(6):545-53.

[70] Ara T, Declerck YA. Interleukin-6 in bone metastasis and cancer progression. Eur J Cancer. 2010;46(7):1223-31.

[71] Rose-John S, Scheller J, Elson G, Jones SA. Interleukin-6 biology is coordinated by membrane-bound and soluble receptors: role in inflammation and cancer. J Leukoc Biol. 2006;80(2):227-36.

[72] Oelzner P, Franke S, Lehmann G, Eidner T, Hein G, Wolf G. The balance between soluble receptors regulating IL-6 trans-signaling is predictive for the RANKL/osteoprotegerin ratio in postmenopausal women with rheumatoid arthritis. Rheumatol Int. 2012;32(1):199-206.

[73] Malinowska K, Neuwirt H, Cavarretta IT, Bektic J, Steiner H, Dietrich H, et al. Interleukin-6 stimulation of growth of prostate cancer in vitro and in vivo through activation of the androgen receptor. Endocr Relat Cancer. 2009;16(1):155-69.

[74] Shariat SF, Andrews B, Kattan MW, Kim J, Wheeler TM, Slawin KM. Plasma levels of interleukin-6 and its soluble receptor are associated with prostate cancer progression and metastasis. Urology. 2001;58(6):1008-15.

[75] Michalaki V, Syrigos K, Charles P, Waxman J. Serum levels of IL-6 and TNF-alpha correlate with clinicopathological features and patient survival in patients with prostate cancer. Br J Cancer. 2004;90(12):2312-6.

[76] Wise GJ, Marella VK, Talluri G, Shirazian D. Cytokine variations in patients with hormone treated prostate cancer. J Urol. 2000;164(3 Pt 1):722-5.

[77] Adler HL, McCurdy MA, Kattan MW, Timme TL, Scardino PT, Thompson TC. Elevated levels of circulating interleukin-6 and transforming growth factor-beta1 in patients with metastatic prostatic carcinoma. J Urol. 1999;161(1):182-7.

[78] Drachenberg DE, Elgamal AA, Rowbotham R, Peterson M, Murphy GP. Circulating levels of interleukin-6 in patients with hormone refractory prostate cancer. Prostate. 1999;41(2):127-33.

[79] George DJ, Halabi S, Shepard TF, Sanford B, Vogelzang NJ, Small EJ, et al. The prognostic significance of plasma interleukin-6 levels in patients with metastatic hormone-refractory prostate cancer: results from cancer and leukemia group B 9480. Clin Cancer Res. 2005;11(5):1815-20.

[80] Chung TD, Yu JJ, Spiotto MT, Bartkowski M, Simons JW. Characterization of the role of IL-6 in the progression of prostate cancer. Prostate. 1999;38(3):199-207.

[81] Steiner H, Godoy-Tundidor S, Rogatsch H, Berger AP, Fuchs D, Comuzzi B, et al. Accelerated in vivo growth of prostate tumors that up-regulate interleukin-6 is associated with reduced retinoblastoma protein expression and activation of the mitogen-activated protein kinase pathway. Am J Pathol. 2003;162(2):655-63.

[82] Lee SO, Chun JY, Nadiminty N, Lou W, Gao AC. Interleukin-6 undergoes transition from growth inhibitor associated with neuroendocrine differentiation to stimulator accompanied by androgen receptor activation during LNCaP prostate cancer cell progression. Prostate. 2007;67(7):764-73.

[83] Wegiel B, Bjartell A, Culig Z, Persson JL. Interleukin-6 activates PI3K/Akt pathway and regulates cyclin A1 to promote prostate cancer cell survival. Int J Cancer. 2008;122(7):1521-9.

[84] Cavarretta IT, Neuwirt H, Untergasser G, Moser PL, Zaki MH, Steiner H, et al. The antiapoptotic effect of IL-6 autocrine loop in a cellular model of advanced prostate cancer is mediated by Mcl-1. Oncogene. 2007;26(20):2822-32.

[85] Pu YS, Hour TC, Chuang SE, Cheng AL, Lai MK, Kuo ML. Interleukin-6 is responsible for drug resistance and anti-apoptotic effects in prostatic cancer cells. Prostate. 2004;60(2):120-9.

[86] Borsellino N, Belldegrun A, Bonavida B. Endogenous interleukin 6 is a resistance factor for cis-diamminedichloroplatinum and etoposide-mediated cytotoxicity of human prostate carcinoma cell lines. Cancer Res. 1995;55(20):4633-9.

[87] Borsellino N, Bonavida B, Ciliberto G, Toniatti C, Travali S, D'Alessandro N. Blocking signaling through the Gp130 receptor chain by interleukin-6 and oncostatin M inhibits PC-3 cell growth and sensitizes the tumor cells to etoposide and cisplatin-mediated cytotoxicity. Cancer. 1999;85(1):134-44.

[88] Feng S, Tang Q, Sun M, Chun JY, Evans CP, Gao AC. Interleukin-6 increases prostate cancer cells resistance to bicalutamide via TIF2. Mol Cancer Ther. 2009;8(3):665-71.

[89] Conze D, Weiss L, Regen PS, Bhushan A, Weaver D, Johnson P, et al. Autocrine production of interleukin 6 causes multidrug resistance in breast cancer cells. Cancer Res. 2001;61(24):8851-8.

[90] Hardin J, MacLeod S, Grigorieva I, Chang R, Barlogie B, Xiao H, et al. Interleukin-6 prevents dexamethasone-induced myeloma cell death. Blood. 1994;84(9):3063-70.

[91] Ara T, Song L, Shimada H, Keshelava N, Russell HV, Metelitsa LS, et al. Interleukin-6 in the bone marrow microenvironment promotes the growth and survival of neuroblastoma cells. Cancer Res. 2009;69(1):329-37.

[92] Rojas A, Liu G, Coleman I, Nelson PS, Zhang M, Dash R, et al. IL-6 promotes prostate tumorigenesis and progression through autocrine cross-activation of IGF-IR. Oncogene. 2011;30(20):2345-55.

[93] Walter M, Liang S, Ghosh S, Hornsby PJ, Li R. Interleukin 6 secreted from adipose stromal cells promotes migration and invasion of breast cancer cells. Oncogene. 2009;28(30):2745-55.

[94] Sullivan NJ, Sasser AK, Axel AE, Vesuna F, Raman V, Ramirez N, et al. Interleukin-6 induces an epithelial-mesenchymal transition phenotype in human breast cancer cells. Oncogene. 2009;28(33):2940-7.

[95] Tamm I, Cardinale I, Krueger J, Murphy JS, May LT, Sehgal PB. Interleukin 6 decreases cell-cell association and increases motility of ductal breast carcinoma cells. J Exp Med. 1989;170(5):1649-69.

[96] Sehgal PB. Interleukin-6 induces increased motility, cell-cell and cell-substrate dyshesion and epithelial-to-mesenchymal transformation in breast cancer cells. Oncogene. 2010;29(17):2599-600; author reply 601-3.

[97] Jilka RL, Hangoc G, Girasole G, Passeri G, Williams DC, Abrams JS, et al. Increased osteoclast development after estrogen loss: mediation by interleukin-6. Science. 1992;257(5066):88-91.

[98] Poli V, Balena R, Fattori E, Markatos A, Yamamoto M, Tanaka H, et al. Interleukin-6 deficient mice are protected from bone loss caused by estrogen depletion. EMBO J. 1994;13(5):1189-96.

[99] Le Goff B, Blanchard F, Berthelot JM, Heymann D, Maugars Y. Role for interleukin-6 in structural joint damage and systemic bone loss in rheumatoid arthritis. Joint Bone Spine. 2010;77(3):201-5.

[100] Roodman GD, Kurihara N, Ohsaki Y, Kukita A, Hosking D, Demulder A, et al. Interleukin 6. A potential autocrine/paracrine factor in Paget's disease of bone. J Clin Invest. 1992;89(1):46-52.

[101] Palmqvist P, Persson E, Conaway HH, Lerner UH. IL-6, leukemia inhibitory factor, and oncostatin M stimulate bone resorption and regulate the expression of receptor activator of NF-kappa B ligand, osteoprotegerin, and receptor activator of NF-kappa B in mouse calvariae. J Immunol. 2002;169(6):3353-62.

[102] Kwan Tat S, Padrines M, Theoleyre S, Heymann D, Fortun Y. IL-6, RANKL, TNF-alpha/IL-1: interrelations in bone resorption pathophysiology. Cytokine Growth Factor Rev. 2004;15(1):49-60.

[103] Kudo O, Sabokbar A, Pocock A, Itonaga I, Fujikawa Y, Athanasou NA. Interleukin-6 and interleukin-11 support human osteoclast formation by a RANKL-independent mechanism. Bone. 2003;32(1):1-7.

[104] Mizutani K, Sud S, Pienta KJ. Prostate cancer promotes CD11b positive cells to differentiate into osteoclasts. J Cell Biochem. 2009;106(4):563-9.

[105] Sato K, Suematsu A, Okamoto K, Yamaguchi A, Morishita Y, Kadono Y, et al. Th17 functions as an osteoclastogenic helper T cell subset that links T cell activation and bone destruction. J Exp Med. 2006;203(12):2673-82.

[106] Pozzi S, Vallet S, Mukherjee S, Cirstea D, Vaghela N, Santo L, et al. High-dose zoledronic acid impacts bone remodeling with effects on osteoblastic lineage and bone mechanical properties. Clin Cancer Res. 2009;15(18):5829-39.

[107] Dhillon S, Lyseng-Williamson KA. Zoledronic acid : a review of its use in the management of bone metastases of malignancy. Drugs. 2008;68(4):507-34.

[108] Zheng Y, Zhou H, Brennan K, Blair JM, Modzelewski JR, Seibel MJ, et al. Inhibition of bone resorption, rather than direct cytotoxicity, mediates the anti-tumour actions of ibandronate and osteoprotegerin in a murine model of breast cancer bone metastasis. Bone. 2007;40(2):471-8.

[109] Green JR. Bisphosphonates: preclinical review. Oncologist. 2004;9 Suppl 4:3-13.

[110] Sasaki A, Boyce BF, Story B, Wright KR, Chapman M, Boyce R, et al. Bisphosphonate risedronate reduces metastatic human breast cancer burden in bone in nude mice. Cancer Res. 1995;55(16):3551-7.

[111] Yoneda T, Sasaki A, Dunstan C, Williams PJ, Bauss F, De Clerck YA, et al. Inhibition of osteolytic bone metastasis of breast cancer by combined treatment with the bisphosphonate ibandronate and tissue inhibitor of the matrix metalloproteinase-2. J Clin Invest. 1997;99(10):2509-17.

[112] Kohno N, Aogi K, Minami H, Nakamura S, Asaga T, Iino Y, et al. Zoledronic acid significantly reduces skeletal complications compared with placebo in Japanese women with bone metastases from breast cancer: a randomized, placebo-controlled trial. J Clin Oncol. 2005;23(15):3314-21.

[113] Saad F, Gleason DM, Murray R, Tchekmedyian S, Venner P, Lacombe L, et al. A randomized, placebo-controlled trial of zoledronic acid in patients with hormone-refractory metastatic prostate carcinoma. J Natl Cancer Inst. 2002;94(19):1458-68.

[114] Guenther A, Gordon S, Tiemann M, Burger R, Bakker F, Green JR, et al. The bisphosphonate zoledronic acid has antimyeloma activity in vivo by inhibition of protein prenylation. Int J Cancer. 2010;126(1):239-46.

[115] Oldfield V, Dhillon S, Plosker GL. Tocilizumab: a review of its use in the management of rheumatoid arthritis. Drugs. 2009;69(5):609-32.

[116] Ito H, Takazoe M, Fukuda Y, Hibi T, Kusugami K, Andoh A, et al. A pilot randomized trial of a human anti-interleukin-6 receptor monoclonal antibody in active Crohn's disease. Gastroenterology. 2004;126(4):989-96; discussion 47.

[117] Illei GG, Shirota Y, Yarboro CH, Daruwalla J, Tackey E, Takada K, et al. Tocilizumab in systemic lupus erythematosus: data on safety, preliminary efficacy, and impact on circulating plasma cells from an open-label phase I dosage-escalation study. Arthritis Rheum. 2010;62(2):542-52.

[118] Shinriki S, Jono H, Ota K, Ueda M, Kudo M, Ota T, et al. Humanized anti-interleukin-6 receptor antibody suppresses tumor angiogenesis and in vivo growth of human oral squamous cell carcinoma. Clin Cancer Res. 2009;15(17):5426-34.

[119] Armstrong AP, Miller RE, Jones JC, Zhang J, Keller ET, Dougall WC. RANKL acts directly on RANK-expressing prostate tumor cells and mediates migration and expression of tumor metastasis genes. Prostate. 2008;68(1):92-104.

[120] Chung TD, Yu JJ, Kong TA, Spiotto MT, Lin JM. Interleukin-6 activates phosphatidylinositol-3 kinase, which inhibits apoptosis in human prostate cancer cell lines. Prostate. 2000;42(1):1-7.

[121] Okamoto M, Lee C, Oyasu R. Interleukin-6 as a paracrine and autocrine growth factor in human prostatic carcinoma cells in vitro. Cancer Res. 1997;57(1):141-6.

[122] Kaighn ME, Narayan KS, Ohnuki Y, Lechner JF, Jones LW. Establishment and characterization of a human prostatic carcinoma cell line (PC-3). Invest Urol. 1979;17(1):16-23.

[123] Zheng Y. The bone microenvironment and its influence on metastatic breast cancer cell growth in bone [dissertation]. Sydney (NSW): University of Sydney; 2008.

[124] Duque G, Watanabe K, editors. Osteoporosis research: animal models, 1st ed. London: Springer; 2011. p. 83-92.

[125] Croucher PI, De Hendrik R, Perry MJ, Hijzen A, Shipman CM, Lippitt J, et al. Zoledronic acid treatment of 5T2MM-bearing mice inhibits the development of myeloma bone disease: evidence for decreased osteolysis, tumor burden and angiogenesis, and increased survival. J Bone Miner Res. 2003;18(3):482-92.

[126] Ottewell PD, Monkkonen H, Jones M, Lefley DV, Coleman RE, Holen I. Antitumor effects of doxorubicin followed by zoledronic acid in a mouse model of breast cancer. J Natl Cancer Inst. 2008;100(16):1167-78.

[127] Koto K, Horie N, Kimura S, Murata H, Sakabe T, Matsui T, et al. Clinically relevant dose of zoledronic acid inhibits spontaneous lung metastasis in a murine osteosarcoma model. Cancer Lett. 2009;274(2):271-8.

[128] Koff JL, Ramachandiran S, Bernal-Mizrachi L. A time to kill: targeting apoptosis in cancer. Int J Mol Sci. 2015;16(2):2942-55.

[129] Halleen JM, Tiitinen SL, Ylipahkala H, Fagerlund KM, Vaananen HK. Tartrate-resistant acid phosphatase 5b (TRACP 5b) as a marker of bone resorption. Clin Lab. 2006;52(9-10):499-509.

[130] Chao TY, Wu YY, Janckila AJ. Tartrate-resistant acid phosphatase isoform 5b (TRACP 5b) as a serum maker for cancer with bone metastasis. Clin Chim Acta. 2010;411(21-22):1553-64.

[131] Zheng Y, Basel D, Chow SO, Fong-Yee C, Kim S, Buttgereit F, et al. Targeting IL-6 and RANKL signaling inhibits prostate cancer growth in bone. Clin Exp Metastasis. 2014;31(8):921-33.

[132] Tawara K, Oxford JT, Jorcyk CL. Clinical significance of interleukin (IL)-6 in cancer metastasis to bone: potential of anti-IL-6 therapies. Cancer Manag Res. 2011;3:177-89.

[133] Zaki MH, Nemeth JA, Trikha M. CNTO 328, a monoclonal antibody to IL-6, inhibits human tumor-induced cachexia in nude mice. Int J Cancer. 2004;111(4):592-5.

[134] Morrissey C, Lai JS, Brown LG, Wang YC, Roudier MP, Coleman IM, et al. The expression of osteoclastogenesis-associated factors and osteoblast response to osteolytic prostate cancer cells. Prostate. 2010;70(4):412-24.

[135] Akimoto S, Okumura A, Fuse H. Relationship between serum levels of interleukin-6, tumor necrosis factor-alpha and bone turnover markers in prostate cancer patients. Endocr J. 1998;45(2):183-9.

[136] Blanchard F, Duplomb L, Baud'huin M, Brounais B. The dual role of IL-6-type cytokines on bone remodeling and bone tumors. Cytokine Growth Factor Rev. 2009;20(1):19-28.

[137] Liu XH, Kirschenbaum A, Yao S, Levine AC. Cross-talk between the interleukin-6 and prostaglandin E(2) signaling systems results in enhancement of osteoclastogenesis through effects on the osteoprotegerin/receptor activator of nuclear factor-{kappa}B (RANK) ligand/RANK system. Endocrinology. 2005;146(4):1991-8.

[138] Liao J, McCauley LK. Skeletal metastasis: Established and emerging roles of parathyroid hormone related protein (PTHrP). Cancer Metastasis Rev. 2006;25(4):559-71.

[139] Chu GC, Zhau HE, Wang R, Rogatko A, Feng X, Zayzafoon M, et al. RANK- and c-Met-mediated signal network promotes prostate cancer metastatic colonization. Endocr Relat Cancer. 2014;21(2):311-26.

[140] Yang J, Weinberg RA. Epithelial-mesenchymal transition: at the crossroads of development and tumor metastasis. Dev Cell. 2008;14(6):818-29.

[141] Jones DH, Nakashima T, Sanchez OH, Kozieradzki I, Komarova SV, Sarosi I, et al. Regulation of cancer cell migration and bone metastasis by RANKL. Nature. 2006;440(7084):692-6.

[142] Santini D, Perrone G, Roato I, Godio L, Pantano F, Grasso D, et al. Expression pattern of receptor activator of NFkappaB (RANK) in a series of primary solid tumors and related bone metastases. J Cell Physiol. 2011;226(3):780-4.

[143] Mori K, Ando K, Heymann D, Redini F. Receptor activator of nuclear factor-kappa B ligand (RANKL) stimulates bone-associated tumors through functional RANK expressed on bone-associated cancer cells? Histol Histopathol. 2009;24(2):235-42.

[144] Fizazi K, Carducci M, Smith M, Damiao R, Brown J, Karsh L, et al. Denosumab versus zoledronic acid for treatment of bone metastases in men with castration-resistant prostate cancer: a randomised, double-blind study. Lancet. 2011;377(9768):813-22.

[145] Park JI, Lee MG, Cho K, Park BJ, Chae KS, Byun DS, et al. Transforming growth factor-beta1 activates interleukin-6 expression in prostate cancer cells through the synergistic collaboration of the Smad2, p38-NF-kappaB, JNK, and Ras signaling pathways. Oncogene. 2003;22(28):4314-32.

[146] Yu H, Kortylewski M, Pardoll D. Crosstalk between cancer and immune cells: role of STAT3 in the tumour microenvironment. Nat Rev Immunol. 2007;7(1):41-51.

[147] Wang L, Yi T, Kortylewski M, Pardoll DM, Zeng D, Yu H. IL-17 can promote tumor growth through an IL-6-Stat3 signaling pathway. J Exp Med. 2009;206(7):1457-64.

[148] Richmond A, Su Y. Mouse xenograft models vs GEM models for human cancer therapeutics. Dis Model Mech. 2008;1(2-3):78-82.

[149] Duluc D, Delneste Y, Tan F, Moles MP, Grimaud L, Lenoir J, et al. Tumor-associated leukemia inhibitory factor and IL-6 skew monocyte differentiation into tumor-associated macrophage-like cells. Blood. 2007;110(13):4319-30.

[150] Kim SW, Kim JS, Papadopoulos J, Choi HJ, He J, Maya M, et al. Consistent interactions between tumor cell IL-6 and macrophage TNF-alpha enhance the growth of human prostate cancer cells in the bone of nude mouse. Int Immunopharmacol. 2011;11(7):862-72.

[151] Li Q, Withoff S, Verma IM. Inflammation-associated cancer: NF-kappaB is the lynchpin. Trends Immunol. 2005;26(6):318-25.

[152] Colotta F, Allavena P, Sica A, Garlanda C, Mantovani A. Cancer-related inflammation, the seventh hallmark of cancer: links to genetic instability. Carcinogenesis. 2009;30(7):1073-81.

[153] Ragab AA, Nalepka JL, Bi Y, Greenfield EM. Cytokines synergistically induce osteoclast differentiation: support by immortalized or normal calvarial cells. Am J Physiol Cell Physiol. 2002;283(3):C679-87.

[154] Morgan RA. Human tumor xenografts: the good, the bad, and the ugly. Mol Ther. 2012;20(5):882-4.

Chapter 7
Appendix / Anhang

7.1 Declaration of Candidate / Eidesstattliche Versicherung

„Ich, Dennis Basel, versichere an Eides statt durch meine eigenhändige Unterschrift, dass ich die vorgelegte Dissertation mit dem Thema: „Antagonizing Autocrine IL-6 Receptor Signaling Inhibits Prostate Cancer Growth in Bone“ selbstständig und ohne nicht offengelegte Hilfe Dritter verfasst und keine anderen als die angegebenen Quellen und Hilfsmittel genutzt habe.
Alle Stellen, die wörtlich oder dem Sinne nach auf Publikationen oder Vorträgen anderer Autoren beruhen, sind als solche in korrekter Zitierung (siehe „Uniform Requirements for Manuscripts (URM)“ des ICMJE -*www.**icmje**.org*) kenntlich gemacht. Die Abschnitte zu Methodik (insbesondere praktische Arbeiten, Laborbestimmungen, statistische Aufarbeitung) und Resultaten (insbesondere Abbildungen, Graphiken und Tabellen) entsprechen den URM (s.o) und werden von mir verantwortet.
Meine Anteile an etwaigen Publikationen zu dieser Dissertation entsprechen denen, die in der untenstehenden gemeinsamen Erklärung mit dem Betreuer, angegeben sind. Sämtliche Publikationen, die aus dieser Dissertation hervorgegangen sind und bei denen ich Autor bin, entsprechen den URM (s.o) und werden von mir verantwortet.

Die Bedeutung dieser eidesstattlichen Versicherung und die strafrechtlichen Folgen einer unwahren eidesstattlichen Versicherung (§156,161 des Strafgesetzbuches) sind mir bekannt und bewusst.“

Datum Unterschrift

7.2 Publications / Anteilserklärung an erfolgten Publikationen

Publikation 1:

Zheng Y, Chow SO, Boernert K, Basel D, Mikuscheva A, Kim S, et al. Direct crosstalk between cancer and osteoblast lineage cells fuels metastatic growth in bone via auto-amplification of IL-6 and RANKL signaling pathways. J Bone Miner Res. 2014;29(9):1938-49 (IF: 6,59).

Beitrag im Einzelnen: Erhebung von *in vitro* Daten, die zeigen, dass humanes IL-6 den Oberflächenrezeptor RANK in der Brustkrebszelllinie MDA-MB-231 hochreguliert und Tocilizumab diesen Effekt reduziert. Andererseits konnte gezeigt werden, dass RANKL die IL-6 mRNA Synthese in MDA-MB-231-Zellen erhöht.

Publikation 2:

Zheng Y, Basel D, Chow SO, Fong-Yee C, Kim S, Buttgereit F, et al. Targeting IL-6 and RANKL signaling inhibits prostate cancer growth in bone. Clin Exp Metastasis. 2014;31(8):921-33 (IF: 3,73).

Beitrag im Einzelnen: Die Planung und Ausarbeitung der Studie erfolgte gemeinsam mit Dr. med. Yu Zheng und Prof. Dr. med. Markus Seibel. Wesentlicher Anteil an der Erhebung der *in vitro* und *in vivo* Daten, wobei ein intra-tibiales und ein subkutanes Mausmodell ausgewertet wurden. Die erhobenen Daten machen einen erheblichen Teil der obigen Publikation aus und bilden die Grundlage für das theoretische Modell.

Unterschrift des Doktoranden

7.3 Curriculum Vitae / Lebenslauf

Mein Lebenslauf wird aus datenschutzrechtlichen Gründen in der elektrischen Version meiner Arbeit nicht veröffentlicht.

7.4 List of Publications / Publikationsliste

7.4.1 Publications / Publikationen

1. Zheng Y, Chow SO, Boernert K, **Basel D**, Mikuscheva A, Kim S, et al. Direct crosstalk between cancer and osteoblast lineage cells fuels metastatic growth in bone via auto-amplification of IL-6 and RANKL signaling pathways. J Bone Miner Res. 2014;29(9):1938-49

   Impact Factor: 6,59

2. Zheng Y, **Basel D**, Chow SO, Fong-Yee C, Kim S, Buttgereit F, et al. Targeting IL-6 and RANKL signaling inhibits prostate cancer growth in bone. Clin Exp Metastasis. 2014;31(8):921-33

   Impact Factor: 3,73

7.4.2 Poster Presentations / Posterpräsentationen

1. **Basel D**, Zheng Y, Zhou H, Buttgereit F, Dunstan CR and Seibel MJ. Treatment with Interleukin-6 Receptor Antibodies Inhibits Prostate Cancer Growth in a Murine Model of Bone Metastasis. Second Asia-Pacific Osteoporosis and Bone Meeting in Gold Coast, Australia 2011.

2. **Basel D**, Zheng Y, Zhou H, Buttgereit F, Dunstan CR and Seibel MJ. Treatment with Interleukin-6 Receptor Antibodies Inhibits Prostate Cancer Growth in a Murine Model of Bone Metastasis. Concord Repatriation General Hospital in Concord, New South Wales, Australia 2011.

7.5 Acknowledgements / Danksagung

I would like to express my sincere appreciation to the following people:

- I'm extremely grateful to Prof. Frank Buttgereit who accepted my application in 2010 for this project and without whom this project would not have been accomplished. I truly appreciate his constant support and patience as well as his steady positive reinforcement.
- I would like to express my deep thankfulness to my supervisor Yu Zheng for his encouragement as well as technical help concerning my project. I am also very grateful for his critical comments on my manuscript. It was an honor to work with him and I'm glad to have met him.
- Profound thanks go to Prof. Markus Seibel for his constant effort and time to make this project possible. It was a privilege to work with him and benefit from his profound academic knowledge.
- I wish to thank A/Prof. Hong Zhou for her great academic wisdom, her assistance for technical questions and her consistent good mood in the lab.
- I also wish to thank the Charité Berlin for providing financial aid and the ANZAC Research Institute for all the support.
- Many thanks go to all the people working in the ANZAC Research Institute and living in the adjacent hospital accommodation. We shared a great experience together and you made this year very special to me.
- Finally, I would like to express my special thanks to my parents for their ever-present support and love.